Multi-timescale shoreline change modelling

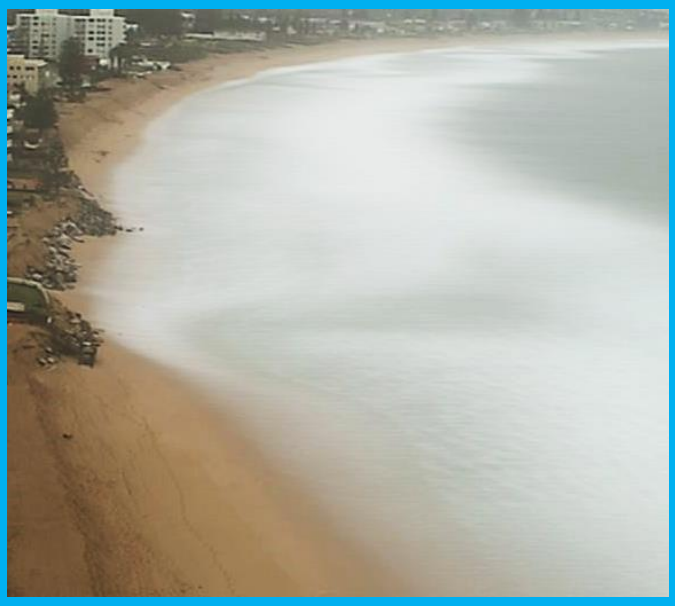

Rob Schepper

Master Thesis

Multi-timescale shoreline change modelling

By

R.B. Schepper

in partial fulfilment of the requirements for the degree of

Master of Science
in Civil Engineering

at the Delft University of Technology,

to be defended publicly on Friday December 21, 2018 at 11:00 AM.

Thesis committee:	Prof.dr.ir. A.J.H.M. Reniers,	TU Delft
	Dr.ir. S. de Vries,	TU Delft, Chair
	Dr. C.A. Katsman,	TU Delft
	Dr. R. Almar,	LEGOS-IRD
	Dr.ir. E.W.J. Bergsma,	LEGOS-CNES
	Dr. M.A. Davidson	University of Plymouth

TU Delft

LEGOS

Preface

This master thesis is about implementing multiple timescales in the equilibrium shoreline prediction model ShoreFor (Shoreline Forecast). I have worked on this thesis for ten months, of which I spent the first five at LEGOS in Toulouse. Here I worked mainly on finding a suitable method to implement multiple timescales. Thereafter, I finalized my thesis in Delft at the Delft University of Technology, where I mainly focussed on writing the report. Finishing the thesis means that my time as a student in Delft ends. I can look back at a great time and can now focus on applying my knowledge about hydraulic engineering.

First of all, I would like to thank all the people from LEGOS who helped me with my research and ensured that my time in Toulouse was helpful, informative and pleasant. A special thanks to Rafael Almar and Erwin Bergsma for their time and supervision on daily basis. They were able to transfer their enthusiasm and knowledge about coastal engineering to me. Moreover, they aided in making the graduation process fluent and efficient.

Secondly, I would like to thank Sierd de Vries, Ad Reniers and Caroline Katsman for their supervision, especially during my time in Delft. A special thanks to Sierd for suggesting me this research topic, making it possible to go to Toulouse and for his feedback and suggestions on this report.

Furthermore, I would like to thank Mark Davidson from the University of Plymouth for his remarks and recommendations about implementing a multitude of timescales in ShoreFor. As the developer of current ShoreFor model, his enthusiasm was a large contributor to my drive in finishing the project.

Finally, I would like to thank my family and friends for supporting me during my time in Delft. A special thanks to my parents, brother and sister for giving me the strength and energy to complete this study.

Rob Schepper
Delft, December 2018

Abstract

Shoreline change is affected by a multitude of complex processes operating at various spatiotemporal scales. Comprehensive multi-year simulations of shoreline changes and forecasts are feasible with process-based models. However, these detailed and computationally expensive numerical simulations do not always lead to increased predictive skill in comparison to simpler shoreline models (Davidson et al., 2013). ShoreFor (Davidson et al., 2013) employs the concept of (dis-) equilibrium of shoreline location following Wright and Short (1985). In this research, the current ShoreFor model (Splinter et al., 2014) is used as baseline and is defined as follows:

$$\frac{dx}{dt} = c * (F(\varphi)^{+} + r * F(\varphi)^{-}) \quad (1)$$

Where x is the shoreline position, t the time, c the response factor, r the erosion ratio and F the forcing, containing a single memory decay factor φ. ShoreFor seeks for an optimum decay factor that best describes the morphological response of a coastal system to the corresponding hydrodynamic forcing. This parameter is measured in days and effectively controls the shoreline response timescale. Currently, the ShoreFor model provides a single value for φ, representing a single dominant shoreline response timescale. As morphological systems can contain multiple dominant timescale responses, a new approach to multi-timescale shoreline change modelling is proposed.

Three video-derived datasets are used to improve the model towards a generally applicable one which incorporates multiple temporal scales: Narrabeen (Australia), Nha Trang (Vietnam) and Grand Popo (Benin). Each dataset has different hydrodynamic- and morphological characteristics. The storm timescale is a dominant mode of shoreline response for Narrabeen, whereas for Nha Trang and Grand Popo the seasonal timescale is the most dominant. Furthermore, all sites are subjected to more modes of shoreline response such that the application of a single memory decay factor will hamper shoreline modelling.

The existing model is improved using 3 steps.

In the first step, the raw wave- and shoreline signals are filtered to distinguish temporal scales. Then filtered temporal scales in shoreline position are forced with the corresponding scales in the wave signals. This part of the model improvement will take the following form:

$$\frac{dx_i}{dt} = c * (F(\varphi)_i^{+} + r * F(\varphi)_i^{-}) \quad (2)$$

Wherein x_i is the shoreline position with temporal scale i and F_i the forcing with scale i. For each temporal scale i, a distinct response factor c and memory decay factor φ is found.

In the second step, the effect of small temporal scales in wave forcing on larger temporal scales in shoreline position is accounted for. The improved model takes this effect into account using the envelope of the filtered wave signals. The envelope is used to force the model and to calculate shoreline change with the same timescale. The second step can be defined as:

$$\frac{dx_j}{dt} = c * \left(F(\varphi)_{i\to j}^{+} + r * F(\varphi)_{i\to j}^{-}\right) \quad (3)$$

In which x_j is the shoreline position with temporal scale j and $F_{i\to j}$ the forcing with scale j determined by the envelope of wave signals with scale i. Note that $j > i$.

In the third and final step, the effect of large temporal scales in shoreline position on smaller scales in shoreline response is accounted for. The efficiency with which waves induce cross-shore sediment transport can be dependent on the large scale shoreline variation. A time varying parameter c is introduced that controls the efficiency with which waves induce cross-shore sediment transport. The shoreline position can then be calculated as follows:

$$x_i(t) = c_j(t) * \int_0^t (F(\varphi,t)_i^+ + r * F(\varphi,t)_i^-)dt \quad (4)$$

Where x_i is the shoreline position with temporal scale i, c_j the dynamic response factor with temporal scale j, and F_i the forcing with scale i. Note that $j > i$. The dynamic response factor varies over time with the shape of the shoreline signal with timescale j: it represents the effect of the large scale shoreline variation with timescale j on shoreline response with timescale i.

In Figure 1, model results (Nha Trang) for both ShoreFor and the improved model are presented, covering the calibration- and validation phase.

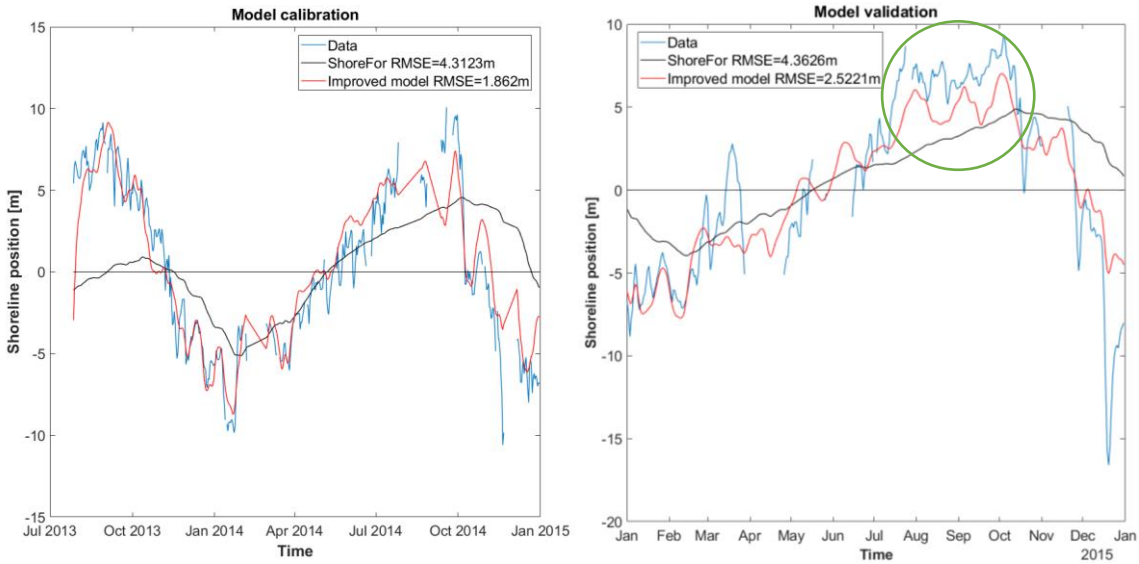

Figure 1: Calibration (left) and validation (right) of ShoreFor (black) and the improved (red) model

The improved model shows better prediction skill for both the calibration- and validation phase. The improved model accurately predicts shoreline response on multiple dominant timescales, for example, the monsoon- (indicated by the green circle) as well as the seasonal timescale. Table 1 presents an overview of the relative model improvement per study site. The root mean squared error (RMSE) is used as an indicator for prediction skill.

Improvement	Calibration	Validation
Nha Trang	+30%	+42%
Narrabeen	+42%	+6%
Grand Popo	+5%	+27%

Table 1: Relative model improvement per site

Contents

Figures:

Tables:

Symbols:
a = shoreline position offset [m]
b = linear trend term [m/year]
c = response parameter [$m^{1.5}s^{-1}W^{-0.5}$]
C_g = shallow water group velocity [m/s]
E_b = significant wave energy at breaking [N/m]
f = variability factor [~]
F = forcing term [$W^{0.5}/m^{0.5}$]
g = gravitational acceleration [m/s^2]
h_b = depth at breaking [m]
H_b = breaking wave height [m]
H_s = significant wave height [m]
k = wave power exponent [~]
m = number of calibration parameters [~]
n = total number of samples [~]
N = total record length [~]
ρ = density [kg/m^3]
P = wave energy flux [Watts]
P_b = breaking wave energy flux [Watts]
φ = memory decay factor [days]
r = erosion ratio [~]
σ = standard deviation of baseline residuals [m]
σ_b = standard deviation of filtered shoreline signals within a timescale bin [m]
σ_x = standard deviation of predicted shoreline signals [m]
$\sigma_{\Delta\Omega}$ = standard deviation of $\Delta\Omega$ [~]
s = beach state [~]
t = time [s]/[hr]/[days]
T_p = peak wave period [s]
w_s = sediment fall velocity [m/s]
x = shoreline position [m]
γ = breaker index [~]
Ω = dimensionless fall velocity [~]
Ω_0 = constant dimensionless fall velocity equilibrium term [~]
Ω_{eq} = time-varying equilibrium condition [~]
$\Delta\Omega$ = dimensionless fall velocity disequilibrium term [~]

1 Introduction

Forecasted shoreline positions are a valuable source in order to adequately manage the coastal zone. If shoreline change is known up front and unwanted erosion/accretion is expected, an efficient solution can be found to mitigate these effects. Especially erosion can endanger one or more services of the coastal system such as recreation and safety (Figure 2).

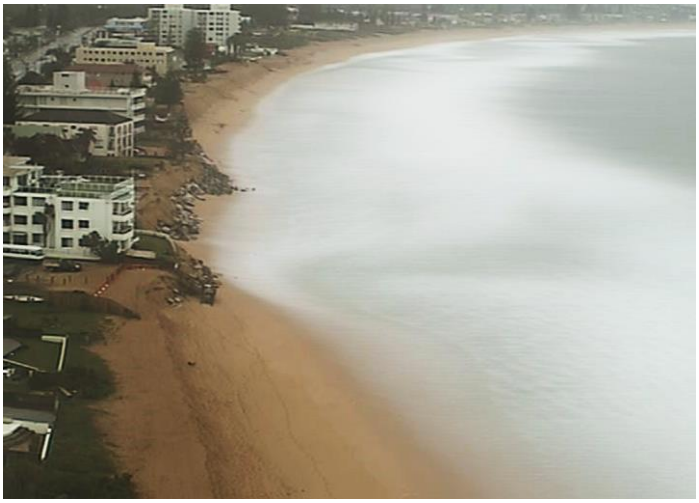

Figure 2: Further coastline erosion will endanger the stability of the buildings (Davidson et al., 2013)

Shoreline migration can be divided into changes due to gradients in longshore sediment transport and gradients in cross-shore sediment transport. Shoreline changes due to gradients in longshore transport are generally active on larger timescales than those of cross-shore sediment transport (except for sea-level variability) (Miller and Dean, 2004). In coastal areas dominated by gradients in longshore sediment transport, shoreline prediction has received significant attention and resulting models have demonstrated reasonable prediction skill. The attempts to predict shoreline changes due to cross-shore sediment transport have been less successful (Davidson and Turner, 2009). The present study will focus on cross-shore sediment transport.

Currently, linear extrapolation of hindcast variables is an often used approach to predict coastline changes of wave dominated systems, where erosion/accretion is dominated by cross-shore processes. However, linear extrapolation is a non-physical modelling approach as it does not account for the actual processes that govern shoreline change, resulting in large uncertainties in coastline prediction (Davidson and Turner, 2009).

Empirical models can be used to predict shoreline change dominated by cross-shore morphological processes. Here, an empirical model called ShoreFor (Shoreline Forecast) will be used. ShoreFor is an equilibrium model which accounts for antecedent- and present forcing conditions to predict shoreline change, as the present morphodynamic state and shoreline position are dependent on past forcing (Davidson et al., 2013). The antecedent forcing conditions are modelled using a weighted average of the antecedent dimensionless fall velocity. This parameter is modelled using a single memory decay factor, which is found through a best-fit analysis by comparison to data. The memory decay factor is an indicator of the dominant timescale of shoreline response. If this parameter is large (>>100 days) the seasonal timescale is dominant and if it is small (<100 days) the smaller (storm) timescale is dominant in determining coastline evolution. The first one is typical for dissipative beaches whereas the latter is typical for intermediate beaches (Splinter et al., 2014).

The single memory decay factor does not yield a problem if a coastal system is dominated by a single timescale. However, if multiple timescales play an equally important role in determining shoreline evolution, model skill deteriorates. An example of such a system is the Nha Trang coastline (Vietnam), where the monsoon- (small timescale) and seasonal variation (large timescale) both play an important role in coastline evolution (Almar et al., 2017). Figure 3 presents the shoreline position time-series at Nha Trang. The seasonal- (red oval) and monsoon (green oval) timescale can easily be identified.

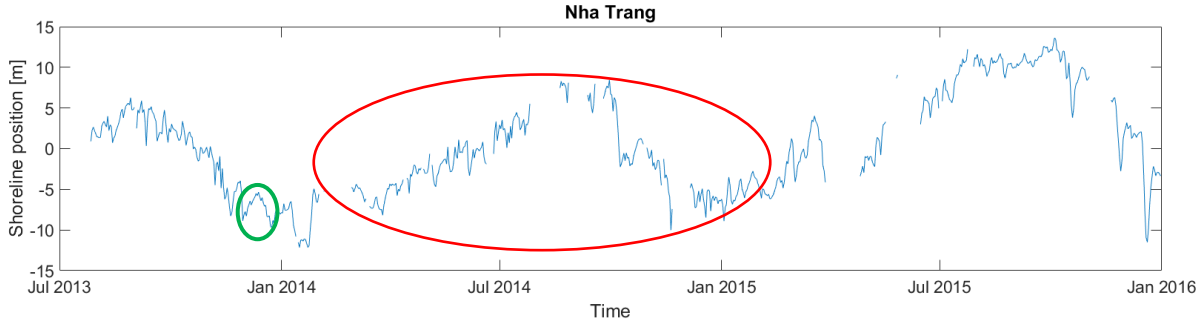

Figure 3: Shoreline position time-series at Nha Trang

1.1 Research questions

Until now, ShoreFor employs a single memory decay factor such that only the most dominant timescale is well represented in shoreline predictions. In case multiple timescales are equally important, but only one predominant timescale is utilized, the model's predictive skill is significantly hampered. To investigate how multiple distinct beach response timescales can be implemented in shoreline predictions using ShoreFor, the following research questions are formulated:

Main question

How are hydrodynamic forcings on multiple timescales (storm – inter-annual) influencing cross-shore shoreline response?

Sub-questions

- What is the relative importance of wave-forcing properties on shoreline response?
- Does the concept of memory decay provide opportunities to describe multiple different forcing timescales (different frequencies) and their effect on shoreline response?
- Can shoreline response be represented by a linear combination using multiple distinct forcing timescales?

1.2 Approach

The approach is divided into five different phases to find a step-by-step solution to the main research question. The phases are: a literature study (background), site descriptions, the methodology for improving ShoreFor, the results using the improved model and the discussion/conclusion of the results.

First, background information is presented about relevant spatiotemporal scales that influence shoreline change. Furthermore, different approaches will be presented to model shoreline evolution at wave dominated beaches. Subsequently, the effects of forcing properties on shoreline location are assessed. Moreover, the past development towards the ShoreFor model is highlighted.

ShoreFor will be improved using three different datasets: at Narrabeen (Australia), Nha Trang (Vietnam) and Grand Popo (Benin). The hydro- and morphodynamic characteristics at these sites are highlighted. Narrabeen counts as a benchmark due to two reasons: firstly, the ShoreFor model is developed using the dataset at Narrabeen which enables for a one-to-one comparison of changes made and secondly, the beach at Narrabeen is well surveyed with multiple sources of hydro- and morphodynamic data available. The datasets at Nha Trang and Grand Popo are of particular interest considering that the morphological evolution is dictated by multiple distinct timescales.

A component analysis is carried out for each site to distinguish between timescales and to find the dominant temporal scales within the hydrodynamic forcing- and beach response time-series. This component analysis requires a filter function which is able to cope with data-gaps. For this reason, a filter function is developed. To validate this filter function, a comparison with the Fourier transform is executed. Moreover, temporal spectra of the hydrodynamic forcing and beach response (constructed with the developed filter function) will be investigated. Thereafter, the model is improved using a combination of a linear superposition-, an upscaling- and downscaling approach, by which all timescales are related to each other. The model improvement will be elaborated using the Nha Trang dataset only, because it is subjected to clear distinct timescales.

After improvement both models are applied to the datasets, where for the improved model multiple distinct timescales are incorporated. For each dataset, two calibration-cases are considered: a calibration on a part of the dataset and a calibration on the whole dataset. Those calibration-cases will be compared to each other on the basis of a grid of interactions between timescales. These grids will reveal the dominant shoreline response timescales.

The discussion section will focus on interpreting the results and model drawbacks are assessed. Thereafter, answers to the main- and sub-questions will be presented in the conclusions section and finally, multiple recommendations are presented for further investigation of model improvement.

2 Background

In the previous chapter, the (equilibrium) model ShoreFor was briefly introduced. This model can accurately predict shoreline change on one dominant timescale only. Before an approach is presented to implement multiple dominant timescales in the model, general background information about modelling shoreline change is considered first (section 2.1). Here, the relevant spatiotemporal will be touched as well as various approaches for modelling shoreline change. Thereafter, the effects of forcing properties on beach response are treated and explained from an equilibrium-model point of view. The effect of the forcing's intensity, duration and sequencing is discussed. Subsequently, ShoreFor's model development is explained. The basis of this model is based on the work of Wright and Short (1985), but the model itself is developed by Davidson et al. (2013).

2.1 Modelling shoreline change

Relevant spatiotemporal scales

Morphological change can be examined at many spatial and temporal scales. These scales range from instantaneous movement of single grains on a timescale of local turbulence to seasonal and long-term movement of large sand bodies such as longshore bars and tidal deltas (Larson and Kraus, 1995). Figure 4 presents such morphological change acting on different timescales. In this idealized time-series two temporal scales can be distinguished: an annual timescale and a timescale of the order of days. As beaches respond differently to different forcing timescales (Almar et al., 2017), each of these forcing timescales can play a distinct role on the evolution of the coast.

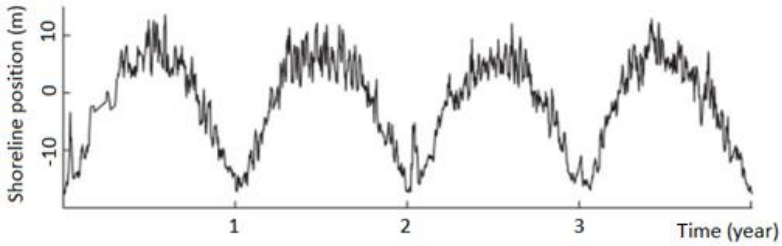

Figure 4: Idealized shoreline position time-series (Milne, Sharma, Flay, & Bickerton, 2013)

Fortunately, space- and timescales are related (Figure 5): larger length scales of certain coastal processes correspond to larger timescales. A timescale is generally interpreted as the period of time required for characteristic hydro- or morphological developments. Due to the relation between temporal- and spatial scales the problem can be simplified, because only a subset of relevant scales is considered. The engineering timescale is probably the most relevant one, as it refers to the range of shoreline changes expected to impact a "structure" during its lifetime. This range generally encompasses everything from storm-induced changes with timescales of the order of hours, up to long-term changes with decadal timescales (Miller and Dean, 2004).

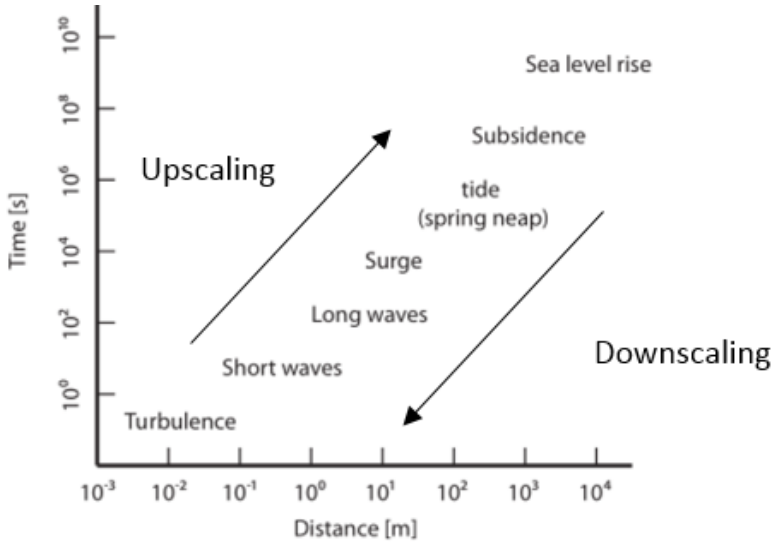

Figure 5: Timescale versus spatial scale for various coastal processes (based on Larson and Kraus, 1995)

Up- and downscaling

Downscaling is a procedure to get information of smaller timescales using larger timescales or in other words, utilize long term processes and interpret them on shorter timescales. For upscaling the opposite is true: information of larger scale processes is based on processes with smaller scales.

However, limitations to this up- and downscaling approach are present. For example, it is not possible to yield accurate information about sea level rise based on the turbulence scale. Or the other way around, one cannot interpret turbulence effects based on sea level rise. Larson and Kraus (1995) investigated these limitations and they classified four different scales, with respect to sediment transport and proposed to what extent these scales can be related. The four different scales are (in ascending order): micro, meso, macro and mega. In Figure 6 this concept is presented.

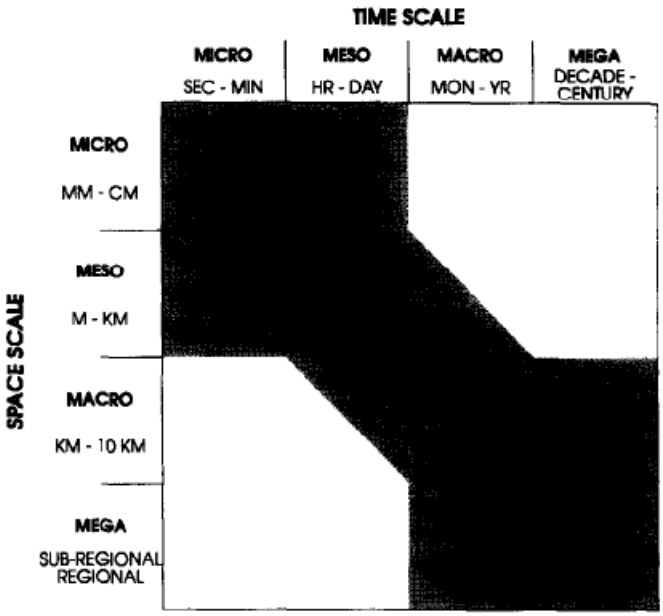

Figure 6: Compatible temporal- and spatial scales for sediment transport and beach morphology (Larson and Kraus, 1995)

Currently no universal theory is present which can be applied to problems with various temporal- and spatial scales. A lot of different theories are available, but each of them has assumptions and limitations which gives models a certain applicability range. Due to these assumptions and limitations, the morphology change at a larger scale is not equal to an integration in time or space of the smaller scale. According to Larson and Kraus (1995), the black areas are the feasible scales to be related to each other and the white areas not. Considering the arguments above, it is for example not realistic to describe sediment transport on a mega scale based on a micro scale.

Types of models

Mainly two modelling approaches can be distinguished for coastal processes on different scales: process-based models and empirical models. The choice for a particular model depends for example on the spatial- and timescales of the processes to be modelled, the purpose of the model and the phase the research is in.

Process-based models

Process-based models are physics-based and employ the mass- and momentum conservation of fluid and sediment to solve physical processes that are important for coastline evolution. Examples of these models are Xbeach and Delft3D. These models can solve a system in three dimensions, but simplifications can be made to simulate the reality in two dimensions. However, the complicated 3D coastal processes hamper a long-term prediction of shoreline change. At the present stage of research, accurate predictions of profile development to derive beach levels and widths is not yet achievable for process-based models on a seasonal time scale (van Rijn et al., 2003). Therefore, empirical models are an important tool to simulate shoreline change on large spatiotemporal scales.

Process-based models utilize the upscaling approach visualized in Figure 5. Note that the feasible relations between the scales (according to Larson and Kraus (1995)) are continuously moving, which means that the transition of the black-white area in Figure 6 is dynamic.

Empirical models

Empirical models often use an equilibrium concept to predict shoreline change. These models state that if the forcing on a beach is constant in time, the beach will reach in an equilibrium with the forcing conditions. Once the equilibrium is reached, the beach width is static and does not change anymore.

Empirical models need a large dataset for calibration purposes. Therefore site-specific calibration is necessary, but this data is not always available. Because of this calibration, only coastal processes observed on the location where the data came from are accounted for. Moreover, empirical models do not explicitly account for all individual processes that force shoreline change, but seeks an overall behaviour pattern as response to the different processes. But the simplicity and computational efficiency make sure that these models are often used.

Another type of empirical models are data-driven models. An example is historical shoreline analyses in which observed shoreline behaviour is used to predict the rate of shoreline change. Data-driven models only account for site-specific processes and a significant amount of data is needed to predict future shoreline developments.

Figure 7 summarizes the available shoreline prediction models, distinguished by their applicability range. Note that this is merely an overview of the models considered in this section. Hence, it does not cover the full spectrum of available models.

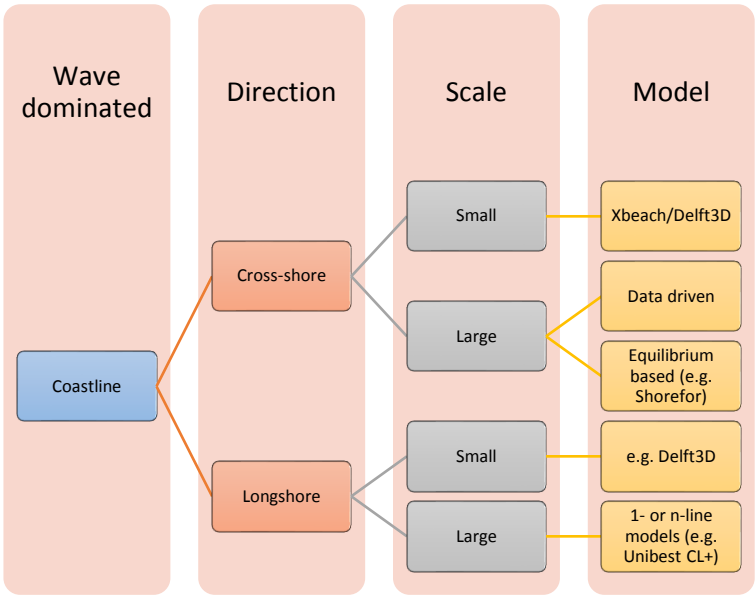

Figure 7: Shoreline prediction model applicability at wave dominated coastlines

The wave-dominated coastline can be divided into two directions: the cross-shore direction and the longshore direction. They can be further divided into two scales: small- and large spatiotemporal scales (since they are related (Figure 5)). Shoreline predictions at wave dominated coastlines in cross-shore direction at small scales, can be modelled with Xbeach or Delft3D. These models are process-based and complicated 3D processes are resolved. Longer term simulations with process-based models is not recommended since they are sensitive to uncertainties in boundary conditions (Splinter et al., 2014). Moreover, assumptions for the small spatiotemporal scales hamper good prediction skill on larger scales. However, Delft3D (and similar models) can be used for shoreline simulations at wave dominated coastlines in longshore direction at small spatiotemporal scales. For the same reasons as in the cross-shore direction, this model cannot be used for simulations at large scales.

For large scales in longshore direction, 1- or n-line models can be used (e.g. Unibest CL+). These models assume that the cross-shore shape is constant and gradients in longshore transport result in a cross-shore translation of the profile. However, these models cannot be used in the longshore direction for small scales, because cross-shore processes dominate here (Splinter et al., 2014). Data-driven or equilibrium based models are suitable for shoreline prediction on a large scale in cross-shore direction.

2.2 Effects of forcing properties on beach response

Beaches erode during storm conditions and accrete after the storm during milder conditions. In addition to this simple storm-recovery cycle, duration, intensity, sequencing and seasonality of forcing events can also play a role. In this section, an elaboration is presented about these parameters from an equilibrium-model point of view: an overall behaviour pattern is sought as response to the different processes.

Forcing intensity

It is well known that a higher forcing intensity (e.g. a higher wave height) will result in erosion of the coastline if that coastline was in equilibrium with the antecedent forcing conditions. Whether accretion or erosion occurs, can be explained by the following formulas implicating the dimensionless fall velocity and the disequilibrium of the dimensionless fall velocity:

$$\Omega = \frac{H_s}{w_s * T_p} \quad (5)$$

$$\Delta\Omega = \Omega_{eq} - \Omega \quad (6)$$

Where H_s is the significant wave height, T_p the peak wave period, w_s the settling velocity, Ω the dimensionless fall velocity, Ω_{eq} the equilibrium dimensionless fall velocity and $\Delta\Omega$ the disequilibrium of the dimensionless fall velocity. A negative disequilibrium will result in erosion of the coastline and a positive disequilibrium will result in accretion.

Figure 8 presents two situations of one beach, forced with different wave heights H_1 and H_2 ($H_2=2*H_1$). If the two situations in Figure 8 have the same sand characteristics and the regular waves have the same wave period, the dimensionless fall velocity is only dependent on the wave height. Hence, different wave heights are expressed with different dimensionless fall velocity values: the first situation (left panel in Figure 8) has a smaller dimensionless fall velocity than the second situation (right panel in Figure 8).

If the shoreline of the first situation (left panel in Figure 8) was in equilibrium with the antecedent waves, this situation determines the equilibrium dimensionless fall velocity value (Ω_{eq}). If the same beach is now forced with waves of wave heights H_2, a disequilibrium is formed according to formula 6. This disequilibrium can be used to explain shoreline change and in this case, erosion can be expected ($\Omega_{eq} < \Omega$). A higher difference in dimensionless fall velocity (a higher disequilibrium), yields a larger coastline change.

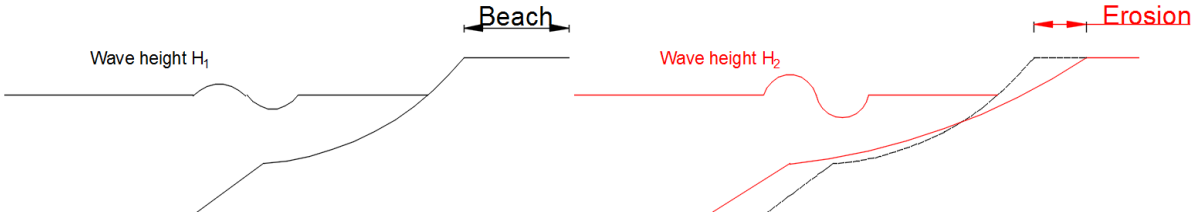

Figure 8: A coastline in equilibrium with waves of wave height H_1 (left). The same coastline will erode to get in equilibrium with waves of wave height H_2, where $H_2>H_1$ (right).

Furthermore, applying this concept indicates that the milder past high-intensity conditions are not able to bring sediment onshore at the same rate, because during the short high-intensity conditions the disequilibrium is larger. This corresponds well with the observed behavior of coastal systems. Note that this is only valid if the duration of the high-intensity conditions is short, otherwise the disequilibria values are the same.

Forcing duration

The effect of forcing duration on coastline change is also quite clear: a larger duration means more available time for the beach to achieve an equilibrium with the forcing conditions. After a certain time, the full erosion/accretion potential is achieved and an equilibrium is reached. Moreover, if higher-intensity conditions are stationary over time and the beach was in equilibrium with the preceding milder conditions, the beach response is approximately exponential in time (Kriebel and Dean, 1993).

Kriebel and Dean (1993) showed that the response timescale to reach an equilibrium with the high-intensity conditions, strongly depends on the breaking wave height and the sediment grain size. They found that larger waves have larger response timescales due to the fact that during larger wave conditions the surf zone is wider and sediment has to be moved further offshore.

Kriebel and Dean (1993) showed using a convolution theory, the role of the forcing duration on beach response (Figure 9). The Beta value expresses the ratio of the erosion timescale to the forcing timescale. If this parameter is large, the forcing duration is relatively short and if Beta is smaller, the forcing duration is larger. Figure 9 shows that during longer forcing durations (Beta = 0.76) the maximum erosion potential ($R(t)/R_\infty$=1) is almost achieved, while this is certainly not the case for the short forcing duration (Beta = 10.6).

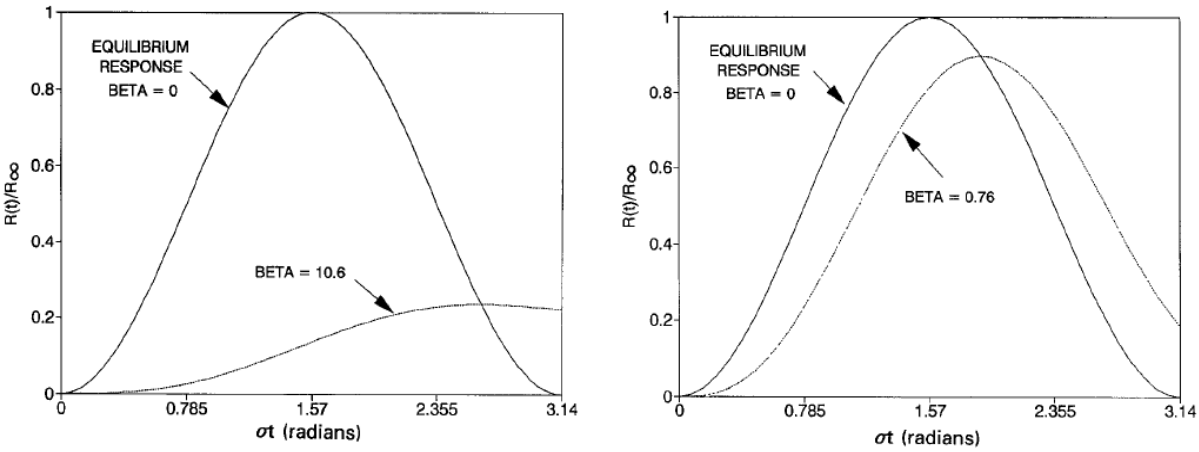

Figure 9: Beach response to forcing events with a different timescale. A larger lasting forcing event (small Beta value, right panel) almost reaches the maximum erosion potential, while this is not the case for the small duration forcing event (left panel) (Kriebel and Dean, 1993).

In Figure 10, the response amplitude of the beach (left) is presented as a function of this same parameter Beta. The declining line indicates that a smaller forcing duration (larger Beta), yields a smaller relative erosion potential ($R(t)/R_\infty$), thus a smaller shoreline change. The inclining line (right) indicates that beach response lags behind the forcing, because the system needs time to respond. A smaller forcing duration (larger Beta) results in a larger relative phase lag between the forcing and shoreline response.

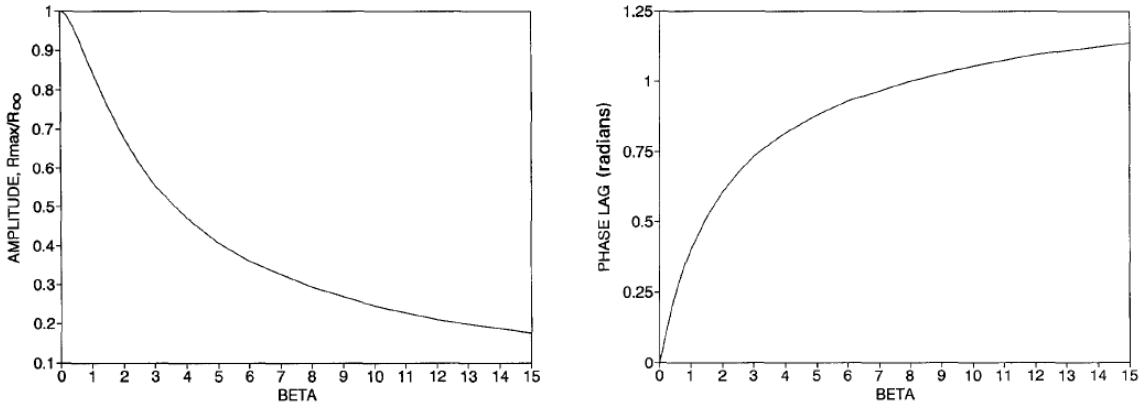

Figure 10: Relative beach response amplitude (left) and phase lag between forcing and beach response (right), due to forcing events with a different timescale (Kriebel and Dean, 1993).

Forcing sequencing

A sequence of high-intensity forcing events is defined as events who successively approach the coastline in a short time interval (order of days –weeks). A short time interval is subsequently defined as when the time between high-intensity forcing events is shorter than the beach recovery time (Coco & Ciavola, 2017).

Lee et al. (1998) showed that a sequence of high-intensity forcing events can act as a single event which has a much higher energy level (higher intensity and duration) and a higher return period. However, opposed to the results of Lee et al. (1998), the analysis of Coco et al. (2014) resulted with the conclusion that sequencing did not result in enhanced erosion. They argued that this could be, because the largest high-intensity forcing event appeared first in the sequence, which was verified by Southgate (1995) who showed that chronology of sequencing also plays a role.

The initial state of the beach is one of the important factors to determine how a beach responses to a sequence of high-intensity forcing events. For example, without a dissipative breaker bar large erosion can be expected, because large quantities of energy reach the shoreline. Subsequently, this energy is then available to erode the beach. The eroded beach volume will then be used to form a dissipative bar, such that the beach approaches an equilibrium with the current forcing. This process makes the subsequent high-intensity forcing events within the cluster less effective in eroding the coastline. If the initial beach system already has a breaker-bar, the following high-intensity forcing events are less effective in eroding the coastline.

Initial beach state and recovery time are not the only factors in determining coastline erosion due to a sequence of high-intensity forcing events. The chronology of the sequencing is also of importance. Yates et al. (2009) showed that two different forcing time-series of wave energy, but with the same average wave energy, resulted in coastline erosion for the first case and an accreted coastline for the second case. They argued that this was due to the different time-series chronology. For the erosive case a period of small waves was followed by a period of larger waves, such that the coastline was in a more accretive state before the high-intensity forcing event. The subsequent larger waves were not dissipated effectively which resulted in large beach erosion. For the accretive case the opposite is true. If one applies this to a sequence of high-intensity forcing events, the beach response to the second event of the cluster is dependent on the beach response to the first event. If the results above are aggregated: the subsequent high-intensity forcing events in a cluster become more ineffective in eroding the coastline, because the coastline is more in equilibrium with the high-intensity conditions.

Another important factor that can play a role in beach response to a sequence of high-intensity forcing events is the water level. For example, if two high-intensity forcing events both approach the shoreline during spring tide conditions, the coast will erode more than when the events coincide with neap tide conditions. With neap tide conditions the waves break further offshore such that less energy is available to erode the coastline.

In addition, the beach recovery period can also be of importance in beach response to a sequence of high-intensity forcing events. The beach recovery can be extremely fast, but also very slow (e.g. when the foredunes are eroded) (Coco and Ciavola, 2017). It is not easy to predict the beach recovery period as it depends on several factors like: the hydrodynamic forcing (relative to the antecedent (high-intensity) conditions) like waves and tides, beach geomorphology, geologic properties, availability of sand, modal beach state and the sand transfer with the foredunes. All these factors hamper a precise prediction of the beach recovery period.

Summarizing, Coco and Ciavola (2017) present several reasons why the erosional response to clusters of high-intensity forcing conditions is generally larger than the sum of the erosional response of each individual high-intensity forcing event that make up the cluster:

1. The equilibrium response of the beach depends on antecedent morphological conditions.
2. The beach may not have been adequately recovered between high-intensity forcing events within clusters.
3. The profile, although recovered, might not have been compacted between high-intensity forcing events.
4. The configuration of offshore sandbars may not be the same during high-intensity forcing events, such that the protective shield might be different.
5. The tidal conditions may be different between high-intensity forcing events that comprise the cluster.

Seasonality of forcing

Recent analyses of the Gold Coast dataset in Australia by Splinter et al. (2017), showed that the beach switched from a seasonally-dominated coastline (before 2005) to a storm-dominated coastline (after 2005) and an erosive trend emerged. This was associated with a seasonality change in high-intensity forcing events. Before 2005, the high-intensity forcing events were dominantly occurring at the start of the year, whereas after 2005 the events occurred throughout the whole year.

Modelling beach response to high-intensity forcing events and sequences of high-intensity forcing events can be carried out using an equilibrium based model. Using such an equilibrium based approach requires a large dataset in which several high-intensity forcing events and sequences of events are included. Moreover, high-frequency data has to be available, because otherwise storms are averaged out.

2.3 ShoreFor's model development

Wright & Short

Wright and Short (1985) came up with six beach states which are related to the width of the beach. Here, only the two extremes are mentioned: the dissipative beach state and the reflective beach state. The dissipative beach state is characterized by fine sandy material, a small beach width and an associated storm wave climate with high energy short waves. Reflective beaches are often found in swell- and monsoon wave climates with low steepness waves and are characterized by sandy coarse material and a large beach width.

Wright and Short (1985) showed that the antecedent forcing conditions have a strong relationship with the present beach state, while the immediate value of the dimensionless fall velocity (Ω, current forcing) has a weak relationship. This is mainly because beaches need time to respond to the associated forcing.

The above implicates that antecedent forcing conditions are of importance when one would like to predict shoreline change. To account for this effect for modelling the shoreline position, the weighted mean of the dimensionless fall velocity is introduced:

$$\Omega_{eq}(t) = \frac{\sum_{i=0}^{2\phi} \Omega_i 10^{-\frac{i}{\phi}}}{\sum_{i=0}^{2\phi} 10^{-\frac{i}{\phi}}} \tag{7}$$

Where $i=1$ on the day before observation, $i=2\varphi$ on 2φ days prior to the day of observation and Ω is the dimensionless fall velocity. The weighting factor decreases to 10% at φ days prior to the observation date. The value of φ depends on the 'memory decay' of the system. If the memory decay is large, the larger timescales are more important for the evolution of the coast (seasonal timescale) and if this parameter is small the smaller timescales are more important (storms timescale) (Splinter et al., 2014).

The morphology of a beach at a certain time is besides the immediate- and antecedent wave conditions also dependent on the sediment characteristics, tide- and wind conditions and the initial beach state. As these conditions change over time, the beach position also changes over time. The range of this variability defines the mobility of a beach.

The time required for the beach and surf zone to evolve from one equilibrium state to another, will be inversely proportional to the available energy. It requires less time to reach a dissipative state than reaching a reflective beach state, because the energy associated with dissipative states is higher so the rate of change is also higher. It is possible that when a high energy storm erodes the beach, the beach state can rapidly switch from a reflective beach to a dissipative beach.

Furthermore, the rate of change is also dependent on the difference between the equilibrium beach state of the current forcing and the initial beach state. The larger the difference, the larger the rate of change. Whether accretion or erosion of the beach occurs, depends if the beach state becomes more dissipative (erosion) or more reflective (accretion). This concept is illustrated in Figure 11.

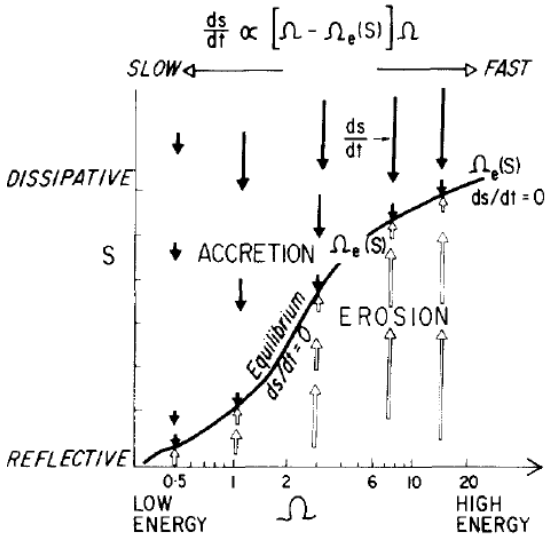

Figure 11: Relationship between morphodynamic equilibrium, relative energy and relative rates of erosion or accretion (Wright and Short, 1985)

Wright and Short (1985) came up with the following model that is based on information described above:

$$\frac{\Delta s}{\Delta t} = b + c\left[\left(\Omega - \Omega_{eq}\right)\Omega^2\right] \tag{8}$$

In which Ω is the instantaneous dimensionless fall velocity, Ω_{eq} the equilibrium value for the state which prevails at the instant in question, $\left(\Omega - \Omega_{\mathrm{eq}}\right)\Omega^2$ the disequilibrium stress, b & c model free parameters and $\Delta s/\Delta t$ the rate of beach state change. This is in line with Figure 11, where a larger disequilibrium $(\Omega-\Omega_{eq})$ yields a larger rate of change of beach state. Furthermore, a larger energy level (Ω^2) also results in a larger rate of change. Moreover, the disequilibrium term $(\Omega-\Omega_{eq})$ will also determine if erosion or accretion occurs. If the waves are milder than the equilibrium ($\Omega<\Omega_{eq}$) accretion will occur and if the waves are steeper ($\Omega_{eq}<\Omega$) erosion can be expected.

ShoreFor

Davidson et al. (2010) developed a one-dimensional equilibrium model for predicting shoreline change, based on their previous two-dimensional model and the work of Wright and Short (1985). The one-dimensional model became simpler and more efficient. The starting point was to develop a model for longshore uniform coasts, such that any longshore gradients in sediment transport are not present.

The developed model (Davidson et al., 2010) is as follows:

$$\frac{dx(t)}{dt} = b + c\left(\Omega_0 - \Omega(t)\right)\Omega^k(t) \tag{9}$$

Wherein x is the cross-shore distance, t the time , b the linear rate of net shoreline progradation or retreat (linear trend), c the optimized response time coefficient, Ω_0 the equilibrium dimensionless fall velocity and Ω the instantaneous dimensionless fall velocity. The parameter k permits a non-linear shoreline response to wave forcing. Note that $(\Omega_0-\Omega)$ is the disequilibrium according to Wright and Short (1985). Moreover, b and c are model free parameters and are determined by calibration of the dataset (by a least-squares method).

Table 2 presents which data is used for calibration, validation and forecasting.

Data	Calibration	Validation	Forecasting
Synthetic wave climate			X
Measured wave climate	X	X	
Shoreline observations	X		

Table 2: Used data per model phase

The model presented above is able to forecast shoreline position changes with reasonable skill, on sites where the seasonal shoreline signal is strong. This is mainly due to the structure of the model: after a Monte Carlo analysis using a synthetic wave climate, the storm responses are averaged out by an averaging procedure and only the seasonal variation remains. Moreover, the forecast converges to a linear trend if the seasonal variability is absent.

Important limitations of the model:

- If a longshore sediment transport gradient is present on a particular site, the model only allows for a linear trend which will remain constant over time.
- Large datasets are needed to calibrate and validate the model (>= 2.5 years)
- In an ideal case, very long time-series of the wave climate should be used to capture storms with large return periods. If these are captured well by the model, it enhances prediction skill for extreme events.
- The effect of tides are not implemented in the model. Davidson and Turner (2009), showed that inclusion of tides can improve the prediction of shoreline change, even in a micro-tidal environment. Tides effectively distribute the impact of a storm over a broader intertidal region, with the effect that increased tidal range generally reduces the response of the shoreline contour.

The model of Davidson et al. (2010), neglected antecedent forcing conditions to forecast shoreline change. However, this dependency on antecedent forcing conditions was already shown by Wright and Short (1985). Moreover, Davidson et al. (2013) showed that at two contrasting sites (Narrabeen and Gold Coast, Australia) the model performance was totally different. The magnitude of the modelled shoreline variability was greatly under-estimated at Narrabeen and the direction of shoreline change was sometimes opposite to the one observed. By inclusion of the antecedent forcing conditions, the model should be able to better predict shoreline change.

The renewed ShoreFor model (Davidson et al., 2013) is given by:

$$\frac{dx}{dt} = b + c^{\mp} P^{0.5} \left(\Omega_{eq}(t) - \Omega(t) \right) \tag{10}$$

In which x is the cross-shore distance, b the linear rate of net shoreline progradation or retreat, Ω_{eq} the time-varying equilibrium dimensionless fall velocity, Ω the instantaneous dimensionless fall velocity, P the incident wave power which represents the flux of wave energy towards the nearshore zone and c a constant separated into two components (c^+ & c^-), where c^+ is the accretion component (when $\Omega<\Omega_{eq}$) and c^- is the erosional component ($\Omega>\Omega_{eq}$). By separating c, the model recognizes that erosion and accretion are governed by different processes (Yates et al., 2009).

The wave power is used instead of the dimensionless fall velocity for the magnitude of the shoreline response, because it better agrees with the observations that shoreline response is dominantly proportional to the available incident deep-water wave power. Yates et al. (2009) showed that an appropriate exponent for the wave height is approximately one, such that the exponent of the wave power becomes 0.5 ($P \sim H_0^2 T$).

A two-step least-squares scheme can be applied, in which the first step isolates shoreline trends caused by long-term gradients in wave forcing. The second step isolates shoreline trends caused by other processes such as a gradient in longshore sediment transport, which are then assigned to parameter *b*.

By implementing a dynamic equilibrium condition, a negative feedback mechanism is implicitly introduced in the model. By including this condition, less extreme shoreline change is modelled when for example the high energy antecedent conditions have already eroded the beach in the past, such that a second storm affects the instantaneous shoreline change less than when the antecedent conditions are not accounted for (Davidson et al., 2013). This corresponds well with beach response observations.

Important limitations of the model:

- Model prediction skills are high for sites where the cross-shore sediment exchange is for the larger part responsible for coastline change.
- The effects of structures and complex sources and sinks of sediment are not accounted for in the present model. Only processes that can be captured by a linear trend in shoreline change, are accounted for by the model. Moreover, a combination of such processes is captured by one parameter, such that a distinct response due to these different processes cannot be visualized.
- As the model is in the early stages of development, there is not much model experience and it has to be proved that the model is of a generic nature. Currently, ShoreFor is most suitable for application in micro-/meso-tidal, energetic, exposed sandy beaches where cross-shore transport processes dominate changes of shoreline position (Davidson et al., 2013).
- The model does not account for short-scale processes, such as alongshore variable bar welding and beach cusp formation. To limit these short scale effects shoreline data can be alongshore averaged.
- Changes in shoreline position of sheltered coastlines or those that experience large tidal variations, are also influenced by changes in mean water level and are expected not to be predicted well by the model. The exclusion of changes in mean water level limits the model predictive skill to El Nino-Southern Oscillation (ENSO) and sea level rise, because these alter the mean water level.

Splinter et al. (2014), made some changes to the ShoreFor model. By the approach they used, the rate of shoreline change is defined as follows:

$$\frac{dx}{dt} = c * (F(\varphi)^{+} + r * F(\varphi)^{-}) + b \tag{11}$$

Wherein *dx/dt* is the rate of shoreline change, *t* the time, *c* the response rate parameter, *b* a linear trend term which is independent of wave forcing and accounts, for example, for shoreline change due to gradients in longshore sediment transport and *F* the forcing term divided into an accretionary (F^{+}) and erosional (F^{-}) component. The erosional forcing term is multiplied by an erosion ratio (*r*), because accretionary- and erosional shoreline responses are governed by different processes. The erosion ratio can be calculated as follows:

$$r = \left| \frac{\sum_{i=0}^{N} \{F_i^{+}\}}{\sum_{i=0}^{N} \{F_i^{-}\}} \right| \tag{12}$$

The erosion ratio is not a model free parameter. It is determined based on the balance between accretion- and erosion forcing in such a way that a long-term equilibrium is maintained. Moreover, it takes care that a zero trend in wave forcing results in a zero trend in shoreline evolution due to cross-shore transport processes. In the calculation of the erosion ratio (formula 12), || indicates the absolute value, {} indicates an operation that removes the linear trend but preserves the record mean and *N* is the total record length. The forcing term, for both the accretionary- and erosional component is determined by:

$$F = P_b^{0.5} \frac{\Delta\Omega}{\sigma_{\Delta\Omega}} \tag{13}$$

In which P_b is the breaking wave energy flux, $\Delta\Omega$ the disequilibrium and $\sigma_{\Delta\Omega}$ the standard deviation of the disequilibrium. The disequilibrium term is divided by the standard deviation of the disequilibrium to make sure that the rate of shoreline change is largely dependent on the breaking wave energy flux (P_b) and response rate parameter (*c*). The disequilibrium itself determines the sign of shoreline change (erosion or accretion). A negative disequilibrium causes erosion and a positive disequilibrium causes accretion. Moreover, the sign of the disequilibrium term is used to divide the forcing term in F^{+} and F^{-}. The breaking wave energy flux can be calculated by:

$$P_b = E_b * C_g \tag{14}$$

$$E_b = \frac{1}{16} * \rho * g * H_{s,b}^2 \tag{14a}$$

$$C_g = \sqrt{g * h_b} \tag{14b}$$

$$h_b = \frac{H_{s,b}}{\gamma} \tag{14c}$$

Wherein the breaking wave energy flux (P_b) is dependent on the significant wave energy at breaking (E_b) and the shallow water group velocity (C_g). The wave energy (E_b) is dependent on the significant wave height at breaking ($H_{s,b}$). The group velocity (C_g) is dependent on the depth at breaking (h_b). The depth at breaking is dependent on the significant wave height at breaking ($H_{s,b}$) and the breaking parameter (γ). The breaking parameter is assumed to be 0.78. The disequilibrium- and sub-terms are given by:

$$\Delta\Omega = \Omega_{\mathrm{eq}} - \Omega \tag{15}$$

$$\Omega_{eq} = \frac{\sum_{i=1}^{2\varphi} \Omega_i 10^{-\frac{i}{\varphi}}}{\sum_{i=1}^{2\varphi} 10^{-\frac{i}{\varphi}}} \quad (15a)$$

$$\Omega = \frac{\mathrm{H_S}}{T_p * w_s} \quad (15b)$$

Where $\Delta\Omega$ is the disequilibrium of dimensionless fall velocity, Ω the instantaneous dimensionless fall velocity and Ω_{eq} the dynamic equilibrium term. Last mentioned is following Wright and Short (1985) and is determined by formula 15a, in which *i* is the number of days in the wave forcing time-series prior to the day of observation, 2φ are the total days that are accounted for in the dynamic equilibrium and φ is the memory decay factor. The weighting of Ω reaches 10% and 1% of the instantaneous value at φ and 2φ prior to the day of observation. Formula 15b indicates that the dimensionless fall velocity is dependent on the significant wave height (H_s), the peak period (T_p) as well as on the sediment fall velocity (w_s).

The memory decay factor (φ) indicates the dominant temporal scale of shoreline response. If this parameter is significantly larger than 100 days, the modelled shoreline response is predominantly seasonal (large temporal scale) and if a small memory decay factor is found (smaller than 100 days), the storm (small temporal scale) shoreline response is dominant. The latter is typical for intermediate beaches while the first is typical for dissipative beaches (Splinter et al., 2014).

The other wave driven model free parameter *c*, represents the efficiency with which waves induce cross-shore sediment transport and is highly dependent on $\bar{\Omega}$, the temporal mean of the dimensionless fall velocity. A negative correlation between the two parameters is observed: if $\bar{\Omega}$ increases, the response factor *c* decreases. Two possible explanations can be derived: At high $\bar{\Omega}$ values, the beach is dissipative with a small gradient and a sand bar. High waves break early on the offshore sand bar causing a wide surf zone. Due to the wide surf zone a lot of energy is already dissipated before it reaches the beach, causing less available energy to move sand and subsequently cause shoreline change. The opposite is true for beaches with a low $\bar{\Omega}$ value. Another possible explanation is that beaches with a low $\bar{\Omega}$ value are typically associated with more complex surf zone morphology, which can induce circulation that moves sediment onshore more efficiently (Splinter et al., 2014).

2.4 Conclusions

Two approaches to model cross-shore sediment transport on a wave-dominated beach can be used: process-based models and equilibrium models. In this research, an equilibrium based model is used. These models state that if the forcing on a beach remains constant in time, the beach will reach equilibrium. Once the equilibrium is reached the beach is static and does not change anymore. These equilibrium models use the downscaling approach: information of smaller timescales is obtained using larger timescales.

A higher ongoing forcing intensity results in increased coastline erosion, if that coastline was in equilibrium with the antecedent milder forcing conditions. Beaches need time to respond towards an equilibrium with ongoing forcing conditions: a higher duration results in more available time for the beach to reach an equilibrium, hence larger shoreline changes. The effect of sequencing of wave conditions is still subject to ongoing research. However, in this study it was found that the erosional response to clusters of high-intensity forcing conditions is generally larger than the sum of the erosional response of each individual high-intensity forcing event that make up the cluster.

The equilibrium based shoreline prediction model ShoreFor is based on Wright and Short (1985), but the model itself is introduced by Davidson (2013). The final model is adapted by Splinter et al. (2014). ShoreFor utilizes the concept of wave-driven equilibrium shoreline response, where a change in wave steepness is the predominant driving factor of shoreline change via on- and offshore transport. The model uses two calibration parameters: the memory decay factor (φ) and the response value (c). The memory decay factor determines the dominant timescale of shoreline response and the response value indicates the efficiency with which waves induce cross-shore sediment transport.

3 Site descriptions

This chapter introduces the hydrodynamic- and morphological characteristics of the three available datasets at Nha Trang (Vietnam), Narrabeen (Australia) and Grand Popo (Benin). These high resolution datasets are utilized, because at all sites multiple dominant beach response timescales are present. In this way, model results can be obtained using a broad spectrum of sandy beaches on three different continents. All three datasets are based on video-derived shoreline positions.

3.1 Nha Trang

Variable	Value
Spring tidal range	<1.6 m (semi-diurnal/diurnal, microtidal)
Grain size: D_{50}	0.4 mm
Settling velocity: w_s	0.0482 m/s
Time span data	27-07-2013/31-12-2015
Data-gap percentage in shoreline time-series	20%
Video system	Unknown (2MP)

Table 3: Summary of the site description at Nha Trang

The Nha Trang beach is situated in Vietnam (Figure 12) and is north-south orientated. In front of the southern part an island-group is present which influences the wave climate. The video system is installed on a location which is considered far enough from the influence of the edges of the bay and beach dynamics are dominated by cross-shore processes (Almar et al., 2017).

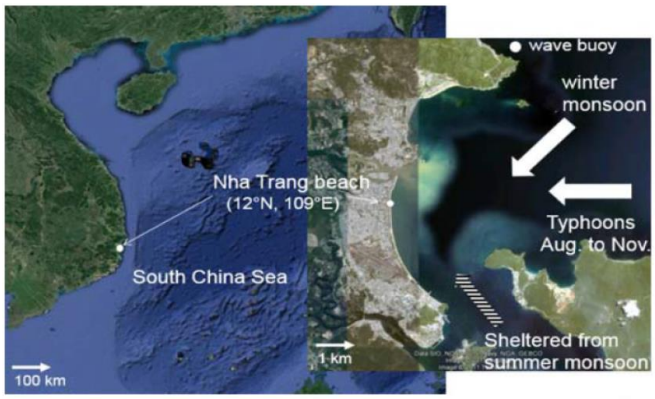

Figure 12: Overview of the location and wave climate at Nha Trang (Almar et al., 2017)

Beach states range from low-tide terrace (LTT) to reflective. The Nha Trang beach is an example of a tropical beach, which are often exposed to short but heavy storms such as typhoons. They can adapt very fast to these storm conditions and can slowly recover under milder conditions during the rest of the year. However, monsoons with a larger temporal scale and relatively high energy are forcing events that can play a role on coastline evolution as well.

The wave climate is influenced by typhoons that mainly occur between August and December. On average the Nha Trang beach is exposed to 4-6 typhoons every year. Additionally, the wave climate is influenced by summer- (wind waves) and winter monsoons (swell waves). However, due to Tre Island, the beach is partly sheltered from summer monsoons that originate in the SE. The beach is heavily affected by winter monsoons, which can generate waves up to 4.0 m.

In Figure 13, wave power- and shoreline position time-series are presented. Note that the dominant seasonal cycle is present in both the shoreline position- and wave power time-series.

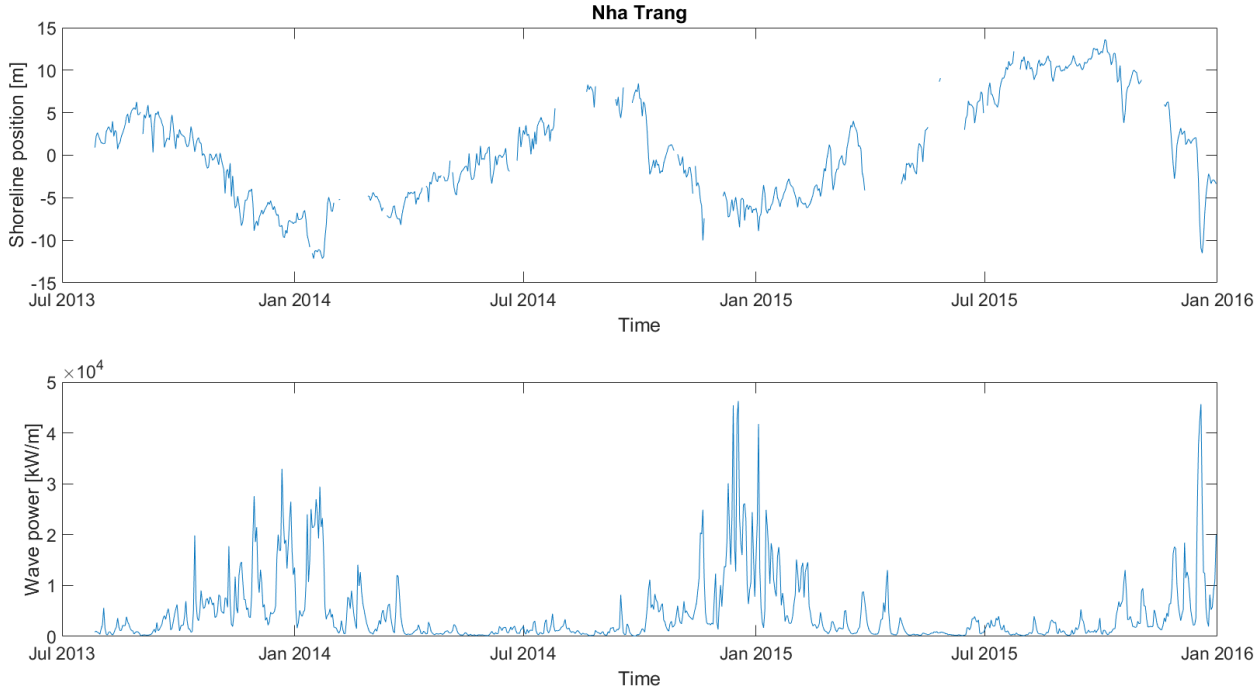

Figure 13: Shoreline position- (top) and wave power (bottom) time-series at Nha Trang

3.2 Narrabeen

Variable	Value
Spring tidal range	<2.0 m (semi-diurnal, microtidal)
Grain size: D_{50}	0.4 mm
Settling velocity: w_s	0.0508 m/s
Time span data	01-08-2004/31-12-2010
Data-gap percentage in shoreline time-series	0%
Video system	Argus

Table 4: Summary of the site description at Narrabeen

The Narrabeen-Collaroy beach is situated near Sydney in the east of Australia. The borders of the beach compartment consist of two headlands. The Narrabeen beach is situated in the north of the compartment and the Collaroy beach is situated in the south (Figure 14). Long term datasets (40 years) are available at the cross-sections indicated with yellow in Figure 14. However, these datasets have a too low (weekly) resolution for the current research. In 2004, an ARGUS system is installed (Figure 14) of which high temporal resolution shoreline position data can be extracted. Three datasets are available: at s = 2200 m, s = 2600 m and s = 3200 m. In this report, data at s = 2200 m is used, because this site is closest to the compartment's center to make sure that the influence of the headlands is minimal.

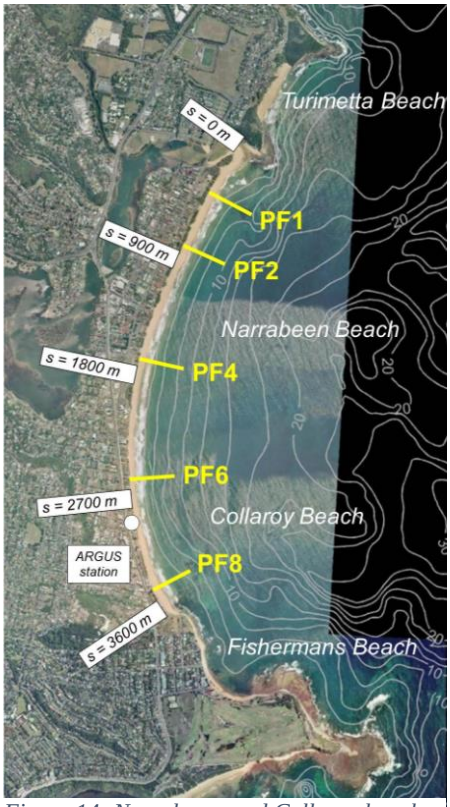

Figure 14: Narrabeen- and Collaroy beach (Narrabeen-Collaroy beach survey program)

Sediment transport is dominated by cross-shore processes (Davidson et al., 2017) and all the beach states (Wright and Short, 1985) can be observed (Davidson et al., 2013).

The deep-water wave climate is dominated by swells from the SSE (mean H_s = 1.6 m and mean T_p = 10 s) that originate from mid-latitude cyclones and reach the beach compartment 5 to 9 times a month. Additionally, the deep-water wave climate exists out of larger waves (H_s = 3 m) that originate from storm events and hit the coastline in any direction. On top of this climate, a small seasonal cycle is present with on average higher waves in the Australian winter- and milder waves in the Australian summer months. On larger timescales, effects of the less energetic ENSO can play a role as well.

In Figure 15, wave power- and shoreline position time-series are presented. Significant storm activity can be observed during the Australian winter months of 2007 (La Niña year), which resulted in a rapid shoreline recession of almost 40 m.

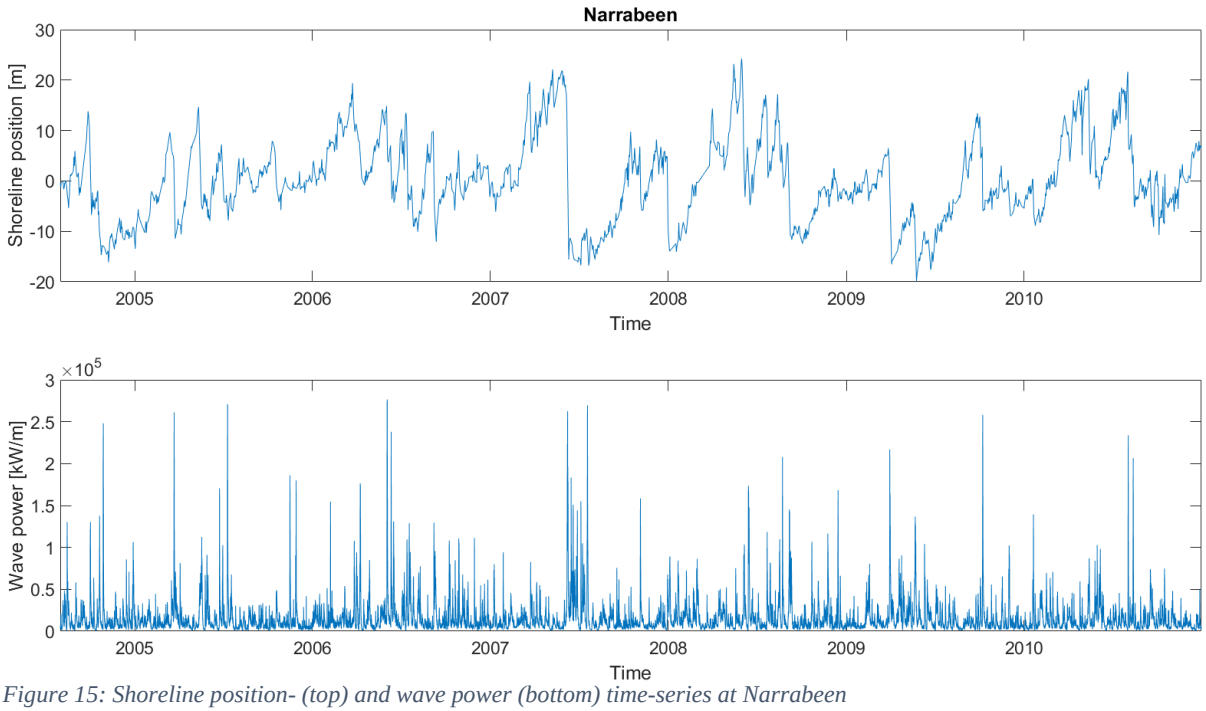

Figure 15: Shoreline position- (top) and wave power (bottom) time-series at Narrabeen

3.3 Grand Popo

Variable	Value
Spring tidal range	<1.8 m (semi-diurnal, microtidal)
Grain size: D_{50}	0.6 mm
Settling velocity: w_s	0.0754 m/s
Time span data	20-02-2013/22-08-2016
Data-gap percentage in shoreline time-series	40%
Video system	VIVOTEK (2MP)

Table 5: Summary of the site description at Grand Popo

The video camera system in Benin is situated near Grand Popo in the Gulf of Guinea (Figure 16). It is an open-ocean, sandy stretch of coast which is situated far from any anthropogenic influences. The nearest (updrift) one is a field of groynes, constructed twenty years ago. The dataset is constructed with images from a VIVOTEK (2MP) system. Note that the amount of data-gaps in the shoreline time-series is quite large (40%).

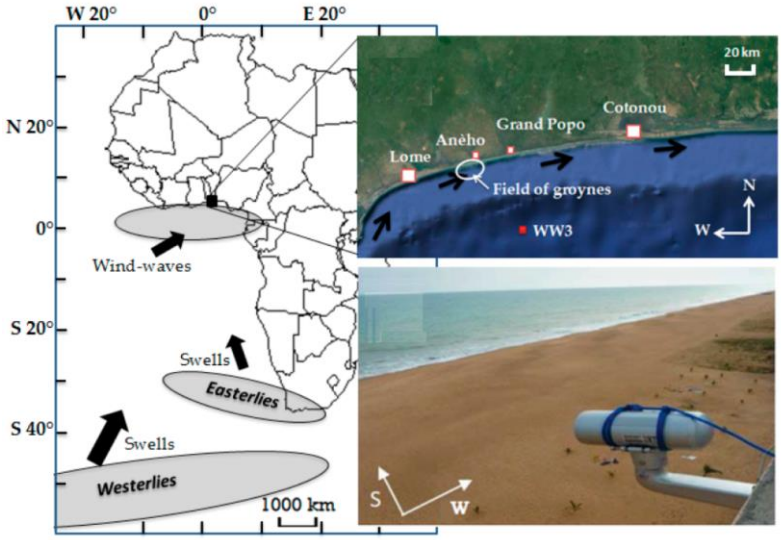

Figure 16: Overview of the location and wave climate at Grand Popo (Ondoa et al., 2017)

The cross-shore beach dynamics are dominated by oblique wind waves from the SSW (Ondoa et al., 2017). Additionally, a major longshore sediment transport (400 000 – 1 000 000 m^3/year) is present, due to oblique incident swell waves. Beach states range from LTT to reflective.

The wave climate consists of wind-waves from the SSW and swells from both the SSW and SSE (Figure 16). The wind-waves have a mean significant wave height of H_s = 1.36 m, a mean peak period of T_p = 9.4 s and originate in the Gulf of Guinea. The swell waves originate from the southern hemisphere at high latitudes.

In Figure 17, wave power- and shoreline position time-series are presented. Note the large quantity of data-gaps in the shoreline position time-series. The shoreline position is dictated by a clear erosive trend, possibly due to gradients in longshore sediment transport. Furthermore, storm- and seasonal fluctuations are present in both time-series.

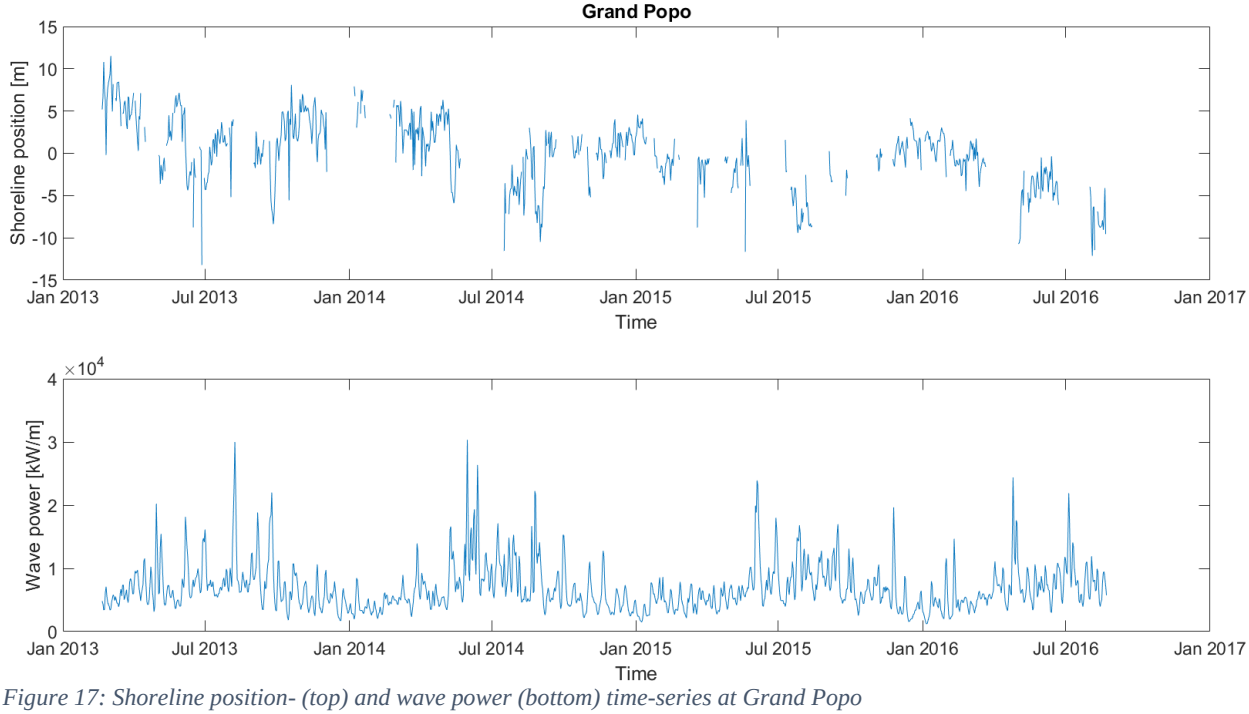

Figure 17: Shoreline position- (top) and wave power (bottom) time-series at Grand Popo

4 Methodology

This chapter introduces the approach for implementing multiple timescales in ShoreFor. The starting point is to check which timescales are present in the wave- and shoreline position signals. For this a filter function is necessary. As multiple filter functions can be used, a comparison between two filter functions is carried out. Thereafter, temporal spectra are presented which indicate the most dominant timescales in the dataset. Subsequently, an approach is presented to implement these multiple dominant timescales in the ShoreFor model. The implementation consists of three distinct steps, which relate multiple timescales to each other. Note that the methodology is elaborated for the dataset at Nha Trang, because clear and distinct dominant timescales are present here.

4.1 Distinguishing temporal scales

In this section, a filter function is presented which is able to distinguish temporal scales and can cope with data-gaps. Moreover, the filter function will be compared with a Fourier transform. Additionally, temporal spectra of hydro- and morphodynamic time-series will be presented.

Comparing filter functions

To investigate which timescales are dominant in the wave- and shoreline position signals and to distinguish between temporal scales, a filter function is developed that is able to cope with data-gaps. The developed filter function utilizes a running average. The elaboration of the developed filter function itself is included in appendix B. If no data-gaps are present, a fast Fourier transform (FFT) filter can determine the most dominant timescales. The FFT filter utilizes sinusoidal waves to reconstruct raw signals.

To check the functionality and (dis)advantages of the developed filter function, a comparison is carried out between the FFT-spectrum and the temporal spectrum calculated with the developed filter function. Both are applied to the wave height- and wave period signal. The result of the two different approaches is presented in Figure 18.

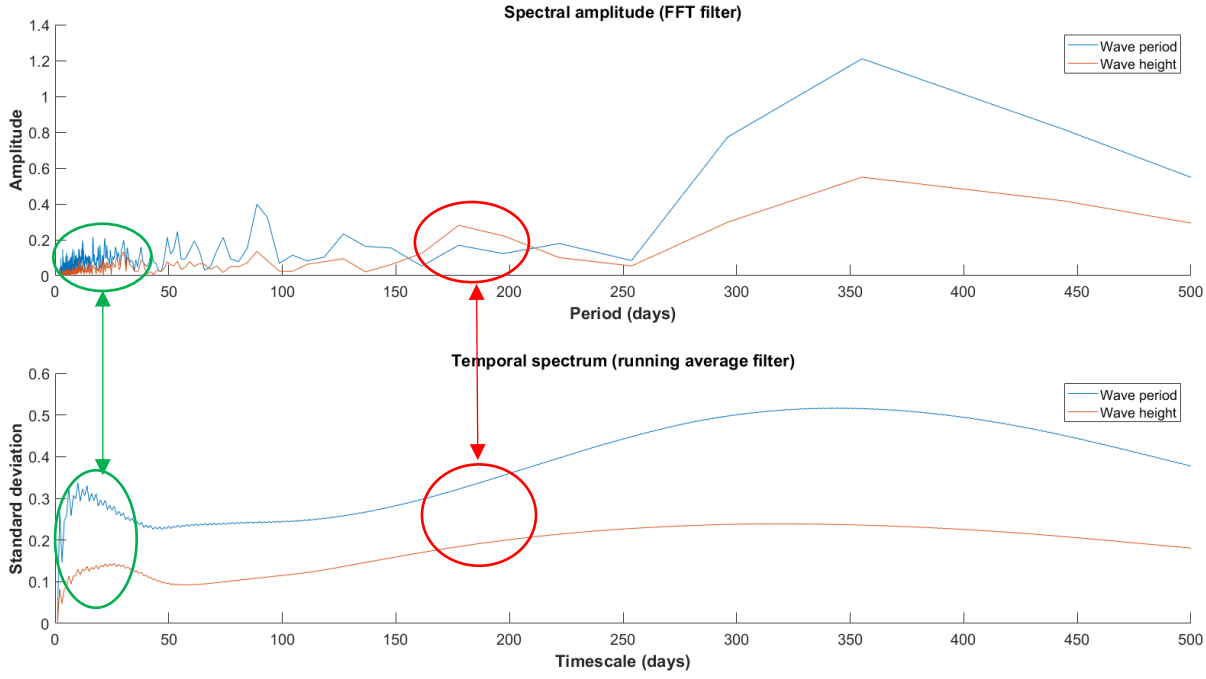

Figure 18: Timescale spectrum generated with the FFT filter (top) and temporal spectrum generated with the running average filter (bottom), applied to the wave period- and wave height time-series at Nha Trang

Figure 18 implies that the resolution for larger timescales is higher when the FFT filter is applied to the time-series. For example, when the FFT filter is applied to the wave height data, it reveals a secondary peak for a timescale of ≈180 days (red ovals). The running average filter only recognizes the timescale with the largest variability: the seasonal timescale (365 days). However, for the smallest timescales (1 to 30 days) the result of the FFT filter is not satisfying, because it does not suggest a dominant timescale at these scales. A dominant timescale is expected in this range due to the observed monsoons at Nha Trang. The temporal spectrum of the running average filter clearly indicates a dominant timescales at ≈20-30 days (green ovals). Additionally, an advantage of the developed filter function is that it can cope with data-gaps.

Both approaches can distinguish- and can indicate dominant timescales, but it is not known beforehand which spectrum gives the right representation. Therefore, the raw wave height signal is partly reconstructed using filtered signals of both approaches, to check which filter function is most suitable to apply.

In Figure 19, three filtered signals are used (each having a distinct temporal scale) from both spectra to reconstruct part of the raw wave height signal. In this case, timescales of 30 days, 182 days and 367 days are used. These timescales correspond to three peaks in the FFT-spectrum (orange line in top panel of Figure 18). Note that the overall resolution of the FFT- and the running average filter is identical: both use 888 distinct filtered signals to decompose the raw wave height signal. Wherein 888 days is the duration (in days) of the raw wave height signal.

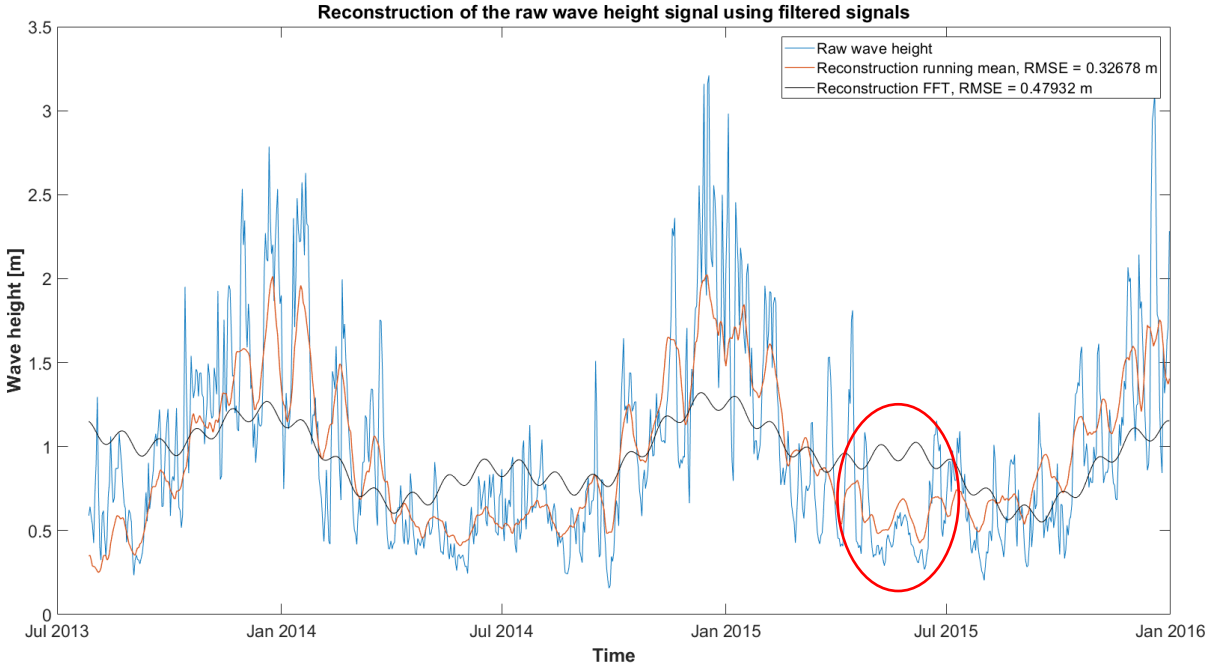

Figure 19: Reconstruction of the raw wave height signal (blue) using filtered time-series generated with the FFT-filter (black) and the running average filter (orange)

Figure 19 indicates that the reconstruction using signals determined with the running average filter is more suitable to apply. The main difference arises from the fact that the filtering approaches are different. The FFT filter decomposes the raw signal into sinusoidal waves with different periods, phases and amplitudes, while the developed filter function utilizes a running mean. Using the FFT filter, it is possible that one particular sinusoidal wave yields a suitable fit to most data, but it can occur that the sinusoidal wave and wave height data are out of phase: not all physical processes can be described by sinusoidal waves with a constant period. For example, in June 2015 (red oval) the reconstructed signal using the FFT filter is out of phase with the wave height data. The reconstructed signal requires more sinusoidal waves with different periods to get a better fit to the data. The other filter does not show such a phenomenon, because it is based on a running mean. For the reasons described above, the filter function based on the running average is used for model improvement.

Dominant timescales

Using the filter function based on the running average, temporal spectra of the shoreline position-, wave height, wave period and wave power time-series can be determined. These spectra indicate the most dominant timescales per signal. The wave power spectrum is included, because changes in shoreline position are best related to changes in wave power (Davidson et al., 2013).

In Figure 20, the temporal spectra at Nha Trang are presented.

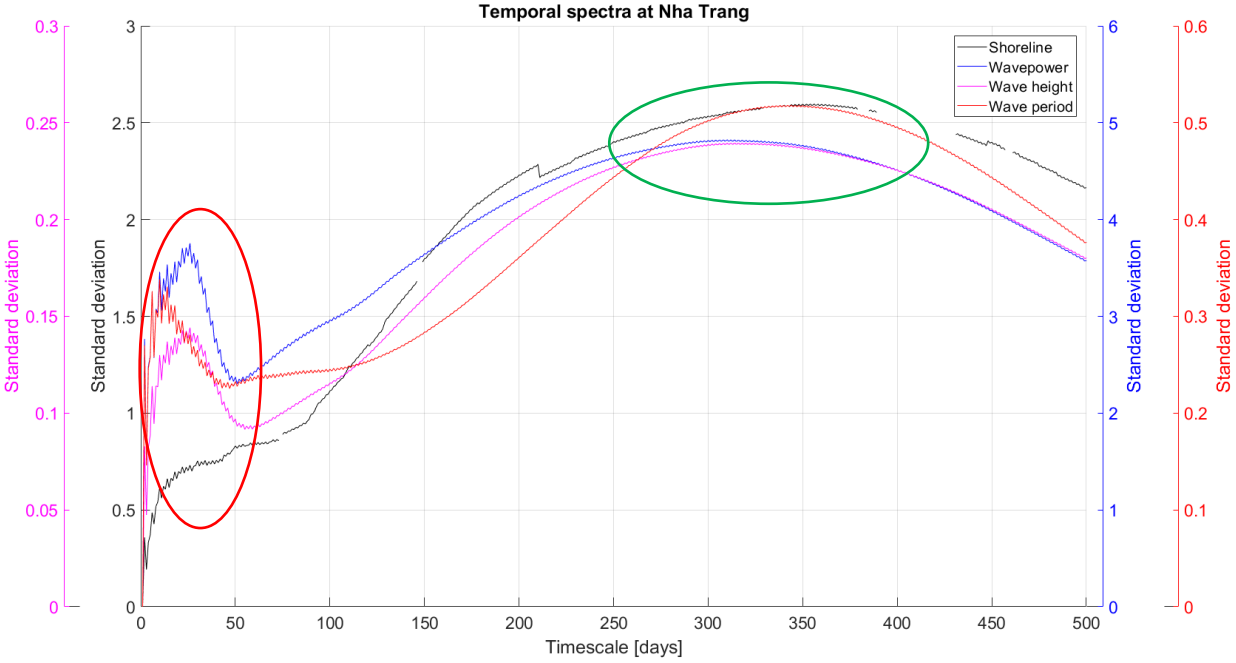

Figure 20: Temporal spectra of the shoreline position, wave height, wave period and wave power at Nha Trang

Figure 20 indicates that two identical dominant temporal scales in the shoreline- and wave power spectrum are present. This can imply that shoreline changes with a certain temporal scale, are driven by waves with a corresponding timescale. The smallest temporal mode corresponds to monsoons with a timescale of ≈20-30 days (red oval) and the largest mode resembles the seasonal variability with a yearly timescale (green oval). Note that only timescales from 1 to 500 days are shown, because they are the most dominant. Furthermore, the discontinuities in the shoreline spectrum are caused by the presence of data-gaps in the shoreline signal.

Table 6 presents an overview of dominant timescales found in the temporal spectra. The temporal spectra at Narrabeen and Grand Popo are included in appendix C.

Dominant timescales in shoreline position	**1st timescale**	**2nd timescale**	**3rd timescale**
Nha Trang	365 days	30 days	
Narrabeen	220 days	60 days	
Grand Popo	365 days	50 days	<7 days
Dominant timescales in wave power			
Nha Trang	365 days	20 days	
Narrabeen	<7 days	60 days	
Grand Popo	365 days	20 days	

Table 6: Overview of dominant timescales in shoreline position- and wave power time-series

Filtered time-series

Figure 21 presents examples of filtered wave height- and shoreline position time-series. Each filtered signal has a distinct timescale. All left panels correspond to shoreline position time-series and all right panels to wave-height time-series. The top panels present the raw signals and the four bottom panels the filtered signals.

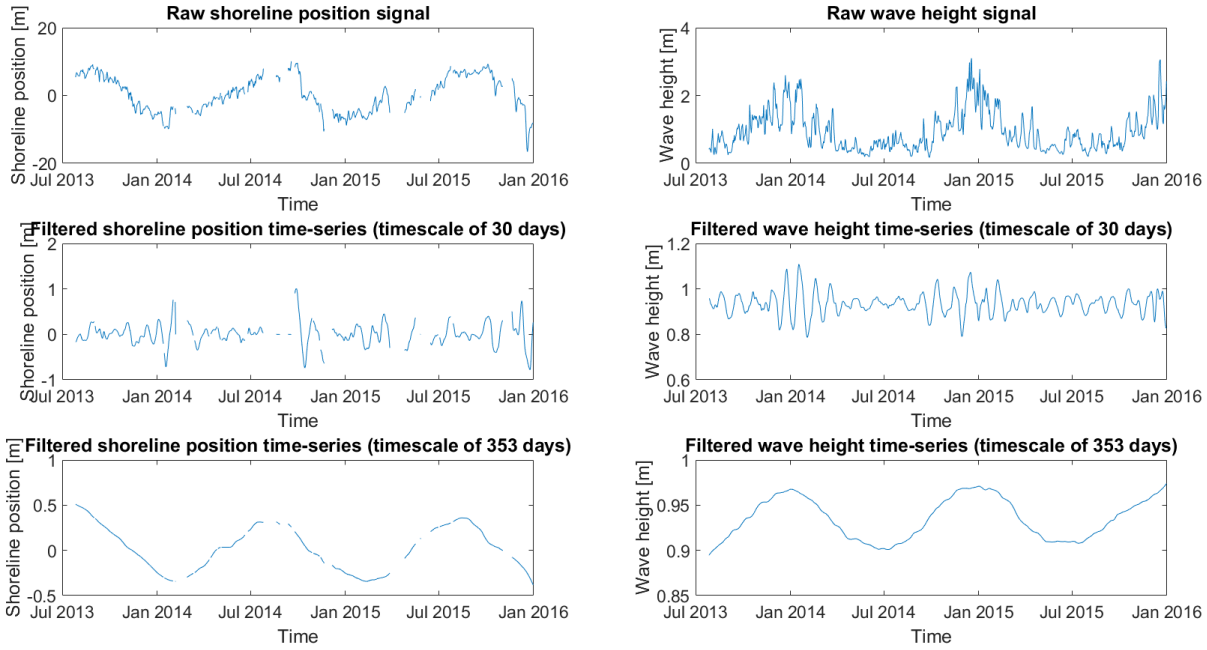

Figure 21: The raw shoreline position signal (top left) and the raw wave height signal (top right). The two lower left panels are two filtered shoreline position time-series with distinct timescales and the two lower right panels are two filtered wave height time-series.

Figure 21 presents only two filtered signals with distinct timescales, found in the raw time-series at Nha Trang. To investigate the effects of multiple timescales in wave forcing on shoreline change, more temporal scales are filtered from the raw wave- and shoreline position signals. The filtered signals in Figure 21 are determined using the temporal spectrum, where parts of the filtered signals in this spectrum are added up (details are described in appendix B). Such a summation of filtered signals will be referred to as a timescale bin.

4.2 Implementing multiple timescales

In the previous section, dominant timescales were identified and an approach was found to filter them out of the raw shoreline- and forcing time-series. In this section, these filtered wave- and shoreline signals are related to each other on multiple temporal scales, using ShoreFor as the benchmark for shoreline prediction. To relate the filtered signals to each other, three new modelling steps are proposed: 1) a linear superposition approach, 2) an upscaling approach and 3) a downscaling approach.

Modelling approach

Figure 22 visualizes the modelling approach by using a synthetic wave- and shoreline spectrum with a certain bin distribution (three bins are used). The shoreline- and wave spectrum have the same bin distribution, such that corresponding timescales can be related to each other.

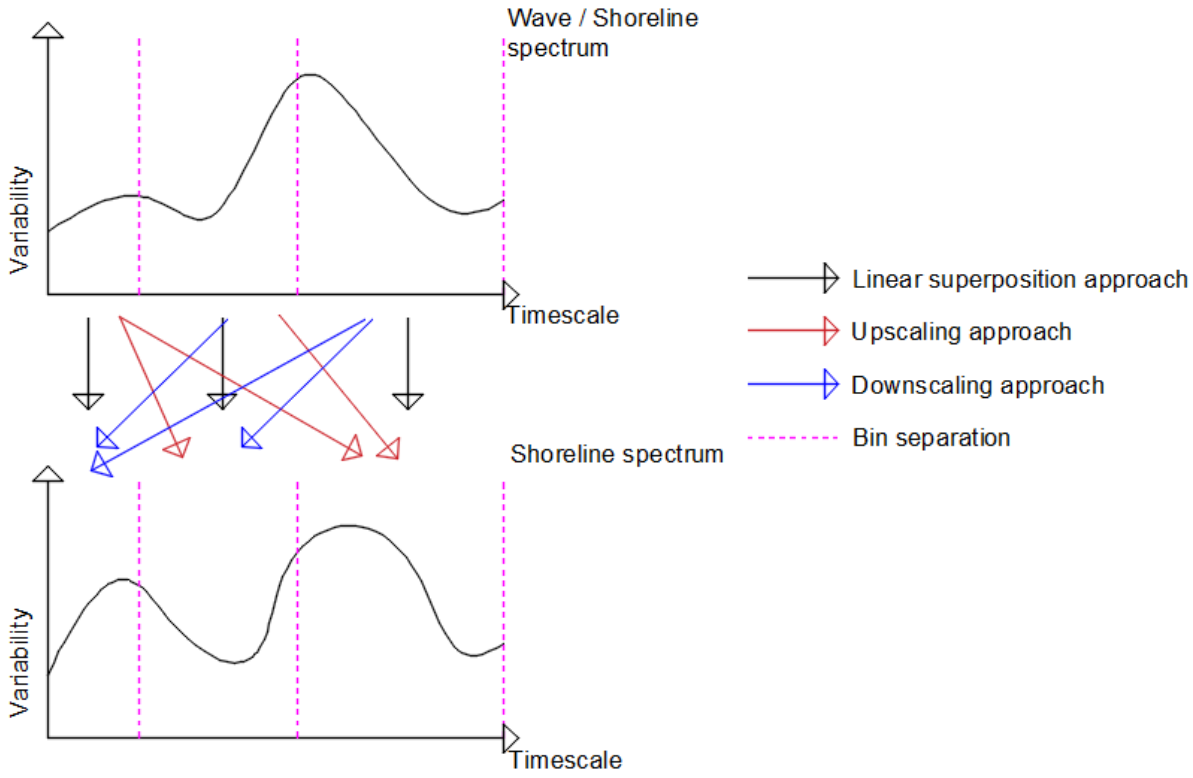

Figure 22: Overview of the new modelling approach

The top spectrum in Figure 22 indicates the wave spectrum when the linear superposition- and upscaling approach are considered, because for these modelling steps waves are directly related to shoreline response. The vertical black arrows indicate that temporal scales in wave forcing are related to corresponding temporal scales in shoreline response, when the linear superposition approach is applied. The red arrows indicate that small temporal scales in wave forcing are related to larger temporal scales in shoreline response, when the upscaling approach is applied. For the downscaling approach, both spectra in Figure 22 represent the shoreline spectrum and the blue arrows indicate that large temporal scales in shoreline variation are related to smaller temporal scales in shoreline response.

Model improvement steps

Before the actual model improvement steps are considered, the following actions were necessary in order to make the data ready to use:

- The bin distribution is based upon an equal amount of shoreline response variation within each bin. Otherwise, ShoreFor's output parameters such as the response rate factor (*c*), are affected by the subjective bin distribution. For the Nha Trang dataset this resulted in 36 bins. Note that this is the maximum amount of bins, such that a significant amount of timescales can be related to each other.
- Raw shoreline- and wave signals are detrended to exclude timescales, which are larger than the length of the dataset. In this way, these large timescales cannot interfere with the smaller timescales. Due to this assumption, the linear trend term in ShoreFor is set to zero.
- All wave- and shoreline data is interpolated, such that all time-series have a temporal resolution of one day. ShoreFor's input consists of shoreline position, wave height and wave period time-series.

As stated above, the total raw wave- and shoreline signals are detrended to get rid of the linear trend term (*b*). However, it is possible that during calibration on a part of the dataset, the model identifies timescales larger than the calibration period as a trend. A forcing imbalance causing a wrong erosion ratio (*r*) and a falsely modelled trend during model validation (black line in Figure 23). To solve the error, all signals used during model validation will be detrended (red line in Figure 23). This results in a better fit to the data.

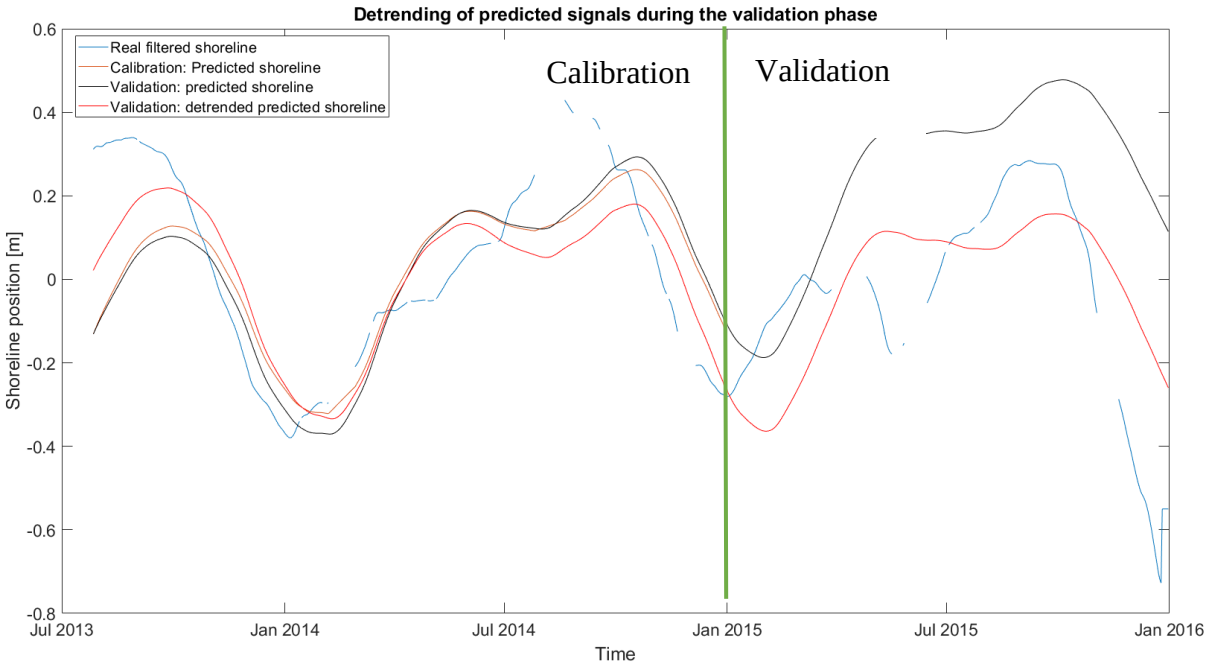

Figure 23: Calibrating the model on a part of the dataset (orange line) can give a clear trend during model validation (black line). Detrending the predicted shoreline signal during model validation solves this error (red line).

Linear superposition approach

The linear superposition approach relates all timescales in wave data (the wave height (H_s) and wave period (T_p)) to corresponding shoreline response timescales. This can be written down as follows:

$$\frac{dx_i}{dt} = c * (F(\varphi)_i^+ + r * F(\varphi)_i^-) \quad (16)$$

In which x is the shoreline position, t the time, c the response factor which indicates the efficiency with which waves induce cross-shore sediment transport, φ the memory decay factor, F the forcing term which is divided into an accretionary- and erosional component and r the erosion ratio which controls trends in data. The subscript i indicates for both the forcing and rate of shoreline change, that corresponding timescales are linked to each other. Using 36 bins for the Nha Trang dataset, the subscript i attains values from 1 to 36. Note that ShoreFor is not adapted (except for the linear trend term), but a linear superposition is carried out using multiple signals with distinct timescales. In Figure 24, ShoreFor's output parameters are presented for each timescale bin, when calibrated on a part of the dataset.

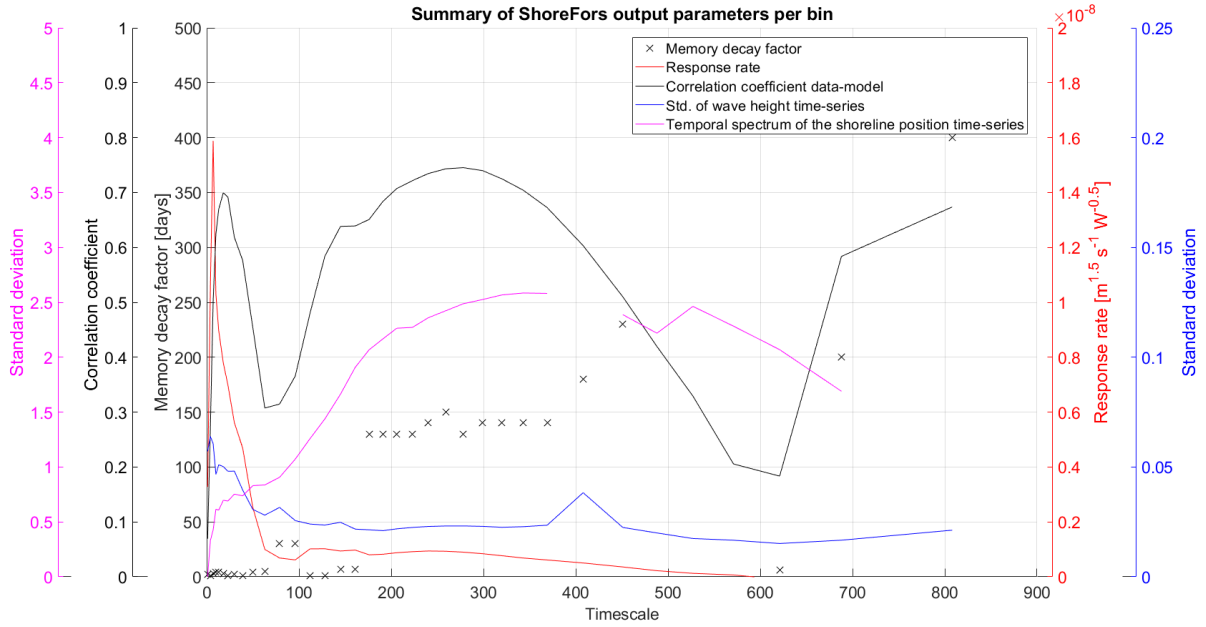

Figure 24: Summary of ShoreFor's output parameters per bin, using the linear superposition approach

As the related timescales become smaller, the response factor (red line in Figure 24) and the amount of variation in the wave height bins (blue line) become larger. The relative increase in response rate is larger than the relative increase in wave height variability. This can have two possible reasons: first is that a higher wave height variability induces a higher efficiency with which waves induce cross-shore sediment transport. Secondly, as the timescales become smaller, multiple waves with different wave heights approach the shoreline in a short period of time. The shoreline is not able to reach an equilibrium and is continuously adapting to changing wave conditions, which results in a higher response value as well. A prerequisite is that the correlation between the data and model results is high enough (black line in Figure 24).

Splinter et al. (2014) found a negative correlation between the memory decay factor (φ) and response factor (c). However, this relationship was based on multiple distinct datasets and not on multiple timescales within a single dataset. Figure 24 suggests that this relationship is also valid for different timescales within the same dataset. This means that small timescale forcing events (e.g. storms), induce sediment transport with a high efficiency causing rapid shoreline change. The beach response to forcing events with a larger timescale is slower and less efficient, as the beach needs more time to respond.

Finally, Figure 24 suggests a relation between the correlation coefficient (correlation between model results and data, black line), the decay factor (black crosses) and the shoreline's timescale distribution (pink line). For timescales from 176 days to 369 days, the decay factor is approximately constant. This is due to the fact that within these bins, the seasonal timescale is dominant. For smaller timescales (1 – 63 days), the decay factor is smaller and in the order of days. The corresponding correlation is highest for ≈20-30 days. This is plausible, because it represents the shoreline response to monsoons. In between these temporal scales, less dominant timescales are present and the decay factor is less dependent on factors named above.

Upscaling approach

Upscaling incorporates the effect of small timescales in wave data on larger timescales in shoreline response and is modelled by using the envelope of filtered wave signals. The envelope creates the timescale-link between the filtered wave height signal and the filtered shoreline signal, where the latter has a larger timescale.

This concept is illustrated in Figure 25: the small timescale raw synthetic wave height time-series are presented in the top panel (blue) as well as multiple envelopes of this signal. Each envelope has a different timescale. In the bottom panel of Figure 25, the raw shoreline position is presented (blue line). This is the total beach response (blue line bottom panel) to the imposed forcing (blue line top panel). From t=400 to t=499, small waves cause shoreline accretion as well as from t=501 to t =600. At t=500 the high intensity forcing event causes major shoreline recession. The total response has a timescale that is larger than the timescale of the forcing. The resulting filtered shoreline response time-series, are provided in the bottom panel as well. If the envelopes of the raw wave height signal and the filtered shoreline position signals are related to each other on corresponding timescales, the effect of small timescales in wave data on larger timescales in shoreline response is accounted for.

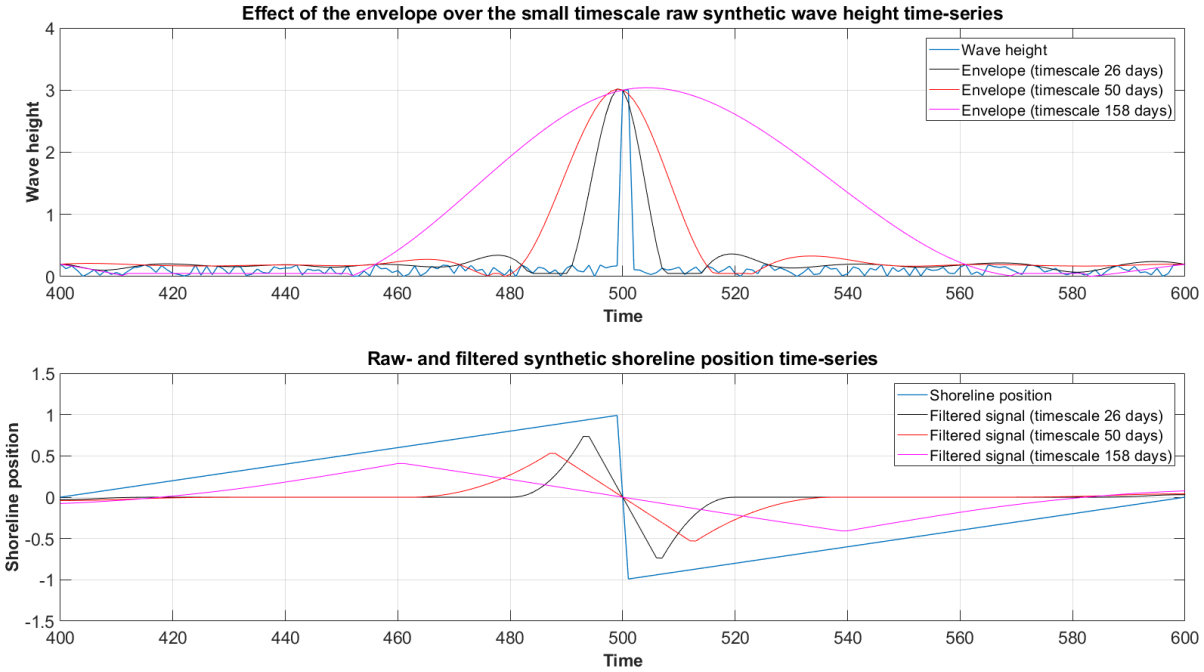

Figure 25: Different envelopes of the small timescale raw wave height time-series (top) and the raw- and filtered shoreline position time-series (bottom). The filtered shoreline position signals are forced with the envelope signals, to account for the effect of small timescales in wave data on large timescales in beach response.

For each filtered wave height signal, multiple envelopes are calculated with distinct timescales. The envelope is determined using spline interpolation, but the timescale of the envelope is determined by the developed filter function. The same approach is applied for the filtered wave period signals, whereupon envelopes of the filtered wave height and wave period signals with corresponding timescales are matched to each other. These two envelopes, with a certain timescale, form ShoreFor's forcing input and will be matched to a filtered shoreline response signal with the identical timescale. The approach can be written down as follows:

$$\frac{dx_j}{dt} = c * \left(F(\varphi)^{+}_{i \to j} + r * F(\varphi)^{-}_{i \to j}\right) \tag{17}$$

Wherein x is the shoreline position, t the time, c the response factor, r the erosion ratio, φ the memory decay factor and F the forcing term. The subscript indices i and j indicate the timescales, where i is the small timescale and j is the larger one ($j>i$). The envelope serves as the link between timescales and is indicated with an arrow. Note that for this modelling step ShoreFor is not adapted, but the forcing is represented differently.

Utilizing the envelope of wave signals has multiple drawbacks:

- High-intensity forcing events already have an effect on the wave height/period, while the event itself did not occur yet.
- The energy present in the wave signals is not conserved by the envelope.

The drawbacks indicate that the envelope is merely a way to model the effects of small timescales in wave data on larger beach response timescales and that it has no clear physical meaning.

Downscaling approach

Beaches can be subjected to erosion-accretion cycles on timescales larger than the storm/monthly timescale (e.g. a seasonal cycle). During these cycles, the beach profile can also differ significantly. During the erosion period, the beach width and slope are small and a breaker bar can be present. During the accretion period, the beach width and slope are large.

Subsequently, when a smaller temporal scale storm/monsoon hits the coastline, the beach response to this forcing event can depend on whether the coastline is eroded or accreted on a larger temporal scale. For an eroded beach where cross-shore sediment transport dominates shoreline change, incoming high-intensity forcing events experience more bottom friction due to a milder slope. The incoming forcing experiences friction for a longer time, causing significant energy dissipation. This dissipated energy cannot be used anymore to drive shoreline change. Moreover, if a breaker bar is present it dissipates high waves of the high-intensity forcing event, before they reach the coastline. Conversely, an accreted beach has a steeper slope causing less dissipation, such that more energy is available to drive shoreline change.

If high-intensity forcing events succeed each other in a short period of time, the effect described above is already implemented in ShoreFor. The dynamic equilibrium condition introduces a negative feedback, constraining excessive shoreline displacement if two high-intensity forcing events approach the coastline shortly after each other. The response due to the second event is lower, because the coastline is more in equilibrium with the high-intensity forcing conditions. This will only be captured by the model if the period between the two high-intensity forcing events is smaller than the memory decay factor.

For the linear superposition approach, the raw wave- and shoreline position signals are filtered and for each distinct timescale bin a memory decay factor will be calculated. The memory decay factor will be small when small (storm) timescales are considered and vice versa for larger temporal scales, as discussed earlier. Considering small (storm) timescales, the time-varying equilibrium condition only accounts for storms that occurred recently and information of larger scales is lost. However, it was stated above that an erosion-accretion cycle on a larger temporal scale can play a role as well on beach response to storms.

To model this effect, a time-varying response factor is used. Note that the response factor represents the efficiency with which waves induce cross-shore sediment transport. It can be expected that the response to storms is higher when the beach is in an overall accreted state (i.e. on a larger temporal scale) and the response to storms is lower when the beach is in an overall eroded state. In Figure 26, this phenomenon is visualized for a synthetic wave- and shoreline signal.

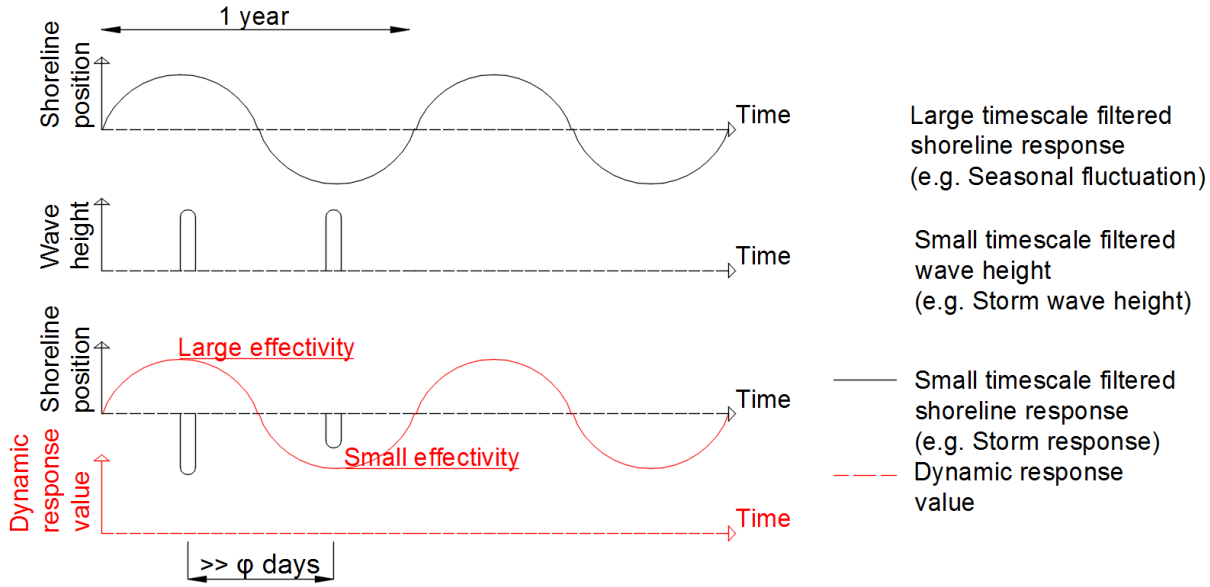

Figure 26: Due to filtering of the wave- and shoreline position signals, the connection between beach response timescales is lost. For storms with the same wave height, the response can be different due to a large scale accretion/erosion cycle of the shoreline. It is not possible to model this with a constant response value. A dynamic response value (red), with the shape of the large scale filtered shoreline response signal, offers the solution. A prerequisite is that the memory decay factor has to be smaller than the period in between the two storms. Otherwise, the negative feedback mechanism (due to the dynamic equilibrium condition) takes care of this effect.

Figure 26 shows three time-series: a large timescale filtered shoreline response signal (seasonal fluctuation, top panel), a small scale filtered wave height signal (storm wave height, center panel) and a combination of a small scale filtered shoreline response signal (storm response) and a dynamic response value (bottom panel). However, the first storm occurs during the seasonal accreted state and the second occurs during the seasonal eroded state. Therefore, the beach response to the two storms is different, while the wave forcing is the same. The memory decay factor is small enough, such that the dynamic equilibrium condition during the second storm is not affected by the first storm. Hence, the different response cannot be modelled using the negative feedback mechanism, because the period in between the storms is too large. Moreover, it cannot be modelled by a constant response value as the wave forcing is the same and the response is different. A dynamic response value with the shape of the large scale filtered shoreline response signal (seasonal fluctuation) offers the solution. It indicates that the sediment transport efficiency is higher for the first storm than for the second storm.

However, the shoreline signal is not available during model validation, which means that the dynamic response value cannot be used. Therefore, the shape of the predicted shoreline signal generated with the linear superposition approach is used. The shape of the dynamic response value is shifted, such that it always attains a positive value. In this way, the only parameter in ShoreFor determining if the coastline erodes or accretes is the disequilibrium term. To implement the downscaling approach, the predicted dynamic response factor is multiplied by the integrated wave forcing:

$$x_i(t) = c_j(t) * \int_0^t (F(\varphi,t)_i^+ + r * F(\varphi,t)_i^-)dt \quad (18)$$

In which x is the shoreline position, t the time, c the dynamic response factor, r the erosion ratio, φ the memory decay factor and F the forcing term. The subscript indices i and j indicate the timescales, where i is the smaller timescale and j the larger one ($j>i$). The subscript index of the dynamic response value indicates that it varies over time with the shape of the shoreline signal with timescale j. Hence, small scale wave- and shoreline position data are related to each other (timescale i), accounting for the fact that a larger scale shoreline variation is present (timescale j). Note that for this model improvement step, the ShoreFor model is adapted. A dynamic response value is used instead of a constant one.

The integrated forcing of the linear superposition approach is used, which incorporates the memory decay factor that is found during that model improvement step. During this step the most suitable memory decay factors were already determined, to match the wave- and shoreline data to each other on corresponding timescales. Normally, an integration constant will be calculated as well, representing the shoreline position offset. This parameter is not important during this model improvement step, as all filtered shoreline signals have a zero mean.

The shape of the dynamic response value is known, but the right variability (i.e. order of magnitude) is not. For this reason is each signal calculated with the downscaling approach multiplied with a factor. This factor makes sure that the variability of each predicted signal is equal to the one which was used to determine the bin distribution. This procedure can be written down as follows:

$$x_i(t) = f * (c_j(t) * \int_0^t (F(\varphi,t)_i^+ + r * F(\varphi,t)_i^-)dt) \quad (19)$$

$$f = \frac{\sigma_b}{\sigma_{x_i}} \quad (20)$$

Wherein f is the factor that makes sure that the variability of the predicted shoreline signal is the same as the one used to determine the bin distribution. σ_b and σ_{xi} represent the standard deviation used to determine the bin distribution and the standard deviation of the predicted signal using the downscaling approach, respectively.

Multiple linear regression analysis

By applying the linear superposition, up- and downscaling approach, multiple shoreline predictions are generated. Not all those predicted signals will contribute in predicting the shoreline change at Nha Trang. To determine which predicted signals contribute the most, a multiple linear regression analysis is carried out. The multiple linear regression analysis determines which combination of all predicted shoreline signals yields the best fit to the raw shoreline signal. Each predicted signal is multiplied by a factor attaining values between zero and one. If the factor is zero, the considered signal does not contribute in predicting shoreline change at Nha Trang and if the factor is one the concerning signal contributes significantly in predicting shoreline change.

It is possible that the multiple linear regression analysis generates a combination of predicted signals, of which some are only included because they increase the fit to the raw shoreline signal. However, the result of the predicted individual signal cannot be explained by physical processes. An example is presented in Figure 27, where the raw synthetic shoreline signal (number one) can be reproduced by a combination of predicted signals two and three. However, signal three is a predicted shoreline signal which is out of phase with the real shoreline signal, such that the result cannot be explained by physical processes. These signals will provide a suitable fit during the calibration phase, but not during the validation phase. Such signals will be referred to as non-physical signals.

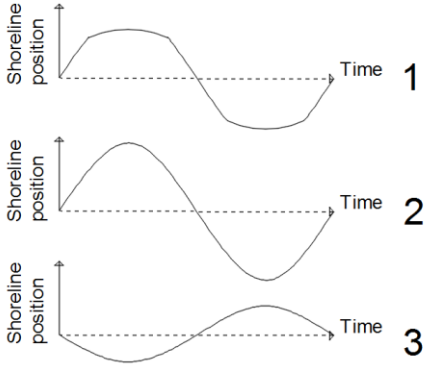

Figure 27: The raw synthetic shoreline signal (top) can be reproduced by predicted signals two and three. However, signal three is a non-physical predicted shoreline signal and may not be used to reproduce signal one.

To exclude non-physical signals from the multiple linear regression analysis, constraints are needed. Non-physical signals can be excluded by only taking predicted signals into account, which have a high correlation with the real filtered shoreline signal. To determine the correlation values for the linear superposition- and upscaling approach the predicted signal can be compared with the real filtered shoreline signal, because the waves are directly related to shoreline change. However, for the downscaling approach a different path is necessary, because the dynamic response value has to be checked on physical relevance and not the resulting predicted signal: the underlying thought of the downscaling approach need to be pursued. The applied approach is elaborated in the following sub-section.

Multiple linear regression constraints for the downscaling approach

The dynamic response value is checked on physical relevance by comparing the modelled response value (i.e. the predicted shoreline position determined with the linear superposition approach) by the real dynamic response value. The real dynamic response value is determined by calculating for each timescale bin, what the response factor has to be over time to match the filtered wave forcing- and filtered shoreline response signals to each other. Note that this calculation is only using signals determined with the linear superposition approach and is ignoring the upscaling approach, because it is not known beforehand which signals determined with the upscaling approach are most suitable to predict shoreline change. The corresponding formula is given by:

$$c_i(t) = \frac{\frac{dx_i}{dt}}{F(\varphi)_i^+ + r * F(\varphi)_i^-} \tag{21}$$

Where x is the shoreline position, t the time, c the response factor, r the erosion ratio, φ the memory decay factor and F the forcing term. The subscript index i indicates that different timescales are considered, corresponding to the filtered signals. To calculate the dynamic response values, the memory decay factors found during the linear superposition approach are used (black crosses on Figure 24). This assumption has to be made because otherwise, the memory decay factor and subsequently the dynamic response value cannot be determined. For the Nha Trang dataset 36 dynamic response values will be calculated using the corresponding 36 memory decay factors of the linear superposition approach.

Subsequently, the 36 dynamic response factors are filtered for the same timescales as the shoreline signal. Thereafter, correlation coefficients (Figure 28) are calculated, representing the correlation between the filtered dynamic response value and the corresponding (with the same timescale) filtered shoreline signal. A strong correlation can suggest a dependency of the dynamic response value on large scale shoreline variation. This can imply that for the prediction of small shoreline response timescales, the response value has to vary over time with the shape of a large scale shoreline variation. This means that the efficiency with which small temporal scale waves induce cross-shore sediment transport is dependent on the large scale beach width variation.

Figure 28 visualizes the correlation coefficients for all different timescale combinations of the filtered dynamic response factor and the filtered shoreline variation. Only combinations in the lower right corner are calculated, because the effect of large timescales in shoreline variation on short timescales in shoreline response is considered. In the figure, the x-axis indicates the timescales in shoreline position and the y-axis the timescales in the dynamic response value. Hence, the red arrow indicates the correlation coefficient between: 1) the calculated dynamic response value (to relate shoreline response and wave forcing to each other on a timescale of 10 days) filtered for a timescale of 13 days and 2) the filtered shoreline variation with a timescale of 13 days.

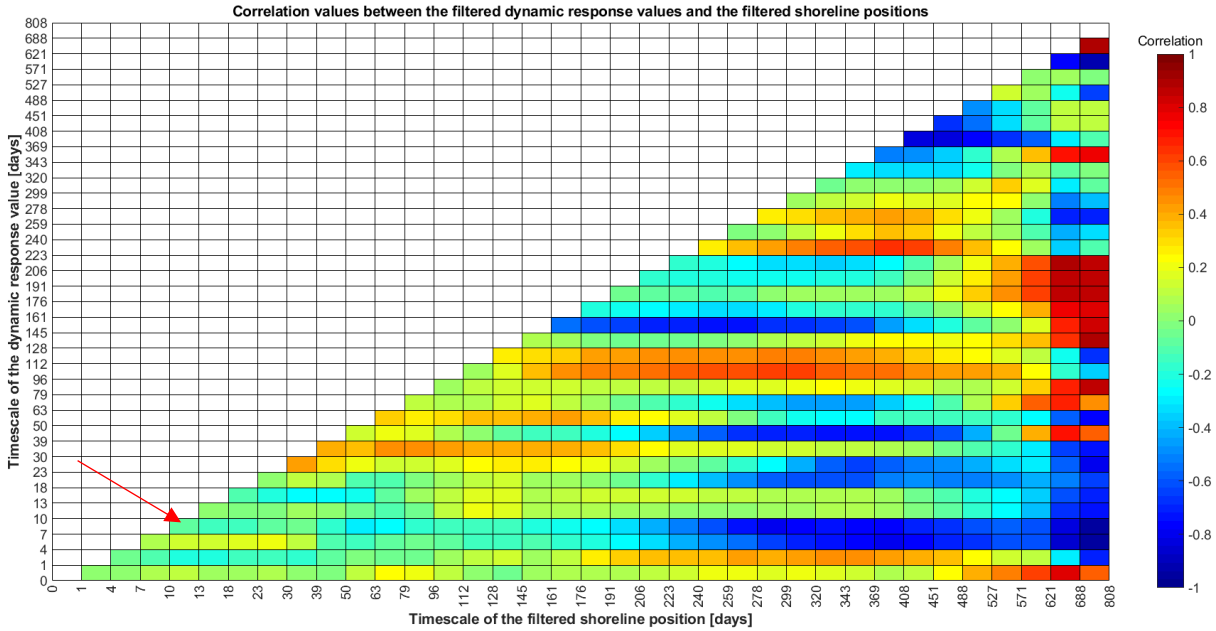

Figure 28: Correlation coefficients between the filtered dynamic response factor and the filtered shoreline variation

The following step of the approach to exclude non-physical signals from the multiple linear regression analysis is to fit a normal distribution to all correlation values per model improvement step. For example, Figure 28 presents all correlation values for the downscaling approach. Subsequently, a percentile is selected for each model improvement step that marks the threshold below which predicted signals (with a too low correlation coefficient) are excluded from the multiple linear regression analysis. In Figure 29, the three normal distributions are presented which are fitted to all correlation values of the corresponding model improvement step.

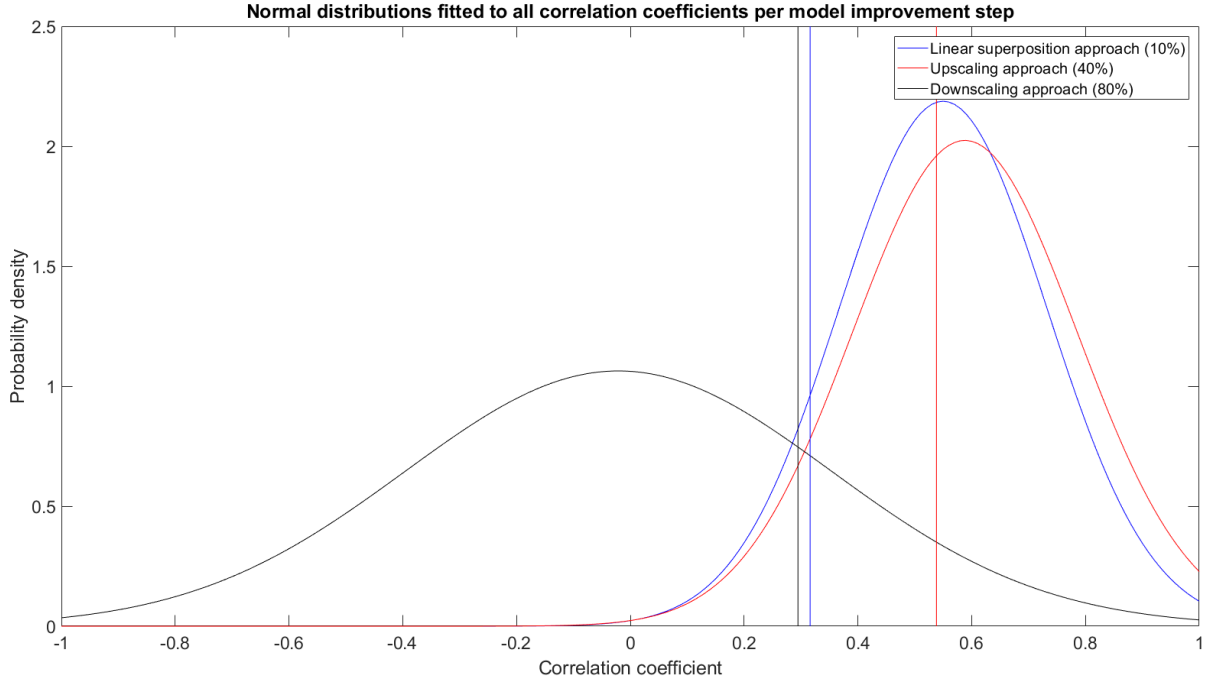

Figure 29: Normal distributions fitted to all correlation coefficients per model improvement step and the corresponding percentile threshold

The percentiles presented in Figure 29, are based on the assumptions made during the model improvement steps and a simple analysis to determine optimal percentiles. These are in this case, percentiles for which the validation phase yields the best results. In this analysis, the percentile of the linear superposition approach was kept steady (10%) and the percentiles for the up- and downscaling approach varied linearly. The linear superposition approach has the smallest percentile (10%), because the filtered wave- and shoreline signals are directly related to each other. The upscaling approach uses the envelope of wave signals to determine the effect of small scale forcing events on larger beach response timescales. However, the envelope is based on spline interpolation and has limited physical relevance. For the downscaling approach, the most assumptions were necessary (e.g. the assumed memory decay factor). It appeared that for the datasets at Nha Trang and Grand Popo, the optimal values were 40% and 80% for the up- and downscaling approach respectively.

Another multiple linear regression constraint is required to exclude the largest timescales from the analysis. This only applies to signals which are predicted using the up- and downscaling approach, as these steps are subjected to the most assumptions/limitations and are the most exposed to inaccuracy of the filter function. The filter function uses a moving average: when timescales become too large the average is affected by the duration of the dataset. For example, in Figure 28 the correlation coefficients for a timescale of 112 days (y-axis) are positively everywhere, except for the last two bins.

A solution to this problem is sought using a generalized extreme value (GEV) distribution. For each temporal scale, it is determined how many times the considered timescale fits in the duration of the dataset. To this data an extreme value distribution is fitted. This distribution is favored, as the difference in values can be an order of magnitude and the values are far from symmetrically distributed. Subsequently, a percentile is adopted below which predicted signals (with a too large timescale) are excluded from the multiple linear regression analysis. Using all three datasets, it appeared that a suitable percentile is 10%. For the Nha Trang dataset this means that predicted shoreline signals determined with the up- or downscaling approach with a timescale larger than 527 days, are not used in the multiple linear regression analysis. The fitted GEV distribution and the corresponding percentile are presented in Figure 30.

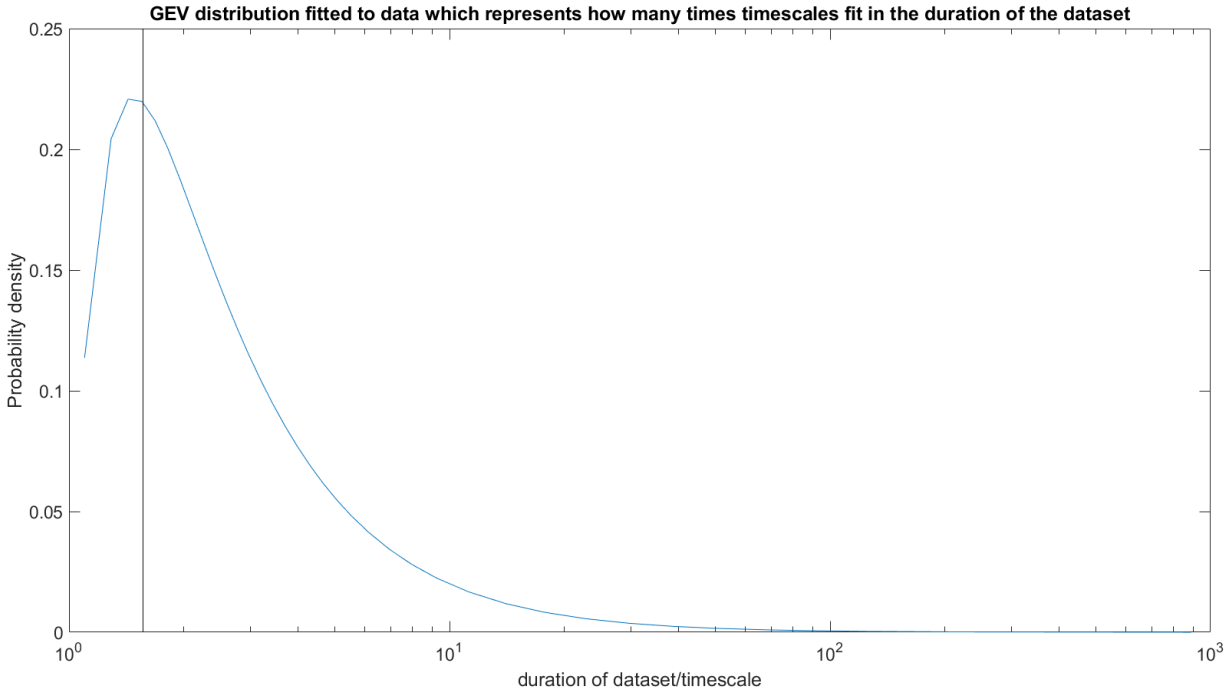

Figure 30: Generalized extreme value distribution and the corresponding percentile to determine the threshold above which too large timescales are excluded from the multiple linear regression analysis

The section below presents an overview of the multiple linear regression constraints per model improvement step. Note that the values below are dataset dependent, but in this case the constraints for the Nha Trang dataset are considered.

Linear superposition approach

For each timescale: predicted signals having a correlation coefficient with the filtered shoreline data below 0.32 (determined using the normal distribution), are not used in the multiple linear regression analysis.

Upscaling approach

For each timescale: predicted signals having a correlation coefficient with the filtered shoreline data lower than 0.54, are not used in the multiple linear regression analysis.

Timescales larger than 527 days (determined using the generalized extreme value distribution) are not used in the multiple linear regression analysis.

Downscaling approach

For each timescale: predicted signals of which the filtered dynamic response value (formula 21) has a correlation coefficient with the filtered shoreline data (Figure 28) lower than 0.29, are not used in the multiple linear regression analysis.

Timescales larger than 527 days are not used in the multiple linear regression analysis. Furthermore, it is possible that ShoreFor is not able to find a proper relation between the wave- and shoreline data during the linear superposition approach. This means that the dynamic response value of the downscaling approach is based on this poor prediction: it has the wrong shape. For this reason, predicted signals of which the dynamic response value is based on linear superposition signals that have a low correlation with shoreline data, will not be used in the multiple linear regression analysis. In this case, a poor prediction means that signals have a correlation coefficient with the filtered shoreline data lower than 0.32.

This section focused on implementing multiple timescales in ShoreFor, using a linear superposition, up- and downscaling approach. Furthermore, constraints for the multiple linear regression analysis are treated, which make sure that the most suitable predicted signals are used for shoreline prediction. The next section will elaborate the results when the improved model is applied to all three datasets.

5 Results

In this chapter, improved model results are analyzed and differences with ShoreFor results are highlighted. Two calibrations cases are considered: a calibration on a part of the dataset and a calibration on the whole dataset. Per dataset, time-series of the calibration- and validation phase are presented, visualizing the improvement and the contribution of each model improvement step over time. Subsequently, the model improvement per timescale is presented, highlighting the fact that multiple beach response timescales are accurately predicted by the improved model. Thereafter, timescale interactions are visualized in the form of a grid, representing the footprint of a dataset. Finally, an overview of model improvements is presented for all datasets.

5.1 Model calibration and validation

Calibration on a part of the dataset

Table 7 summarizes important parameters corresponding to model calibration for the dataset at Nha Trang, when calibrated on a part of the dataset. Later on, a calibration on the whole dataset is carried out and differences are highlighted. Parameters corresponding to calibration on the whole dataset are presented within the brackets. Note that the amount of timescale bins is the same for both calibration cases.

Calibration at Nha Trang	
Calibration period	27-07-2013/31-12-2014 (27-07-2013/31-12-2015)
Constraints linear superposition approach	Correlation >0.32 (0.40)
Constraints upscaling approach	Correlation >0.54 (0.55) & timescales <= 527 days
Constraints downscaling approach	Correlation >0.29 (0.30) & timescales <= 527 days
Amount of timescale bins	36

Table 7: Multiple linear regression constraints and dataset information at Nha Trang

Table 8 summarizes important parameters corresponding to model calibration for the dataset at Narrabeen.

Calibration at Narrabeen	
Calibration period	01-08-2004/31-12-2007 (01-08-2004/31-12-2010)
Constraints linear superposition approach	Correlation >0.43 (0.35)
Constraints upscaling approach	Correlation >0.42 (0.26) & timescales <= 851 days
Constraints downscaling approach	Correlation >0.36 (0.32) & timescales <= 851 days
Amount of bins:	48

Table 8: Multiple linear regression constraints and dataset information at Narrabeen

Table 9 summarizes important parameters corresponding to model calibration for the dataset at Grand Popo. Note that for this dataset only eight bins are used. The storm response timescale has a significant amount of variability relative to the seasonal one, which means that the variability within each bin is high and the amount of bins is low.

Calibration at Grand Popo	
Calibration period	20-02-2013/22-11-2015 (20-02-2013/22-08-2016)
Constraints linear superposition approach	Correlation >0.14 (0.11)
Constraints upscaling approach	Correlation >0.33 (0.31) & timescales <= 342 days
Constraints downscaling approach	Correlation >0.24 (0.09) & timescales <= 342 days
Amount of bins:	8

Table 9: Multiple linear regression constraints and dataset information at Grand Popo

Nha Trang

Figure 31 presents the results when ShoreFor and the improved model are applied to the dataset at Nha Trang (top panel), as well as the contribution of each model improvement step over time (bottom panel). Note that the latter is cumulative. Moreover, the red line in the bottom panel is the total predicted shoreline change determined with the improved model, which is identical to the red line in the top panel.

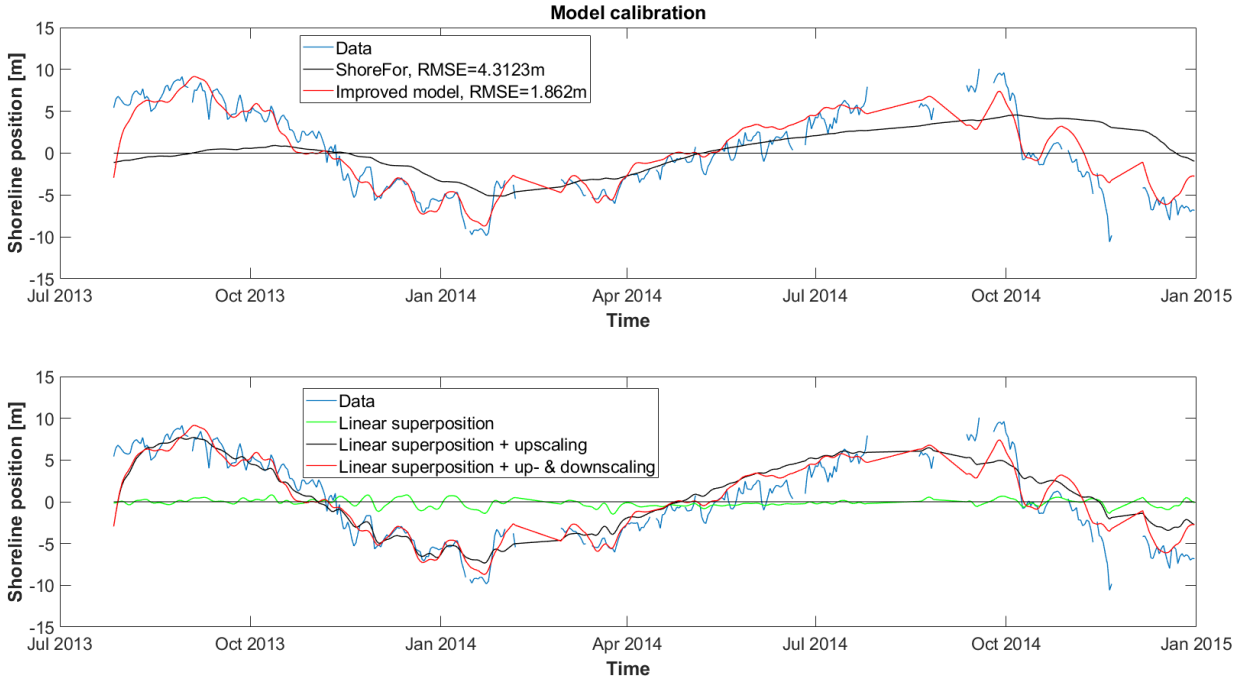

Figure 31: Model calibration at Nha Trang: difference in modelling results using ShoreFor and the improved model (top panel) and the contribution of each model improvement step over time (bottom panel)

ShoreFor is only able to accurately model the seasonal shoreline change and the response to monsoons is poorly predicted. The memory decay factor for the dataset at Nha Trang is 130 days, which confirms that the seasonal shoreline response is dominant. The improved model is able to predict the shoreline evolution better than ShoreFor. The RMSE between the data and the ShoreFor prediction is 4.31m, whereas for the improved model a RMSE of 1.86m is found. The biggest contributor to shoreline prediction of the improved model, is the effect of small timescales in wave data on larger timescales in beach response (upscaling, black line in lower panel). Using this upscaling approach, a suitable fit for the seasonal variation is found. Moreover, modelling the effect of large shoreline variation timescales on smaller beach response timescales (downscaling, difference between the red- and black line in the lower panel) makes sure that the monsoon response is captured as well.

Narrabeen

Figure 32 presents the results when ShoreFor and the improved model are applied to the dataset at Narrabeen (top panel), as well as the contribution of each model improvement step over time (bottom panel).

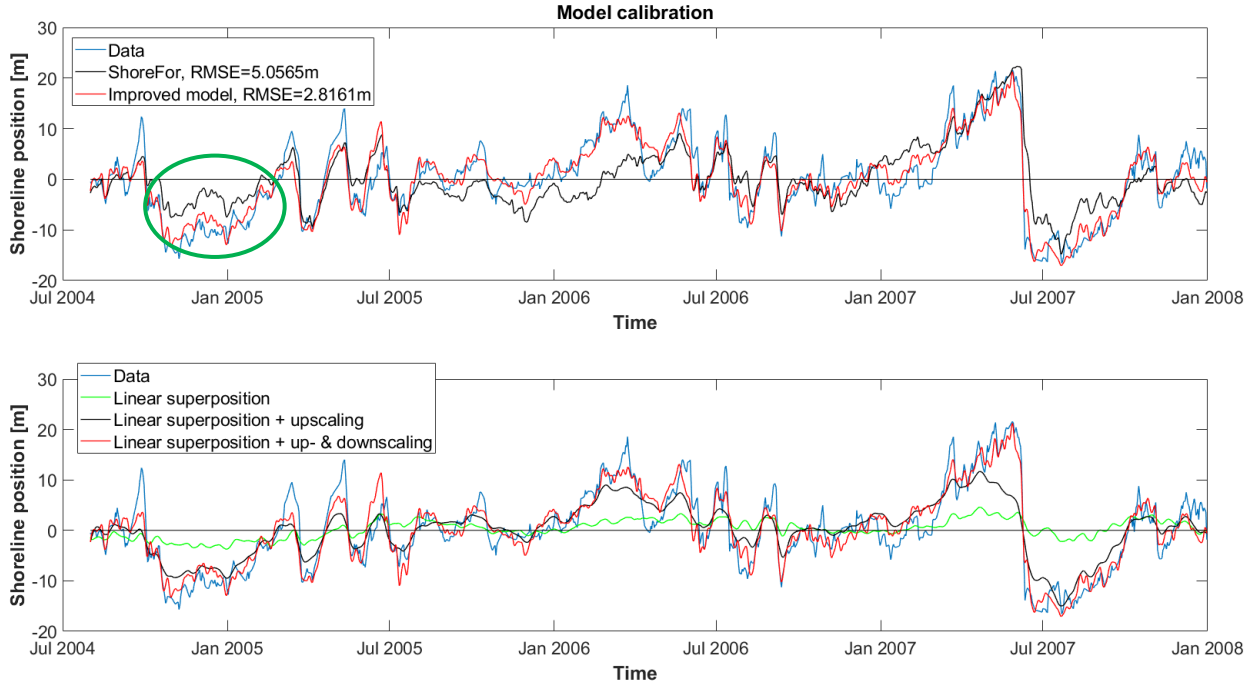

Figure 32: Model calibration at Narrabeen: difference in modelling results using ShoreFor and the improved model (top panel) and the contribution of each model improvement step over time (bottom panel)

ShoreFor is able to predict the storm response quite well, but the larger scale shoreline variations not. The memory decay factor at Narrabeen is 55 days, which confirms that the storm response is dominant. The improved model yields a significant increase in prediction skill compared to ShoreFor. The RMSE between the data and ShoreFor prediction is 5.06m, whereas the improved model results in a RMSE of 2.81m between data and prediction. Especially when the shoreline is accreted or eroded on a larger timescale (larger than the storm timescale), the improved model result fits better to the data. This occurs for example in the Australian summer months of November 2004 until March 2005 (green oval), where the large erosion period is predicted well by the improved model. The storm timescale (order of days) is represented well by both models. All three model improvement steps contribute significantly to the total predicted shoreline signal. The larger timescales are predicted by the linear superposition- and upscaling approach and the smaller (storm) timescale are modelled with the downscaling approach.

Grand Popo

Figure 33 presents the results when ShoreFor and the improved model are applied to the dataset at Grand Popo (top panel), as well as the contribution of each model improvement step over time (bottom panel).

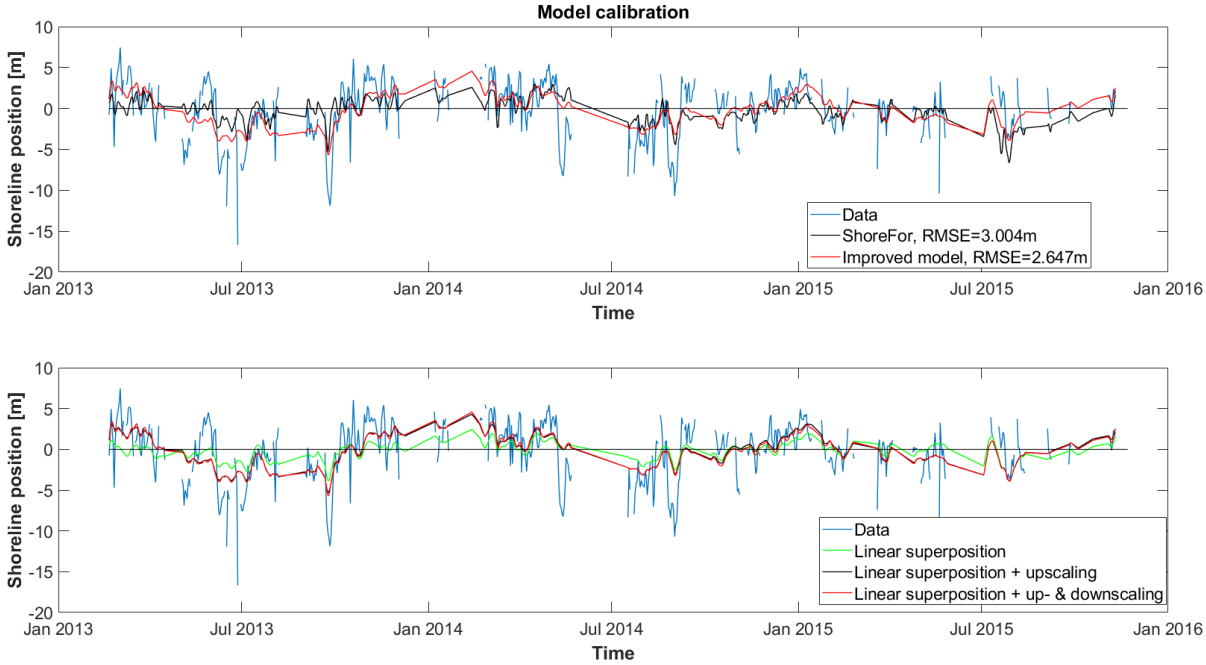

Figure 33: Model calibration at Grand Popo: difference in modelling results using ShoreFor and the improved model (top panel) and the contribution of each model improvement step over time (bottom panel)

The difference in prediction skill between ShoreFor and the improved model is minor. Both models predict the seasonal variation well, but the storm timescale not. The contribution of the linear superposition- and upscaling approach is high. The signals generated with the downscaling approach have almost no contribution to the shoreline change prediction at Grand Popo. However, the storm timescale is a dominant mode of shoreline response. It is possible that due to the small amount of bins, the improved model is not able to find a relation between waves and shoreline response, such that the storm response can be captured. Using a limited amount of bins, timescales within a bin are not distinct enough such that suitable interactions cannot be found. Another possible explanation is that due to a large amount of noise and data-gaps the prediction skill for the storm timescale is limited, because in that bin the noise is highest.

Model validation

During model validation, wave data (wave height and wave period) is used as only model input and calibration parameters are not adjusted anymore. Moreover, the combination of predicted signals (determined by the multiple linear regression analysis) that modelled shoreline change during the calibration phase, is also responsible for modelling shoreline change during model validation.

Nha Trang

Figure 34 presents the results when ShoreFor and the improved model are validated with the dataset at Nha Trang (top panel), as well as the contribution of each model improvement step over time (bottom panel).

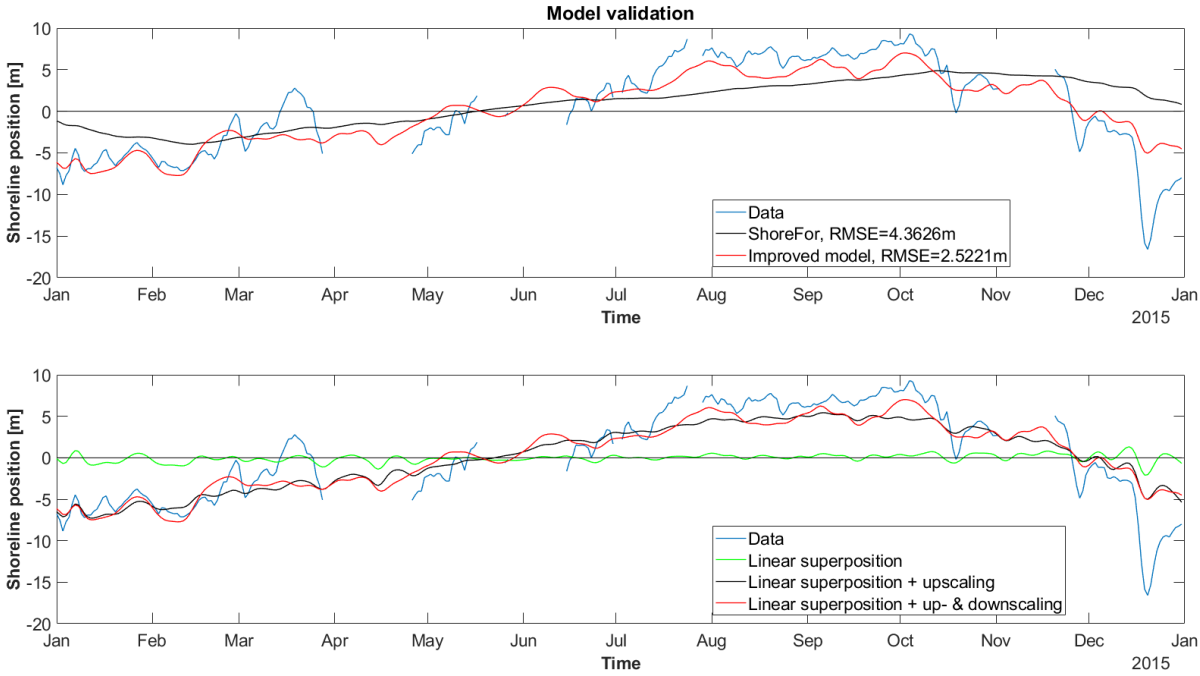

Figure 34: Model validation at Nha Trang: difference in modelling results using ShoreFor and the improved model (top panel) and the contribution of each model improvement step over time (bottom panel)

The improved model yields a better prediction during the validation phase too. Besides the seasonal variation, the improved model captures the monsoon response as well. The RMSE between the data and the ShoreFor prediction is 4.36m, whereas for the improved model a RMSE of 2.52m is found.

The Akaike's information criterion (AIC) is specifically designed to compare models with a different number of calibration parameters (m):

$$AIC = n * (\log(2\pi) + 1) + n * \log(\sigma^2) + 2m \quad (22)$$

In which n is the total number of samples and σ^2 is the variance of the model or baseline residuals. If the difference between the baseline and model AIC (ΔAIC) exceeds 1.0, a significant model improvement is acquired (Davidson et al., 2013).

The model improvement is significant for the calibration phase (57%, Table 10) as well as for the validation phase (42%), when the RMSE is used as an indicator for prediction skill. The significant model improvement is also indicated by the ΔAIC score for the calibration phase. However, the ΔAIC score for the validation phase is zero, indicating negligible improvement due to a too large number of calibration parameters. For the improved model the total predicted shoreline signal consists out of multiple signals with distinct timescales. For each predicted signal, two calibration parameters are present: the memory decay factor (φ) and the response value (c). In total, 72 calibration parameters are used causing a low/zero ΔAIC score.

	Calibration	**Validation**
ShoreFor (RMSE [m])	4.31	4.36
Improved model (RMSE [m])	1.86	2.52
Improvement	**+57%**	**+42%**
ΔAIC	174	0

Table 10: RMSE between data and model prediction for both models and the ΔAIC value for the dataset at Nha Trang

Narrabeen

Figure 35 presents the results when ShoreFor and the improved model are validated with the dataset at Narrabeen (top panel), as well as the contribution of each model improvement step over time (bottom panel).

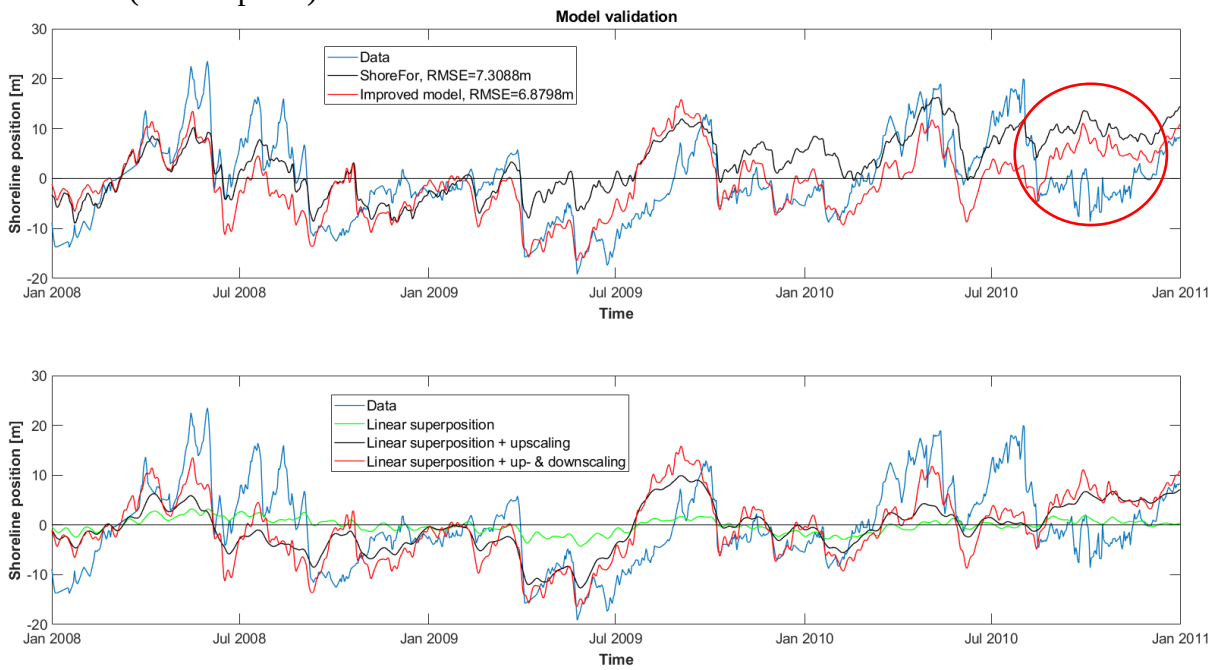

Figure 35: Model validation at Narrabeen: difference in modelling results using ShoreFor and the improved model (top panel) and the contribution of each model improvement step over time (bottom panel)

A comparison of the validation results of both models reveals that the differences are not significant. The smaller (storm) timescales are predicted with considerable skill for both models. However, neither model is capable in predicting large timescale shoreline variations. For example, from July 2010 until January 2011 (red oval) both ShoreFor and the improved model (black- and red line in the top panel, respectively) are not predicting the large scale variation well. A possible explanation for the poor validation result is that the calibration period is too short, such that the improved model cannot capture the large scale shoreline variations well.

For the calibration phase the model improvement is significant (44%, Table 11). However, for the validation phase the improvement is minor (6%), when the RMSE is used as an indicator for prediction skill. The significant model improvement during calibration is also reflected in the ΔAIC score. In that case, the large number of calibration parameters (131) is justified, as they result in significant model improvement. However, for the validation phase the large number of calibration parameters is not causing significant model improvement, which is reflected in the ΔAIC score.

	Calibration	**Validation**
ShoreFor (RMSE [m])	5.06	7.31
Improved model (RMSE [m])	2.82	6.88
Improvement	**+44%**	**+6%**
ΔAIC	378	-307

Table 11: RMSE between data and model prediction for both models and the ΔAIC value for the dataset at Narrabeen

Grand Popo

Figure 36 presents the results when ShoreFor and the improved model are validated with the dataset at Grand Popo (top panel), as well as the contribution of each model improvement step over time (bottom panel).

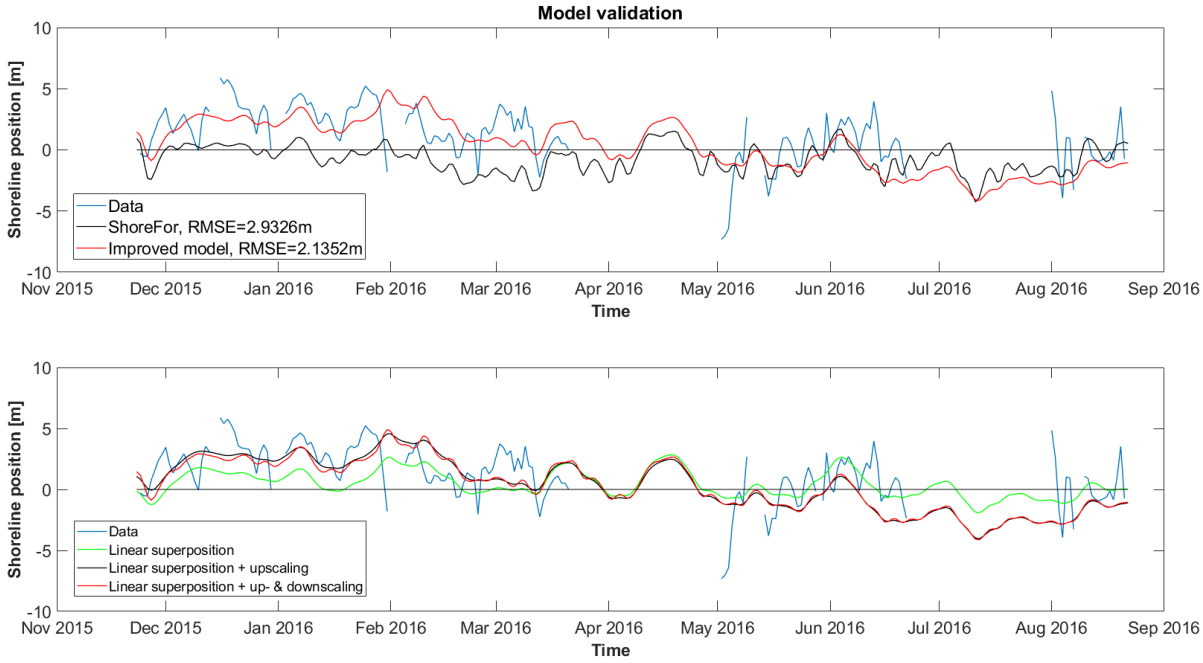

Figure 36: Model validation at Grand Popo: difference in modelling results using ShoreFor and the improved model (top panel) and the contribution of each model improvement step over time (bottom panel)

For the validation phase the model improvement is significant compared to ShoreFor, in which signals determined by the upscaling approach contribute most to the improvement. Those signals are responsible for the prediction of the seasonal variation as was already determined during the calibration phase. The storm timescale was not captured well during model calibration, so it is also poorly modelled in the validation phase.

For the calibration phase the model improvement is minor (12%, Table 12). However, considering the ΔAIC score the large number of calibration parameters (26) yields significant model improvement. For the validation phase the improvement is significant (27%) when the RMSE is used as an indicator for prediction skill, but not when the ΔAIC score is considered. Apparently the baseline residuals of the improved model are too large compared to the increased number of calibration parameters.

	Calibration	**Validation**
ShoreFor (RMSE [m])	3.00	2.93
Improved model (RMSE [m])	2.65	2.14
Improvement	**+12%**	**+27%**
ΔAIC	19	-46

Table 12: RMSE between data and model prediction for both models and the ΔAIC value for the dataset at Grand Popo

Calibrated on the whole dataset

In this section, improved model results are presented and compared with the results using ShoreFor when calibrated on the whole dataset. For the important parameters corresponding to model calibration is referred to Table 7, Table 8 and Table 9 (data within the brackets).

Nha Trang

Figure 37 presents the results when ShoreFor and the improved model are applied to the whole dataset at Nha Trang (top panel), as well as the contribution of each model improvement step over time (bottom panel).

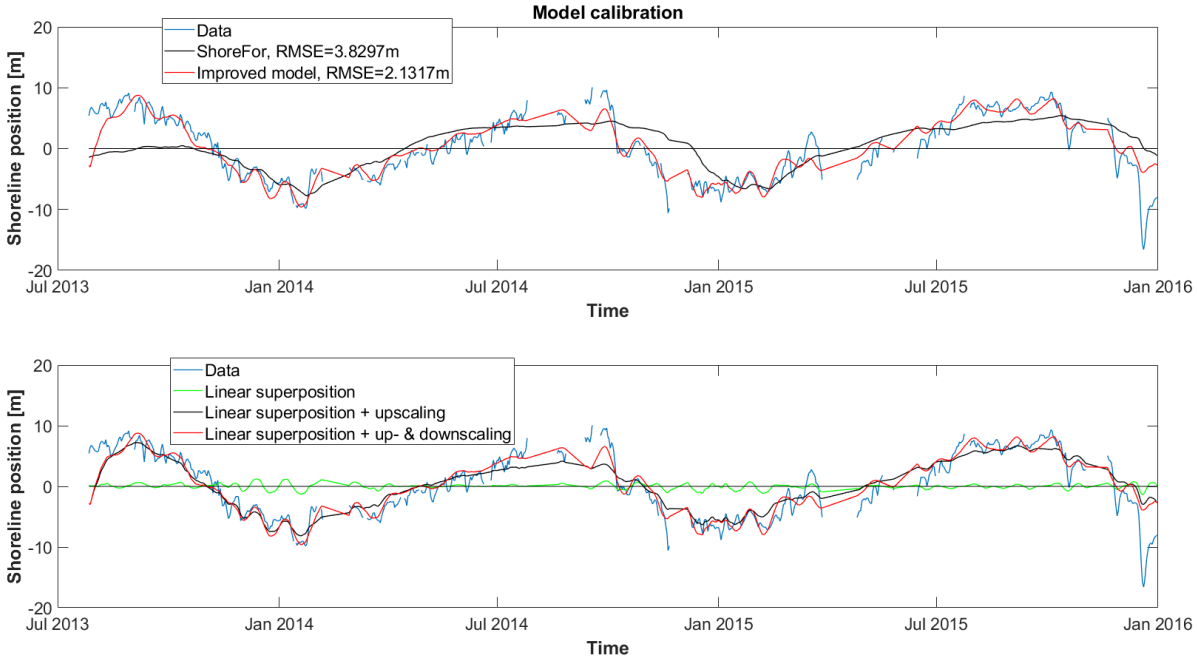

Figure 37: Model calibration at Nha Trang: difference in modelling results using ShoreFor and the improved model (top panel) and the contribution of each model improvement step over time (bottom panel)

The improved model yields a better fit to the raw shoreline signal compared to the result using ShoreFor. ShoreFor is only able to accurately predict the seasonal variation and does not predict the shoreline response to monsoons. The improved model is able to predict the shoreline response to monsoons and the seasonal variation. Moreover, the seasonal variation is better predicted when the improved model is applied. Shoreline signals generated with the upscaling approach are responsible for the prediction of the seasonal variation. Signals generated with the downscaling approach are responsible for the prediction of the monsoon response.

Narrabeen

Figure 38 presents the results when ShoreFor and the improved model are applied to the dataset at Narrabeen (top panel), as well as the contribution of each model improvement step over time (bottom panel).

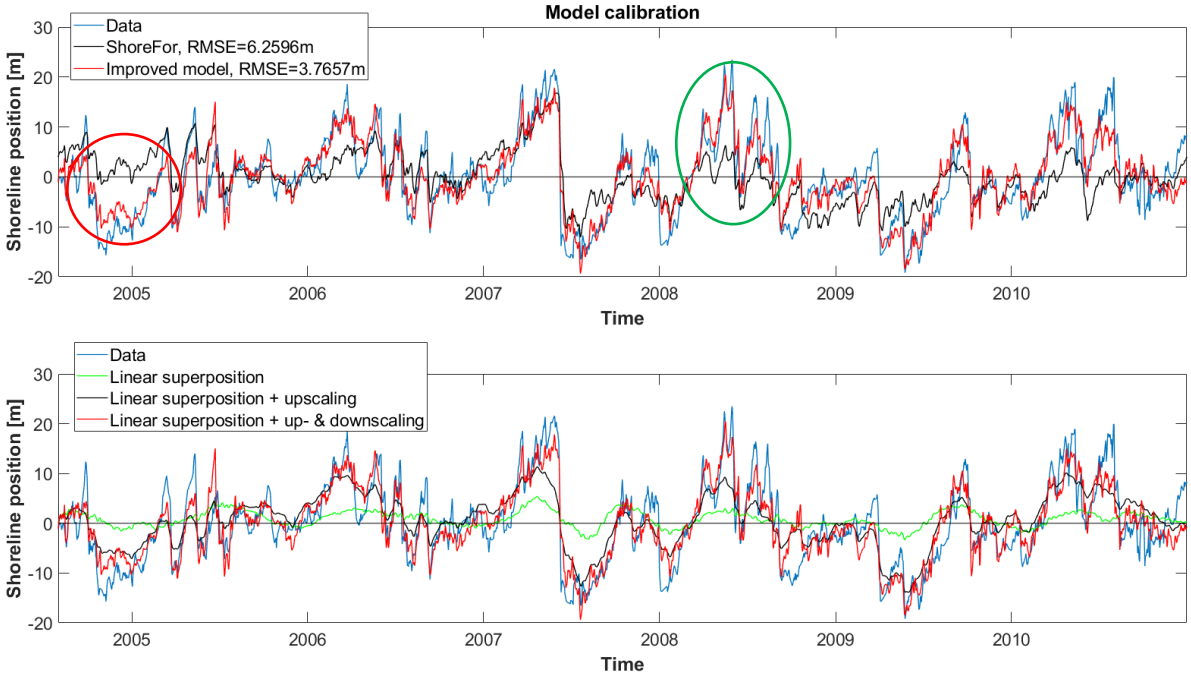

Figure 38: Model calibration at Narrabeen: difference in modelling results using ShoreFor and the improved model (top panel) and the contribution of each model improvement step over time (bottom panel)

When the improved model is calibrated on the whole dataset the prediction skill gain is significant, compared to the ShoreFor model. The improvement is due to a better prediction for larger timescales. This is for example clearly indicated at the end of 2004 to the beginning 2005 (red oval). When applying ShoreFor, the limited prediction skill for larger timescales causes that the storm response offset is poor for large periods of time. The larger timescales (larger than the storm timescale) are predicted by the linear superposition- and upscaling approach. The downscaling approach makes sure that the storm response is modelled. Even the response to large accretion/erosion events are captured by the downscaling approach (green oval).

Grand Popo

Figure 39 presents the results when ShoreFor and the improved model are applied to the dataset at Grand Popo (top panel), as well as the contribution of each model improvement step over time (bottom panel).

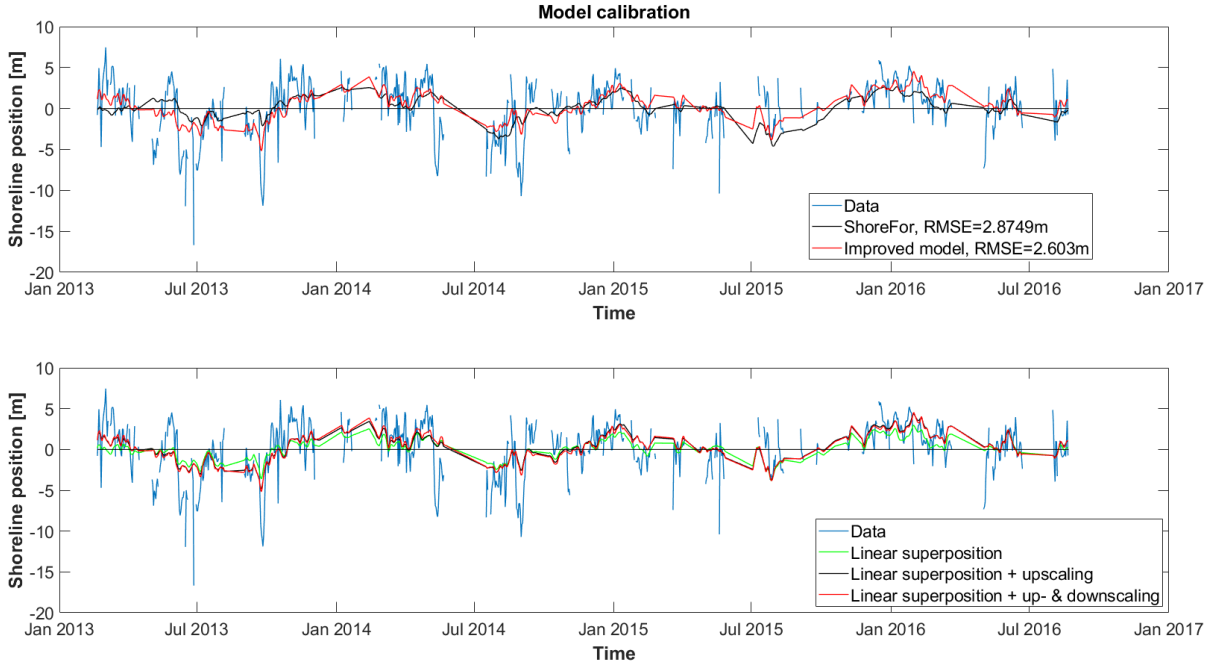

Figure 39: Model calibration at Grand Popo: difference in modelling results using ShoreFor and the improved model (top panel) and the contribution of each model improvement step over time (bottom panel)

The model improvement is negligible compared to the result using ShoreFor. The seasonal timescale is predicted with reasonable skill by the linear superposition approach and the storm timescale is not captured well by the model.

5.2 Model improvement per timescale

This section presents the model improvement per timescale for all the three datasets, where the RMSE is used as an indicator for prediction skill. The errors are determined by filtering the total predicted signals and calculate the RMSE by using the real filtered shoreline signal.

Nha Trang

Figure 40 presents the model improvement per timescale for the dataset at Nha Trang.

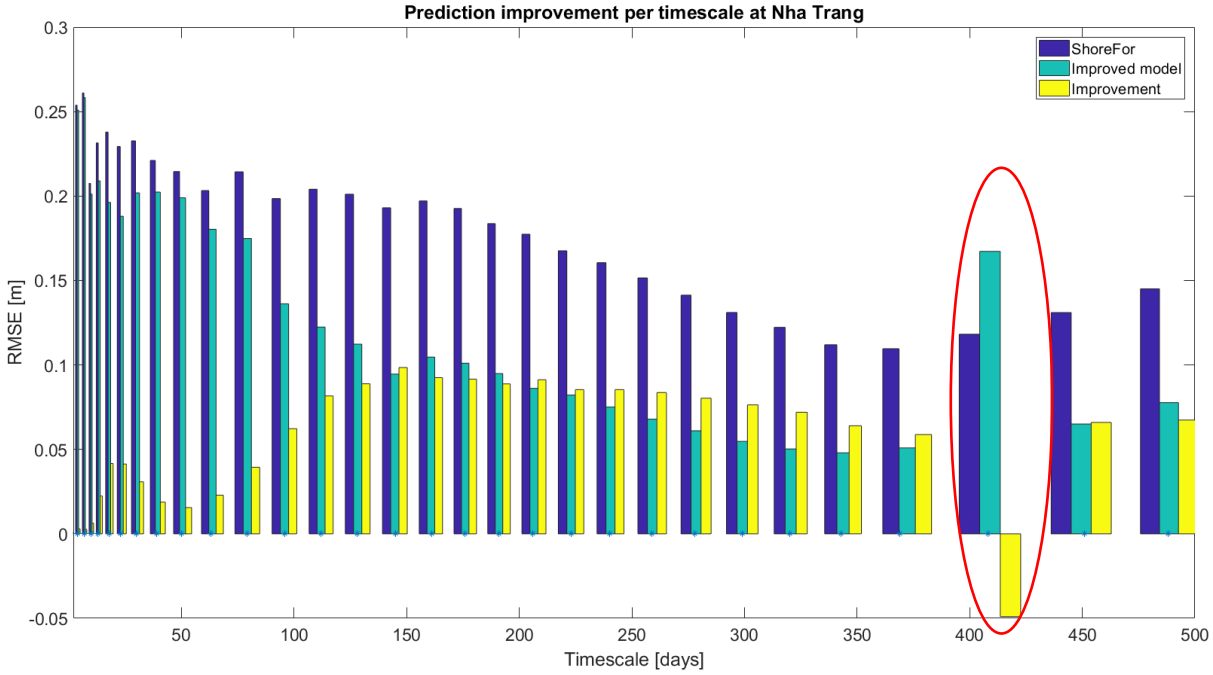

Figure 40: Model improvement per timescale for the dataset at Nha Trang

The improvement is large for monsoon timescales (≈30 days). These timescales are poorly captured by ShoreFor, because only the most dominant timescale is accurately predicted. The other significant improvement is for timescales smaller than the seasonal one. Those timescales make sure that the seasonal variation is better captured when the improved model is applied. As the seasonal timescale is approached, the improvement decays where after it increases again when the timescales become larger. Note that the improvement for a timescale of 408 days is negative (red oval). This is due to the fact that the bin distribution is affected by the data-gaps.

Narrabeen

Figure 41 presents the model improvement per timescale for the dataset at Narrabeen.

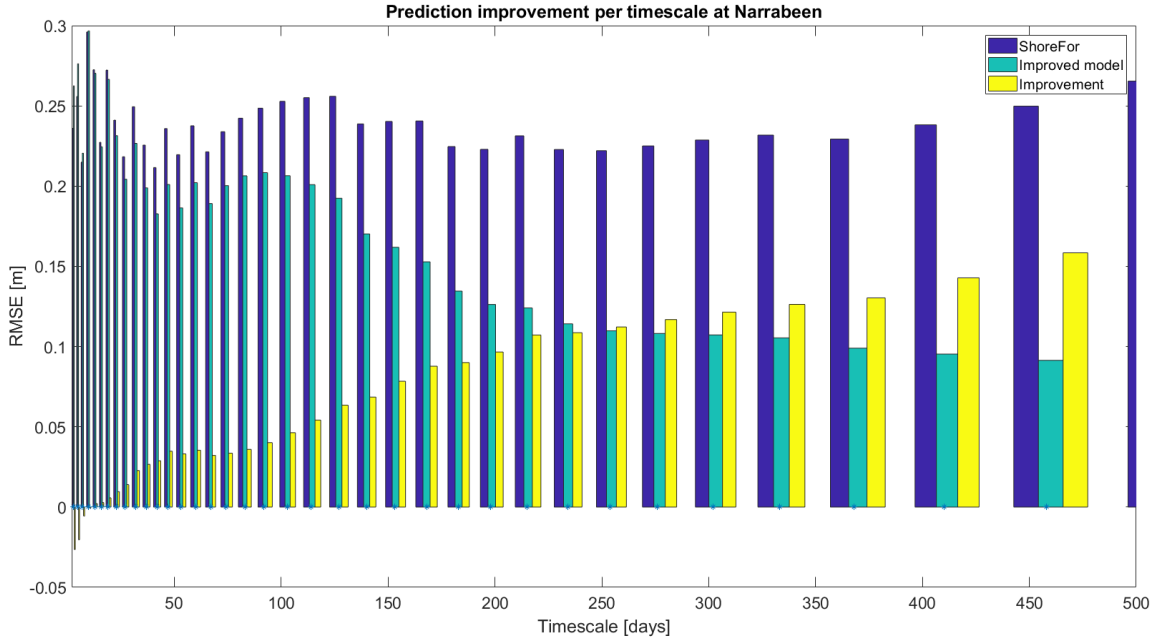

Figure 41: Model improvement per timescale for the dataset at Narrabeen

The histogram indicates that large timescales contribute the most to model improvement. ShoreFor is capable of predicting the dominant storm response timescales accurately (small improvement), but large timescales are not modelled with sufficient skill (large improvement). The improved model is able to predict multiple timescales as the storm- and larger timescales are both predicted well.

Grand Popo

Figure 42 presents the model improvement per timescale for the dataset at Grand Popo.

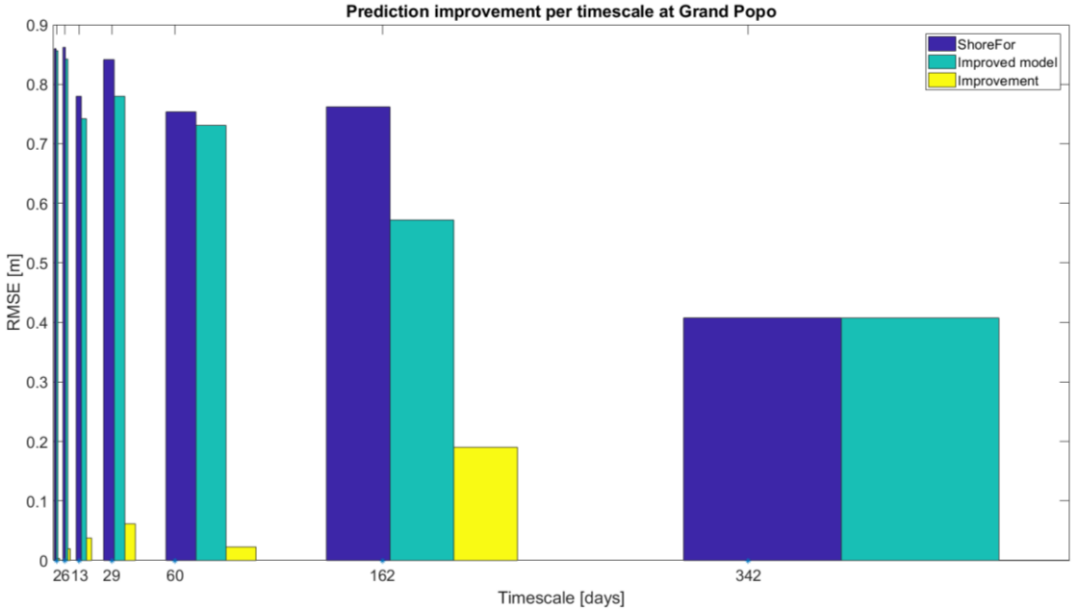

Figure 42: Model improvement per timescale for the dataset at Grand Popo

The improvement is largest for timescales below the seasonal scale. This phenomenon was also clearly visible at the Nha Trang dataset. Moreover, for the monthly timescale some improvement is made as well. The RMSE for the smallest timescales remain high, which could be expected based on the modelled shoreline response time-series.

5.3 Timescale interactions

The previous sections focused on the overall difference in model results between ShoreFor and the improved model. First in the form of shoreline position time-series, thereafter the improvement per timescale was considered where the RMSE was used as indicator for model prediction skill. However, the structure of the total predicted shoreline signal using the improved model consists out of multiple predictions with distinct timescales. These timescales are interacting with each other as was explained in chapter 4. Which timescales are interacting with each other, will be elaborated in this section. Moreover, the structure of the downscaling approach is treated corresponding to signals which are of major important in predicting shoreline change. From that analysis it becomes clear why timescales are interacting.

To visualize the timescale interactions, grids are presented in which the standard deviation of all predicted signals is plotted. The diagonal represents the standard deviation of signals predicted with the linear superposition approach and the black axes (from x to y) can be used to check which timescales are involved. For the standard deviation of signals generated with the upscaling approach, the black axes (from x to y) can be used as well, because the approach relates the waves directly to shoreline change. All signals in the upper left corner represent the upscaling approach as indicated by the figure. The lower right corner of the grid represents the standard deviation of signals generated by the downscaling approach. For those signals, the red axes (from x to y) need to be used, as this approach determines the effect of large timescales in shoreline data on smaller timescales in shoreline response. Note that a large standard deviation indicates a large contribution to the total shoreline change.

Nha Trang

Figure 43 presents the timescale interactions at Nha Trang when calibrated on a part of the dataset.

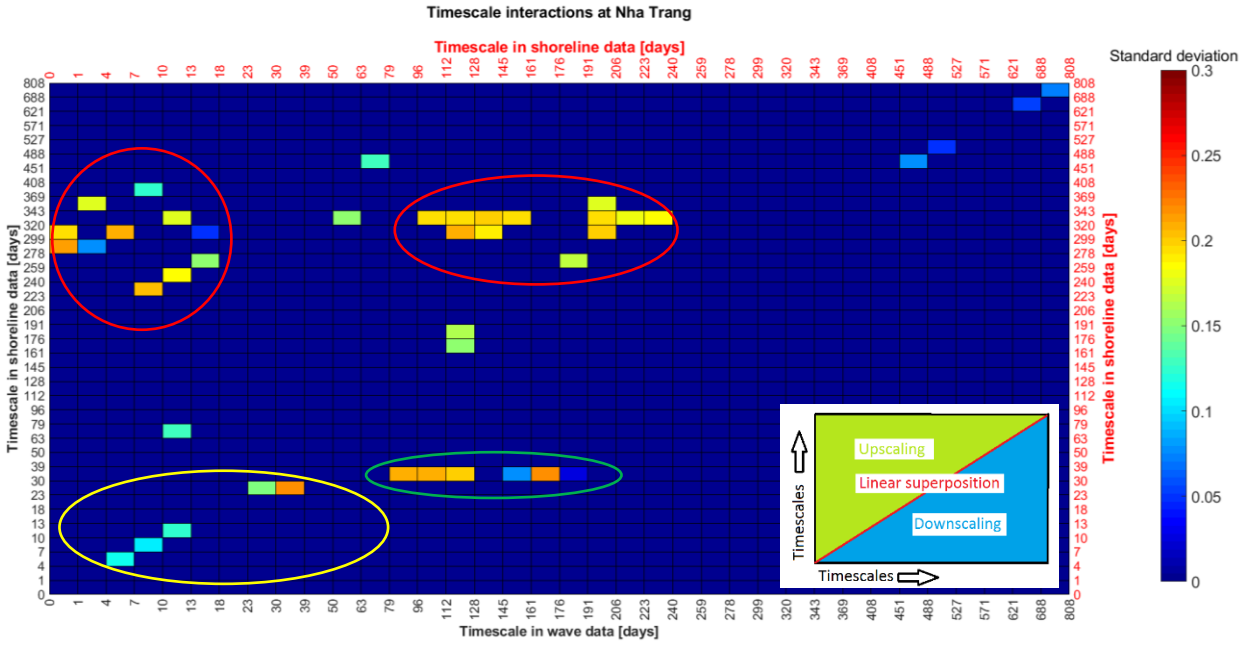

Figure 43: Timescale interactions at Nha Trang when calibrated on a part of the dataset

The figure indicates that seasonal timescales (order of 1 year) are a dominant mode of shoreline change (red ovals), which is modelled by the upscaling approach. Moreover, the upscaling approach contributes most to the predicted shoreline signal. This means that small timescales in wave data have a large effect on the seasonal shoreline response. Shoreline response to monsoons is represented by the downscaling approach (green oval). Hence, the response to monsoons is affected by the shoreline variation on a larger temporal scale. Shoreline response to timescales smaller than the monthly timescale is represented by the linear superposition approach (yellow ovals). For those scales, no timescale interactions are present.

Figure 44 presents the timescale interactions at Nha Trang when calibrated on the whole dataset.

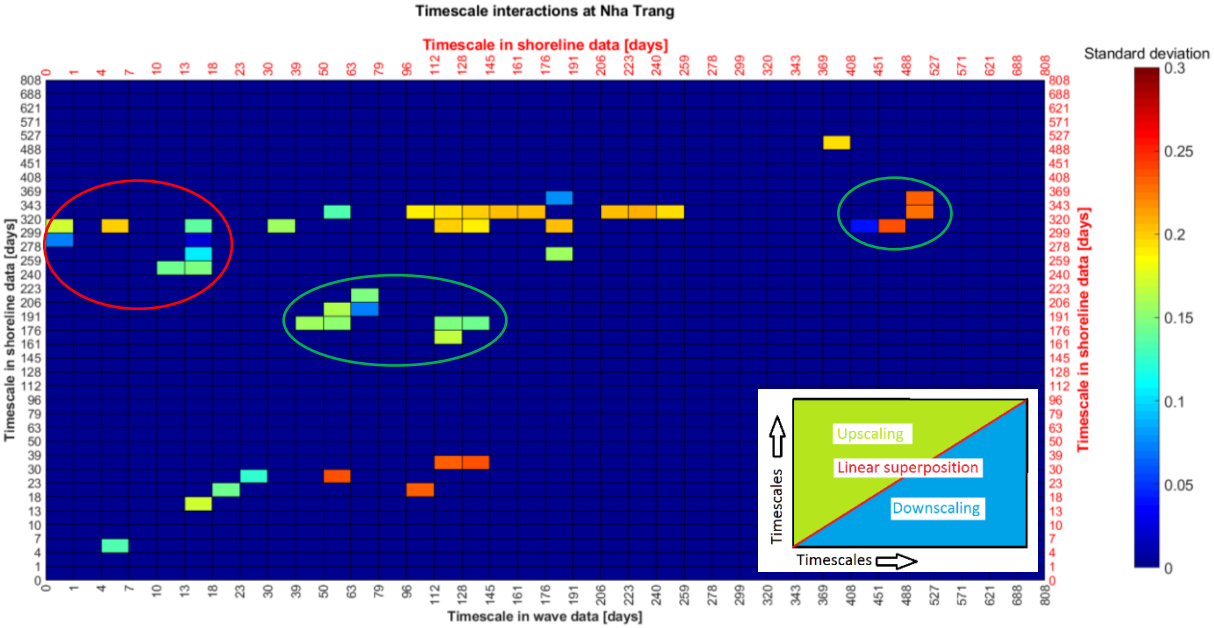

Figure 44: Timescale interactions at Nha Trang when calibrated on the whole dataset

Figure 44 reveals that most signals which are important for shoreline prediction when calibrated on a part of the dataset, also contribute to shoreline change when calibrated on the whole dataset. The seasonal response is still modelled using signals generated with the upscaling approach and the monsoon response is modelled using signals determined with the downscaling approach. The difference with Figure 43 is that the cluster representing the effect of the smallest timescales in wave data on seasonal response (red oval in Figure 44), is less important. Moreover, two new clusters are formed (green ovals). One represents the effect of timescales in wave data of ≈2-4 months on shoreline response with a timescale of ≈200 days. The other cluster represents the effect of timescales in shoreline variation of ≈500 days on the seasonal response.

Narrabeen

Figure 45 presents the timescale interactions at Narrabeen when calibrated on a part of the dataset.

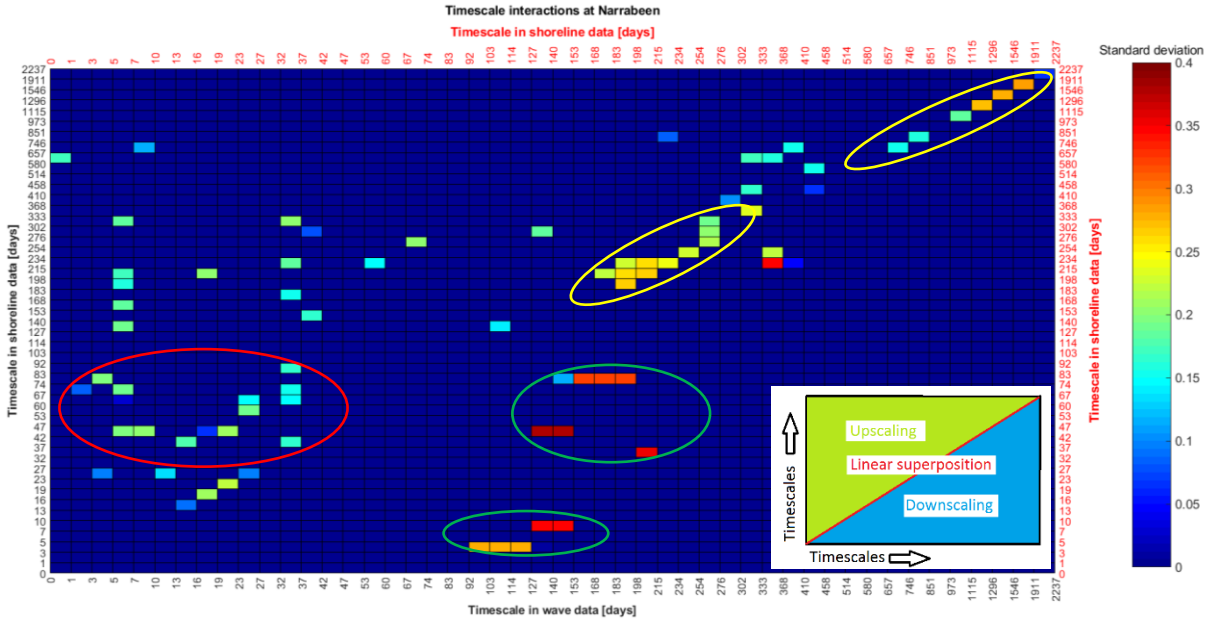

Figure 45: Timescale interactions at Narrabeen when calibrated on a part of the dataset

Figure 45 indicates the presence of five timescale clusters. If one compares this grid of timescale interactions with the one at Nha Trang (when calibrated on a part of the dataset (Figure 43)), it can be observed that at Narrabeen less distinct timescale interactions are present. Especially the upscaling approach generates multiple signals with various timescale interactions.

The linear superposition approach generates two clusters (yellow ovals in Figure 45) of which one consists out of timescales of approximately 215 days and the other out of the largest timescales in the dataset. The latter is due to the multiple linear regression constraints, mentioned in Table 8. The largest timescales are excluded from the up- and downscaling approach due to inaccuracy of the filter function. Hence, the linear superposition approach is responsible for modelling the most dominant timescale (≈215 days), which means that at this scale no timescale interactions are present. The upscaling approach generates one less distinct cluster (red oval), by which the other dominant timescale in beach response is modelled (≈60 days). It represents the effect of daily to monthly timescales in wave data on timescales in shoreline response of approximately 60 days. The downscaling approach generates two clusters (green ovals). Both represent the effect of timescales in shoreline variation of approximately 140 days on smaller timescales in shoreline response: the storm response timescale and a timescale of approximately 60 days. The other dominant timescale in beach response is also modelled by the downscaling approach and is thus affected by shoreline variations on a larger scale. Note that this is valid for the storm response as well.

Figure 46 presents the timescale interactions at Narrabeen when calibrated on the whole dataset.

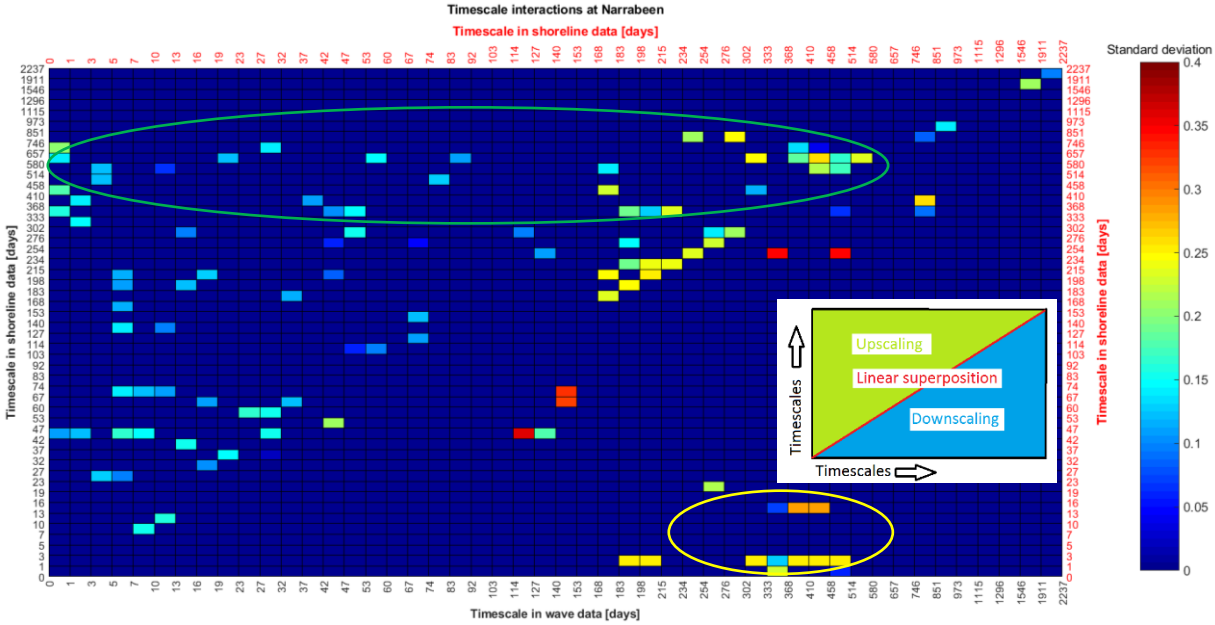

Figure 46: Timescale interactions at Narrabeen when calibrated on the whole dataset

Two new timescale clusters can be recognized in Figure 46 (indicated by the yellow and green ovals), when the grid of interactions is compared to the one in Figure 45. The yellow oval indicates that storm response timescales are not dependent anymore on shoreline variation with a timescale of approximately 140 days, but on shoreline variations with a seasonal timescale. The green oval expresses that all timescales in wave forcing cause shoreline change on timescales slightly larger than the seasonal one.

The fact that the new timescale cluster for the upscaling approach is present could have been expected. During model validation, the improvement at Narrabeen was not significant due to absence of distinct large timescales. The new cluster represents shoreline response with timescales of the order 1 to 2 years. Apparently, those timescales were not caught during calibration on a part of the dataset, causing minor improvement during model validation. It is hypothesized that the large accretion/erosion event of June-July 2007 is responsible for this. This event dominates model calibration on a part of the dataset, such that it affects timescale interactions. Another possible explanation is that the calibration period is too short to capture these timescales.

Moreover, less distinct clusters of timescales are present at Narrabeen, with the result that the shoreline is difficult to predict. No clear seasonal variation is observed in the shoreline position time-series. Such a variation is easier to predict because of the cyclic process. A comparison of Figure 44 and Figure 46 emphasizes this. The grid of timescale interactions at Nha Trang shows a clear timescale cluster for the upscaling approach (seasonal variation) while the grid at Narrabeen shows scattered timescale interactions. These predicted signals corresponding to the upscaling approach yield a suitable fit to the shoreline data during model calibration, but during validation this combination of signals is less representative for shoreline change.

Grand Popo

Figure 47 presents the timescale interactions at Grand Popo when calibrated on a part of the dataset.

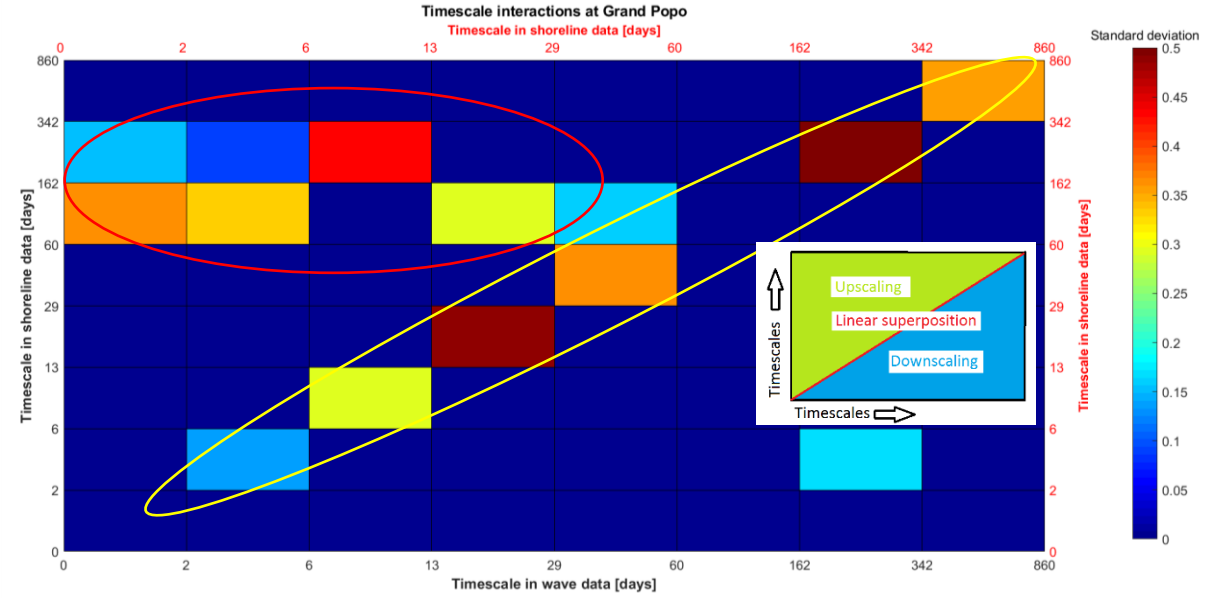

Figure 47: Timescale interactions at Grand Popo when calibrated on a part of the dataset

The largest contribution to shoreline change is modelled using the linear superposition- and upscaling approach. Two distinct clusters can be recognized. The upscaling approach represents the effect of timescales in wave data smaller than the monthly timescale (<=29 days) on beach response with timescales from 60 to 342 days (red oval). The other cluster represents the effect of waves with timescales larger than the storm timescale (>6 days) on shoreline response with corresponding timescales (yellow oval). As was already observed in the time-series, the downscaling approach has almost no contribution to shoreline change at Grand Popo. It was stated that this was due to the large amount of noise present at the small (storm) timescales.

Figure 48 presents the timescale interactions at Grand Popo when calibrated on the whole dataset.

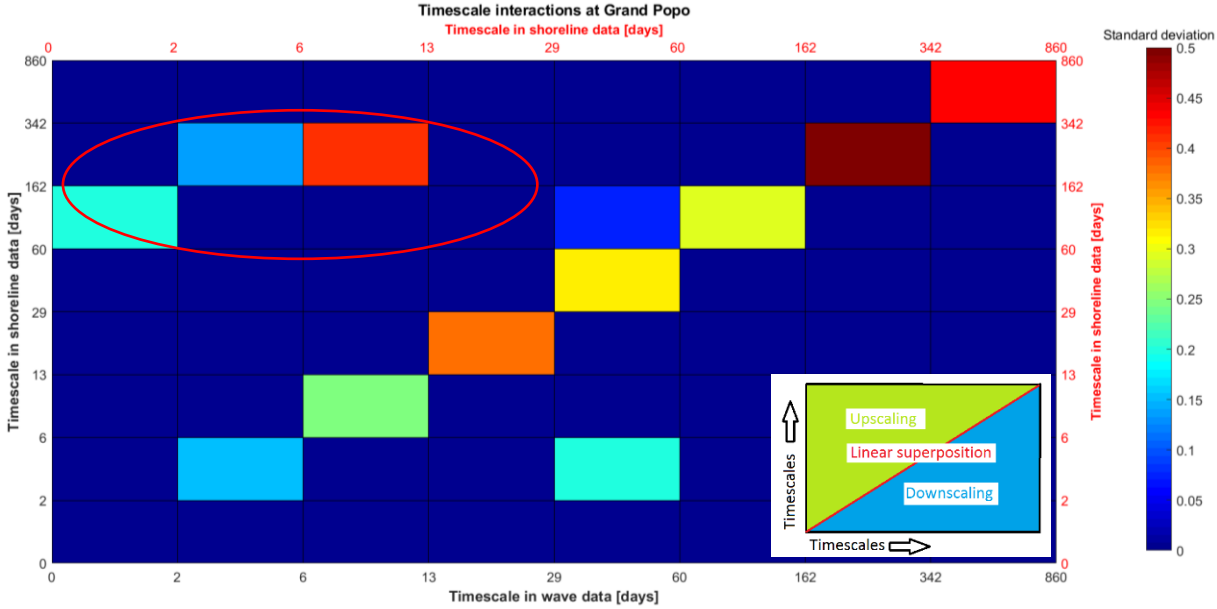

Figure 48: Timescale interactions at Grand Popo when calibrated on the whole dataset

The difference with the grid of timescale interactions when calibrated on a part of the dataset (Figure 47) is not significant. The largest difference arises from the fact that the predicted signals generated with the upscaling approach, contribute less to the total predicted shoreline change (red oval). The linear superposition approach is responsible for almost all predicted signals. This means that at Grand Popo, timescale interactions are limited and shoreline change is driven by waves with a corresponding timescale.

Timescale interactions of the downscaling approach

The section below elaborates the structure and variability over time of one particular signal generated with the downscaling approach. The considered signals have a large variability as indicated by the grids of interactions. Here, a single signal within a cluster of variability is described. Only predicted signals determined with the downscaling approach are presented, because these are subjected to the most complicated underlying physical concept.

Calibration on a part of the dataset at Nha Trang

At the Nha Trang dataset, one timescale-cluster corresponding to the downscaling approach was involved (green oval in Figure 43). The considered signal within the cluster represents the effect of shoreline variation with a timescale of 176 days on the monthly beach response (39 days) (green oval).

Figure 49 visualizes the composition of the downscaling approach. In the top panel, the filtered wave height with a timescale of 39 days (black) and the raw shoreline signal (blue) are presented as well as the real filtered shoreline signal (pink) and the dynamic response value (red). Note that the latter has the shape of the predicted shoreline signal using the linear superposition approach. The predicted- (shape of the red line) and real filtered shoreline signal match quite well, except in August 2014. A local accretion maximum is present while a local minimum is predicted (black oval in top panel). If a poorly predicted shape for the dynamic response factor is used, the underlying model assumptions are not valid anymore and the wrong conclusions will be drawn. However, Figure 43 indicates that the resulting predicted shoreline signal (black line in bottom panel) has a large contribution to the total predicted shoreline change. The reason for this is that the monsoons in October 2014 have a large impact on shoreline response (large response value), because the shoreline was in an overall accreted state. The beach profile was not able to effectively dissipate incoming energy, causing major shoreline change.

The falsely predicted secondary peak of the predicted shoreline signal (red oval in the top panel) has little consequence. This is due to the small wave forcing in the summer of 2014 (June until August), causing that the higher dynamic response value does not result in significant errors.

The response to monsoons is in phase with the corresponding forcing, as the memory decay factor is one day. Using the linear superposition approach, the modelled response to waves with the same wave height (and wave period) (green arrows) is the same. The real response to those waves is different (orange arrows), because the shoreline is accreted/eroded on a larger scale. To model this effect the dynamic response value has to be larger/smaller for these particular moment in time, which is implemented in the downscaling approach. The resulting predicted signal is indicated by the black line in the bottom panel.

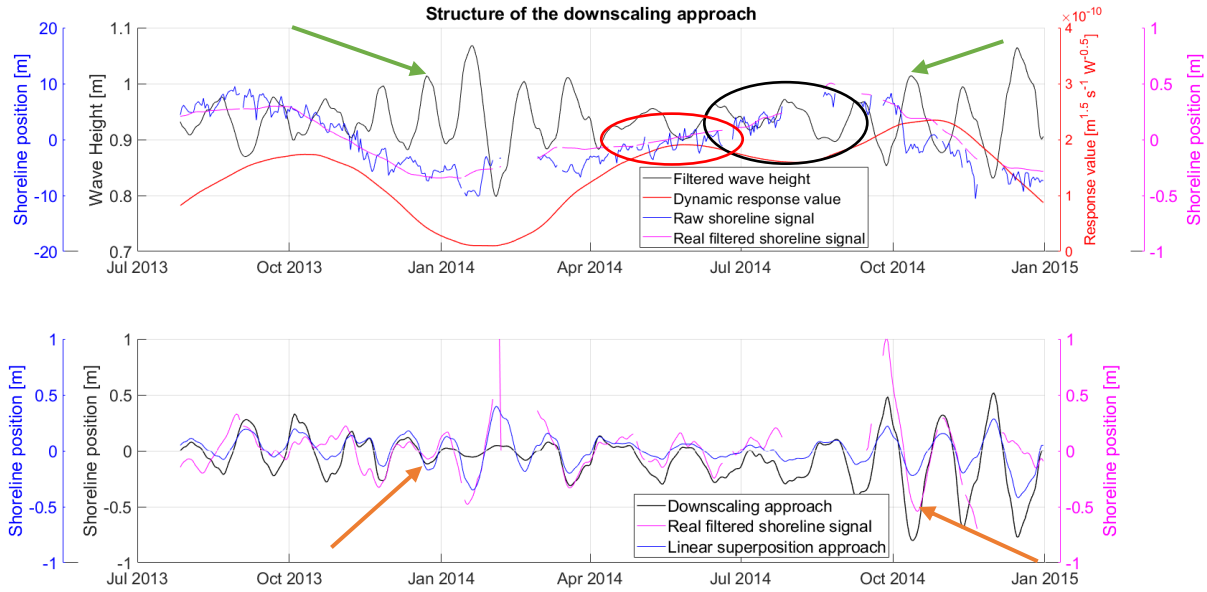

Figure 49: The composition and variability over time of a signal generated with the downscaling approach. The figure visualizes the effect of shoreline variation with a timescale of 176 days on shoreline response with a timescale of 39 days.

Calibration on the whole dataset at Nha Trang

Figure 50 presents the composition of the downscaling approach, representing the effect of shoreline variation with a timescale of 527 days on shoreline response with a timescale of 343 days.

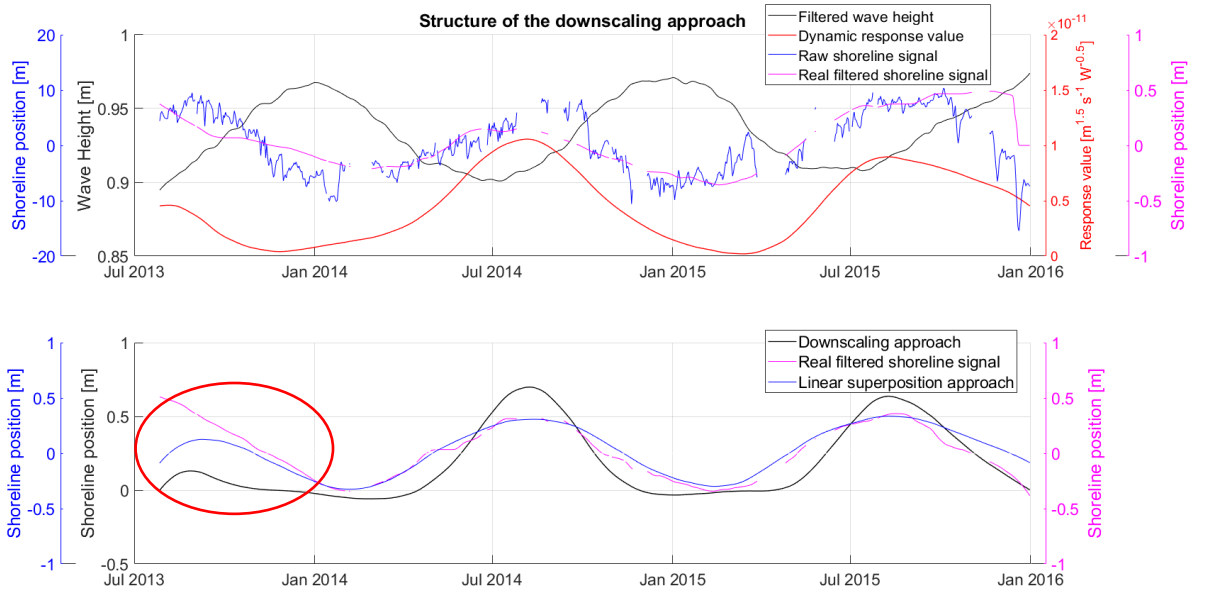

Figure 50: The effect of shoreline variation with a timescale of 527 days on shoreline response with a timescale of 343 days

The predicted shoreline signal using the downscaling approach (black line in the bottom panel) is a skewed signal with minor shoreline retreat during winter months and a major accretion peak during summer months. This signal can represent the fact that the shoreline is partly protected from summer monsoons, giving the beach opportunity to accrete under influence of smaller waves. If this is the case, it means that the underlying thought of the downscaling approach is not justified here. Moreover, this predicted shoreline signal was not used when calibrated on a part of the dataset, because of model spin-up (red oval in the bottom panel). The effect of the predicted signal using the downscaling approach (black line in the bottom panel) can easily be identified in the bottom panel of Figure 37 (difference between the black and red line): it is causing a clear accretion peak in the summer months.

Calibration on a part of the dataset at Narrabeen

For the Narrabeen dataset, two timescale-clusters corresponding to the downscaling approach are involved in the prediction of the shoreline (green ovals in Figure 45). The composition of the signal of the first cluster is presented in Figure 51, representing the effect of shoreline variation with a timescale of 183 days on shoreline response with a timescale of 83 days.

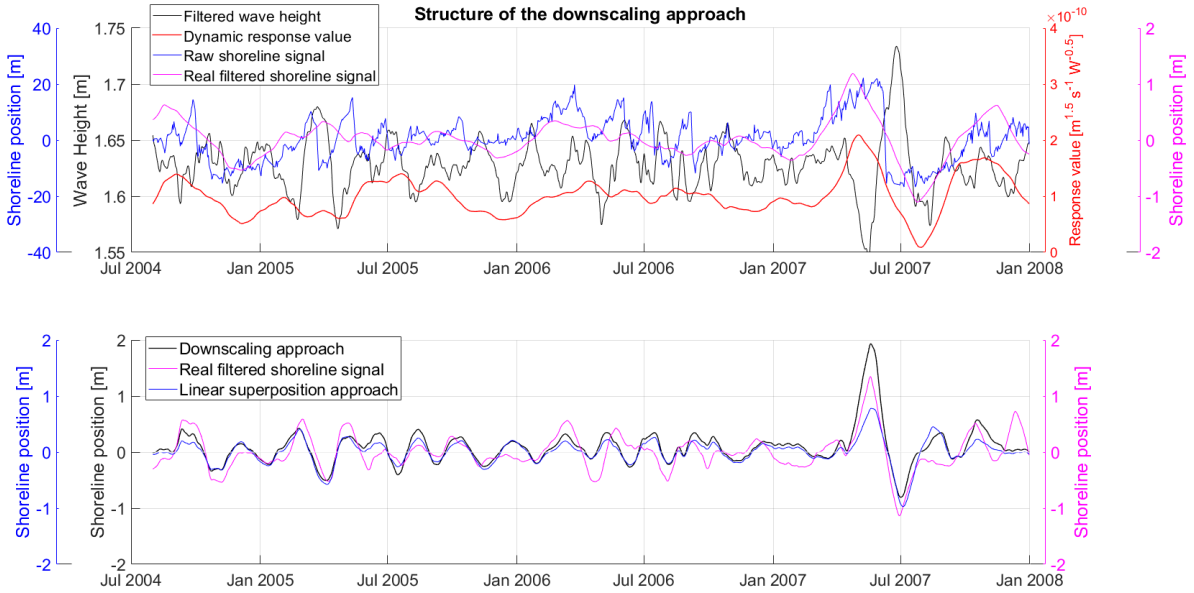

Figure 51: The effect of shoreline variation with a timescale of 183 days on shoreline response with a timescale of 83 days

The effect of the dynamic response value is limited, because the predicted shoreline signal generated with the linear superposition approach (blue line in the bottom panel) and the predicted shoreline signal determined with the downscaling approach (black line in bottom panel) are not significantly different. The largest difference is in 2007, where the predicted accretion using the downscaling approach is considerably larger compared to the predicted accretion using the linear superposition approach. This is due to the dynamic response value (red line in the top panel), because it attains an almost twice as high value during this period compared to the rest of the dataset.

In order to adequately model the large accretion event in May-June 2007, it appears that during this period the sediment transport efficiency of small waves is larger than to similar waves in the dataset. This cannot be modelled using a constant response factor, causing that the predicted signal generated with the linear superposition approach is not used for the prediction of the total shoreline signal.

The composition of the signal of the second cluster is presented in Figure 52, corresponding to the effect of shoreline variation with a timescale of 153 days on shoreline response with a timescale of 10 days.

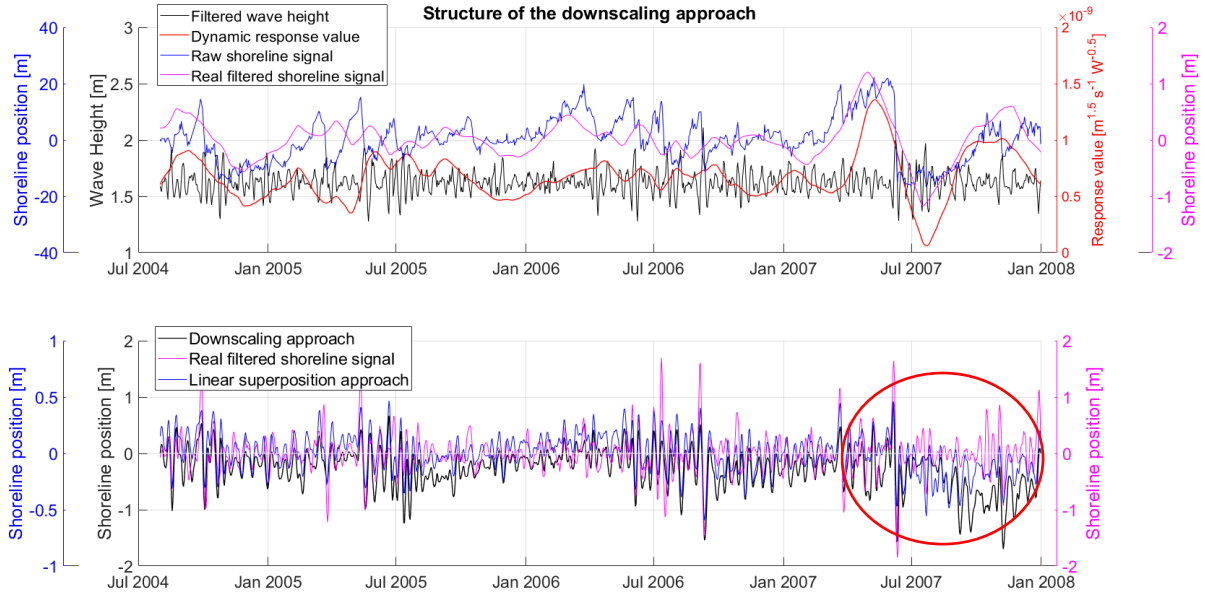

Figure 52: The effect of shoreline variation with a timescale of 153 days on shoreline response with a timescale of 10 days

Figure 52 indicates that small (storm) timescales can be predicted with a significant amount of skill (black line compared to the pink line in the bottom panel). However, both the predicted signal generated with the linear superposition approach and the predicted signal determined with the downscaling approach vary on larger timescales. For example, such a large scale variation occurs from July 2007 until January 2008 (red oval). This large scale variation can be due to an imbalance of erosion/accretion forcing on a larger timescale. Over the total dataset this balance is governed by the erosion ratio such that no trend in wave forcing results in no trend in the predicted shoreline signal. However, on smaller timescales an imbalance can be present for a certain period. This causes erosion/accretion events on timescales larger than the storm timescale.

Because no variation on a larger scale is present in the real filtered shoreline signal (pink line in the bottom panel), amplitudes are kept low during ShoreFor's optimization (due to a low response value) when the linear superposition approach is applied. The amplitude of the predicted signal generated with the downscaling approach, is determined based on the variability within each timescale bin. This results in different signal variabilities for the two approaches as is highlighted by the different y-limits used in the bottom panel of Figure 52.

Figure 53 presents the same time-series as visualized in Figure 52, but only for the year 2007. The memory decay factor for the prediction of shoreline response with a timescale of 10 days, is 8 days. This means that the dynamic equilibrium condition (accounting for the negative feedback mechanism) in July 2007 is not dependent anymore on the waves that cause the large erosion event in June 2007. However, the real response (pink line in the bottom panel) to the storms in July 2007 is different than the response to the first large storm in June 2007. The storm response in July 2007 is still dependent on the large erosion event in June 2007: the storms in July 2007 have a smaller response as the coastline is more in equilibrium with the high forcing. The downscaling approach captures this effect by using a dynamic response value. With a constant response value as used by the linear superposition approach, those different responses cannot be modelled correctly.

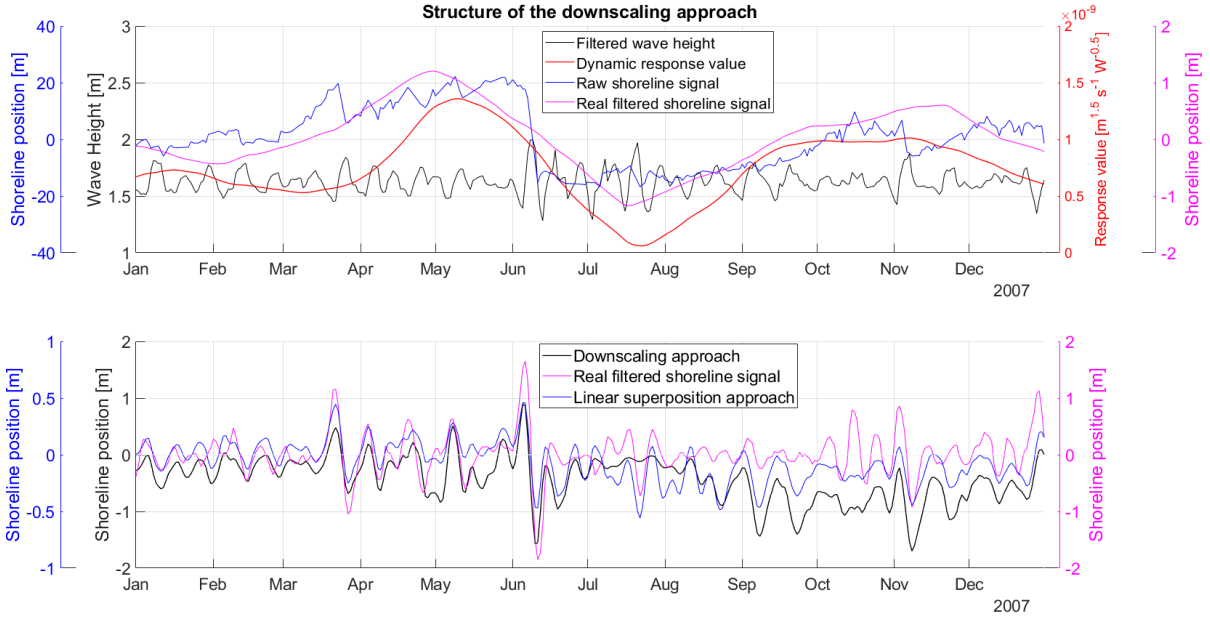

Figure 53: Effect of large timescales in shoreline position (153 days) on smaller timescales in shoreline position (10 days) (limited timespan)

During the multiple linear regression analysis it is determined that the predicted signal generated with the downscaling approach (black line in the bottom panel) can better be used for the prediction of the storm response timescale than the predicted signal determined with the linear superposition approach (blue line in the bottom panel). In this case, several reasons can play a role: First, the variability of the predicted signal generated with the downscaling approach is larger than the variability of the predicted signal determined the linear superposition approach. Secondly, in the total shoreline signal (Figure 32), the large scale variations (red oval in Figure 52) are partly countered by other predicted signals of the downscaling approach or correspond well to the large scale shoreline variation. Hence, the combination of all predicted signals generated with the downscaling approach makes sure that the storm response timescale and the corresponding large scale variations are represented well by the model. Thirdly, the predicted signals generated with the downscaling approach are yielding a better representation of the storm response (apart from the large scale variations) as indicated by Figure 53. This means that the storm response at Narrabeen is dependent on whether the coastline is eroded/accreted on a larger scale.

5.4 Summary model results

In this section a summary of the model results is presented. Per dataset, it will be shown which combination of model improvement steps yields the best model result. Moreover, the dominant timescales and the timescale interactions are highlighted.

Nha Trang

The shoreline at Nha Trang (Vietnam) is subjected to a dominant seasonal response, which can be modelled best using the upscaling approach. This means that small timescales in wave signals (< 1 year) have a large effect on seasonal shoreline response. The less dominant monsoon response can be modelled best by the downscaling approach. This indicates that the response to monsoons is not equal throughout the year. Beach response to monsoons (20-30 days) is larger when the shoreline is accreted on a larger scale (4-6 months). Due to an overall accreted beach state, the beach profile is not able to effectively dissipate incoming wave energy, causing major shoreline changes. Adversely, when the coastline is already eroded on a larger scale the monsoon response is therefore smaller.

Narrabeen

The beach at Narrabeen (Australia) has a significant amount of beach response timescales. The most dominant mode of shoreline response (≈220 days) can best be modelled using the linear superposition approach. Hence, this response is caused by corresponding timescales in wave forcing: no interaction between timescales is present. The storm response can be modelled using the downscaling approach. This indicates that the response to storms (<3 days) is not equal throughout the year, but dependent on whether the coastline is eroded or accreted due to the seasonal variation (1 year). This is identical at Nha Trang, where the monsoon response is dependent on the seasonal variation. The effect of small timescales in wave data (< 2 months) on larger beach response scales is significant, but the beach response timescales are less distinct than at Nha Trang: no clear cluster of timescales can be recognized. This is logical because other than the most dominant beach response timescale (≈220 days), the temporal spectrum is not indicating other dominant beach response modes.

Grand Popo

The shoreline at Grand Popo (Benin) is subjected to a dominant seasonal response, which can be modelled best using a combination of the linear superposition- and upscaling approach. This implies that the effect of storm to seasonal timescales in wave data on seasonal response is significant. Other, less dominant timescales can be modelled with the linear superposition approach as well: the predicted signals generated with the linear superposition approach are contributing most to the total shoreline change prediction. This suggests that the interaction between timescales is limited at Grand Popo. The downscaling approach is not contributing significantly to the overall shoreline response. It is hypothesized that this is due to the large amount of noise present in the shoreline signal.

5.5 Overview model improvements

Table 13 provides an overview of the model improvements for all datasets. Per dataset the RMSE between model prediction and data is presented for the two calibration cases: calibration on a part of the dataset and calibration on the whole dataset. Moreover, the RMSE for the validation phase is presented as well. Three modelling cases are provided per dataset: firstly, ShoreFor is applied without the linear trend term (as used in this report) and secondly, ShoreFor is applied including the linear trend term (as used in Splinter et al., 2014) and thirdly, the improved model is applied as introduced in this thesis. All raw wave- and shoreline signals are detrended (to get rid of linear trends) to establish the results of the first- and third modelling cases. The input-signals used by the second model (both wave- and shoreline data) are subjected to linear trends. The improvement percentage is calculated by comparing ShoreFor- and improved model results, in which for ShoreFor the modelling case with the lowest RMSE is chosen. Note that an overview of the ΔAIC scores is included as well.

RMSE [m]	**Part of dataset**		**Whole dataset**
	Calibration	***Validation***	***Calibration***
Nha Trang			
ShoreFor (without linear trend)	4.31	4.36	3.83
ShoreFor (with linear trend)	2.67	-	3.73
Improved model	1.86	2.52	2.13
Improvement	**+30%**	**+42%**	**+43%**
ΔAIC [-]	174	0	225
Narrabeen			
ShoreFor (without linear trend)	5.06	7.31	6.26
ShoreFor (with linear trend)	4.88	-	5.38
Improved model	2.82	6.88	3.77
Improvement	**+42%**	**+6%**	**+30%**
ΔAIC [-]	378	-307	679
Grand Popo			
ShoreFor (without linear trend)	3.00	2.93	2.87
ShoreFor (with linear trend)	2.79	-	2.73
Improved model	2.65	2.13	2.60
Improvement	**+5%**	**27%**	**5%**
ΔAIC [-]	19	-46	26

Table 13: Overview of the model improvements per dataset

The difference in RMSE between ShoreFor with- and without linear trend term is not significant except at Nha Trang when calibrated on a part of the dataset (2.67m and 4.31m, respectively) and at Narrabeen when calibrated on the whole dataset (5.38m and 6.26m, respectively). The difference at Nha Trang can be due to the strong seasonal variation, where the phase of the seasonal shoreline variation is different at the start- and end of the dataset. It is possible that ShoreFor recognizes this as a trend while this is not the case. However, due to this modelled trend, a better fit to the shoreline signal is found. At Narrabeen no clear trend can be identified. However, the results indicate that when ShoreFor is applied, the shoreline position at Narrabeen can better be modelled by including the linear trend term.

6 Discussion

The ShoreFor model (Splinter et al., 2014) is improved by using three distinct steps (i.e. the linear superposition-, upscaling- and downscaling approach) to account for multiple temporal scales. Each step creates multiple shoreline predictions with different temporal scales. Thereafter, a multiple linear regression analysis is carried out to determine which combination of predicted signals can be used best for the prediction of the raw shoreline signal. The combination of predicted signals is plotted in a grid to present an overview of timescale interactions. The memory decay factor in ShoreFor yields an indication of the dominant mode of shoreline response (Splinter et al., 2014). For the improved model, the grid of timescale interactions yields an overview of the multiple temporal scales involved. For datasets with a large memory decay factor (determined by ShoreFor), the grid of interactions also implies that large timescales are important for coastline prediction. For datasets with a small memory decay factor the opposite is true. It can be stated that both models are able to find the most dominant mode of shoreline response, but the improved model is capable of finding multiple, less dominant temporal scales as well.

The largest model improvement is at Nha Trang for both the calibration- and validation phase, when the RMSE is used as indicator for prediction skill. This is due to the fact that multiple dominant beach response timescales play an almost equal role in determining coastline evolution (Almar et al., 2017). ShoreFor is only capable of accurately predicting shoreline response to a single dominant timescale (the seasonal response), causing poor model performance. By including multiple distinct timescales a large improvement is made, because the other dominant timescales are accurately predicted as well. These multiple distinct timescales (monsoon- and seasonal variability) can easily be identified in the grid of timescale interactions.

At Narrabeen model improvement is significant during the calibration phase, but not during the validation phase. It is hypothesized that the large accretion/erosion event in June-July 2007 is responsible for this in combination with a too short calibration period. This event is dominant during model calibration, such that it affects the timescale interactions. Using a larger calibration period (i.e. the whole dataset), the large accretion/erosion event in June-July 2007 becomes less dominant and large timescales become more dominant. These large beach response timescales were not captured during model calibration on a part of the dataset, causing a poor validation result.

For the dataset at Grand Popo improvement is made for both phases, but for the calibration phase the improvement is minor. The third dominant (small) timescale in shoreline response (Table 6) is considered to mainly exist out of noise. Due to this noise the bin distribution is affected, such that only 8 timescale bins are used. It is hypothesized that the improved model cannot find suitable relations between the filtered wave- and shoreline time-series, because the timescales are poorly separated from each other. However, during model validation the improvement is significant. This is mainly due to the fact the validation period is short. Because the time-span centre of the dataset (January 2015 to January 2016) is subjected to a significant amount of data-gaps, a suitable trade-off between the calibration- and validation period is hampered.

An important aspect is the difference between grids of interactions when calibrated on a part of the dataset and on the whole dataset. If these grids of timescale interactions are identical, it means that the calibration period when calibrated on a part of the dataset is long enough and that dominant timescales stay dominant over time. For the datasets at Nha Trang and Grand Popo, the timescale of the dominant seasonal response is constant over time as can be confirmed by the two grids of interactions. For the dataset at Narrabeen, the two grids of interactions differ significantly, causing a poor result during model validation.

A comparison between grids of interactions (when calibrated on the whole dataset) reveals properties of the different modelling steps. If a seasonal variation (large timescale) is present in the raw shoreline position time-series, the upscaling- or linear superposition approach makes sure that this variation is captured. Storm to monthly (small) timescales are mostly captured by the downscaling approach. This partly shows that the different approaches model the correct beach response timescales, because downscaling is a procedure to get information of smaller timescales using larger timescales (vice versa for upscaling). However, where the seasonal/large timescale variability is modelled well in all cases, the prediction of smaller timescales (daily to weekly) can still be improved. Especially at Nha Trang and Grand Popo this is the case. Multiple aspects can play a role with respect to the poor prediction skill at small timescales. For example, because the smallest timescales are most sensitive to noise.

A relation is present between the temporal spectra and grids of timescale interactions. For each site, the dominant temporal scales of shoreline response and wave power (visualized by the temporal spectra) can be found in the grids of interactions as well. Hence, the spectra indicate up front a degree of interactions between timescales. Moreover, the timescale distributions can be used to determine if the improved model is favorable with respect to ShoreFor. In Figure 54 synthetic spectra are presented. If multiple dominant timescales are present in the spectra, the model improvement will be significant (for the calibration- and validation phase). If merely one dominant timescale is present, a limited model improvement is expected. An example of a limited model improvement is the dataset at Narrabeen. Both the wave power spectrum and the shoreline spectrum (Figure 69) imply that only one timescale is the most dominant, causing a limited improvement for the validation phase.

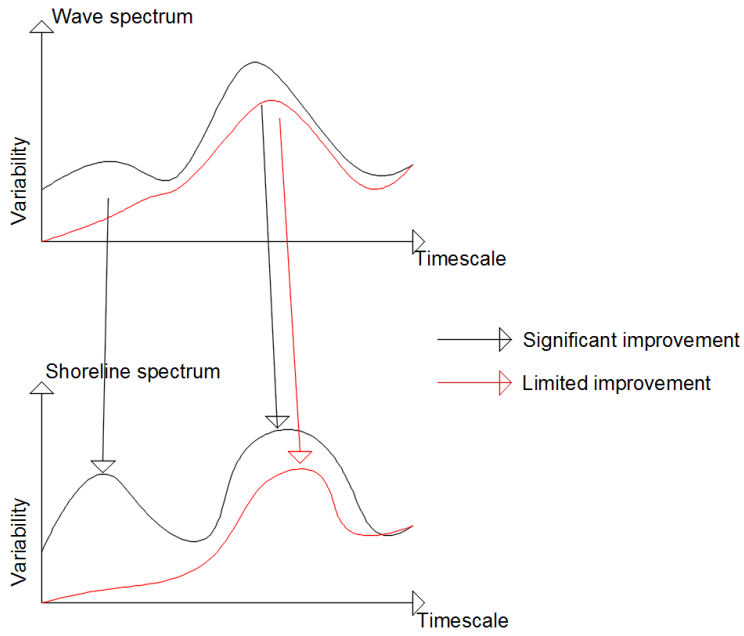

Figure 54: Synthetic spectra indicating whether or not the improved model is favorable with respect to ShoreFor

Model drawbacks

In this research, ShoreFor is used as benchmark to predict shoreline change. Hence, the same limitations mentioned in Splinter et al. (2014) apply to the improved model as well. The only difference is that multiple timescales are implemented in the improved model, whereas ShoreFor only accurately determines the most dominant shoreline response timescale. However, the approach used for implementing multiple temporal scales poses new model limitations.

First, the constraints for the multiple linear regression analysis are important for the determination of timescale interactions. The current constraints are determined based upon a simple optimization process, but it cannot be guaranteed that all chosen signals represent the correct physical processes. As a consequence, the individual structure of a predicted signal within a timescale cluster always need to be checked. For example, at Nha Trang when calibrated on the whole dataset: a skewed predicted signal generated with the downscaling approach (black line in the bottom panel of Figure 50) was chosen by the multiple linear regression analysis. The minor shoreline retreat during winter months and major accretion during summer months represents the fact that the shoreline is partly protected from summer monsoons. This gives the beach opportunity to accrete under influence of smaller waves. However, the underlying thought of the downscaling approach is not justified in that case, such that the predicted signal had to be excluded from the multiple linear regression analysis.

Secondly, ShoreFor is constructed such that the computation time is limited (order of seconds/minutes depending on the dataset duration). However, the improved model is computationally less efficient as a large number of signals need to be filtered and predicted. For the longest dataset (Narrabeen) the running time easily exceeds one hour.

Thirdly, the modelling structure of the improved model is not efficient (Figure 55). Currently, the bin-distribution is such that the maximum amount of bins is used. Note that this distribution was based on an equal amount of shoreline variability within each bin. Subsequently, shoreline signals are predicted for all timescale interactions (i.e. the three model improvement steps), for the calibration- and validation phase. Thereafter, the multiple linear regression (MLR) analysis is carried out utilizing signals of the calibration phase. This determines which combination of predicted signals can be used best to represent the raw shoreline signal. The same combination of signals responsible for modelling shoreline change during model calibration, is used for the validation phase as well. The signals used for model validation, were already predicted before the MLR analysis was carried out. However, before the MLR analysis it is not necessary to predict all the signals for the validation phase, because only a selection is used for modelling shoreline change.

Figure 55: Current modelling structure of the improved model

Fourthly, the temporal spectra and filtered shoreline position and forcing signals are highly dependent on the developed filter function. The developed filter function has limitations and a certain accuracy, such that timescale errors are made (appendix B).

Fifthly, some drawbacks/inaccuracies arise from the implementation of the up- and downscaling approach. More precisely, due to the timescale-links: for the upscaling approach the envelope creates the link and for the downscaling approach the dynamic response value provides the link between timescales. However, the envelope lacks a strong physical underlying meaning and is merely an approach to determine the effect of small timescales in wave data on larger beach response timescales. The downscaling approach has a stronger underlying meaning as small timescales in beach response are dependent on larger scale shoreline variations. To model this, the dynamic response value should correspond to the shape of these larger scale shoreline variations. However, these shoreline variations are not available during model validation and the predicted signal determined with the linear superposition approach is used. This predicted signal is not exactly identical to the real shoreline signal and poses inaccuracies within the model. Note that predicted signals with a very large inaccuracy are excluded from the multiple linear regression analysis by the imposed constraints.

Finally, Table 13 shows that during model validation, the ΔAIC scores are negative or zero when all the various cases and datasets are considered. This indicates that too many calibration parameters are used for model improvement.

7 Conclusions

In this thesis, the equilibrium shoreline prediction model ShoreFor (Shoreline Forecast) is improved by allowing for the implementation of multiple morphological timescales. ShoreFor was not able to accurately model shoreline change on multiple dominant timescales due to the use of a single memory decay factor, where the memory decay factor describes the dominant response time of cross-shore sediment exchange. The improved model identifies which timescales are present in the forcing- and shoreline signals by applying a filter function. The filtered forcing- and shoreline signals (with different timescales) are related to each other and are interacting. This is modelled using three new- and distinct steps: a linear superposition-, an upscaling- and downscaling approach. In the first step, corresponding timescales in the wave- and shoreline data are related to each other. In the second step, the effect of small timescales in wave forcing on larger scales in shoreline response is determined, where the envelope of the wave forcing provides the timescale-link. In the third step, the effect of large timescales in shoreline variation on smaller timescales in shoreline response is determined, in which a dynamic response factor provides the timescale-connection. The dynamic response factor encapsulates the fact that sediment transport efficiency varies over time. To illustrate the improved model, it has been applied to three sites where high resolution data encompassing multiple timescales is available: at Nha Trang in Vietnam, Narrabeen in Australia and Grand Popo in Benin.

The relative importance of ongoing and antecedent wave-forcing properties on shoreline response is illustrated during this study. A higher ongoing forcing intensity results in increased coastline erosion, if that coastline was in equilibrium with the antecedent milder forcing conditions. Beaches need time to respond towards an equilibrium with ongoing forcing conditions: a higher duration results in more available time for the beach to reach an equilibrium, hence larger shoreline changes. The effect of sequencing of wave conditions is still subject to ongoing research. However, in this study it was found that the erosional response to clusters of high-intensity forcing conditions is generally larger than the sum of the erosional response of each individual high-intensity forcing event that make up the cluster.

The concept of memory decay provides opportunities to describe multiple different forcing timescales and their effect on shoreline response. If corresponding filtered timescales are related: a small memory decay factor indicates that temporal scales in the filtered wave- and shoreline position time-series are small. Large factors indicate large timescales of shoreline response and wave forcing. Hence, different timescales are described by using the memory decay factor in combination with filtering.

Shoreline response can be represented by a linear combination using multiple distinct forcing timescales. The three model improvement steps relate multiple timescales to each other, in which numerous shoreline signals on different temporal scales are predicted. Which linear combination of predicted signals can be used best for coastline prediction is determined by the subsequent multiple linear regression analysis, based on a comparison with the measured shoreline position data. The temporal scales involved in shoreline change are disclosed by the succeeding grid of timescale interactions.

Table 14 presents an overview of the relative model improvement per study site. The root mean squared error is used as an indicator for the prediction skill.

Improvement	Calibration	Validation
Nha Trang	+30%	+42%
Narrabeen	+42%	+6%
Grand Popo	+5%	+27%

Table 14: Relative model improvement per site

The improved shoreline prediction model outperforms ShoreFor on sites where multiple dominant forcing- and beach response timescales are present (e.g. Nha Trang). Temporal spectra of the raw shoreline position- and wave power time-series indicate in advance if multiple temporal scales are present. Hence, they can be used to assess which model can be applied best.

8 Recommendations

In this report, a method is presented to improve shoreline predictions in comparison with the ShoreFor model. The improved model is able to accurately predict shoreline change due to multiple dominant forcing timescales, unlike the ShoreFor model. However, the improved model is in an early stage of development and poses new assumptions and limitations, which means that it can be subject to further research. In this section, some recommendations are highlighted.

First of all, the computation time of the model is significantly enlarged due to the filtering of signals in combination with the amount of timescale bins used: multiple signals need to be predicted instead of only one. Code optimization using pre-allocation and vectorization can decrease the computation time.

Secondly, the modelling structure of the improved model is not efficient (left structure in Figure 56). The suggested structure of the improved model is presented on the right hand side in Figure 56. The first step is identical to the one of the current structure: filtering the raw signals, such that the maximum amount of bins is used. Subsequently, shoreline signals are predicted, but only for the calibration phase. Thereafter, the MLR analysis is carried out to determine the timescale interactions: the model is calibrated. The next modelling step is to predict shoreline signals for the validation phase. However, only a selection of signals are predicted (determined by the MLR analysis). This suggested approach will result in a more efficient model and a decreased computation time.

For the forecasting phase the same approach mentioned in Davidson et al. (2010) is recommended: generate multiple synthetic wave time-series to encapsulate the statistical properties of the measured wave field. Subsequently, use these synthetic series in a Monte Carlo simulation to drive the calibrated model and generate multiple (e.g. one thousand, as used in Davidson (2010)) shoreline prediction time-series. The ensemble-average of these shoreline forecasts can be taken, such that it results in a single forecast.

In the forecasting phase, multiple shoreline predictions are generated as stated above. Each of these shoreline predictions are also generated using multiple signals with distinct timescales. This will result in large computation times. Another suggestion is therefore to implement a bin optimization-loop within the modelling structure (Figure 56), such that an optimum amount of bins is reached considering prediction skill in combination with the amount of bins used. The Akaike's information criterion (AIC) can be used to find the optimum amount of bins, which is designed to compare models with different numbers of calibration parameters. Where in this case, the number of calibration parameters is dependent on the amount of bins used.

Instead of bin optimization another approach can be used as well: only select the most dominant timescale components which are indicated in the grid of timescale interactions. Or in other words, only select the clusters of timescales. However, this is a subjective approach as this selection is based on visual inspection. A more suitable approach would be to utilize similar methods as used for wave input reduction.

The approaches above to minimize the amount of predicted signals (and hence calibration parameters) during the validation- and forecasting phase, can also be used to ensure that all ΔAIC scores in Table 13 will be positive. In that case, both indicators for model improvement (RMSE and ΔAIC) will suggest that the improved model always outperforms ShoreFor.

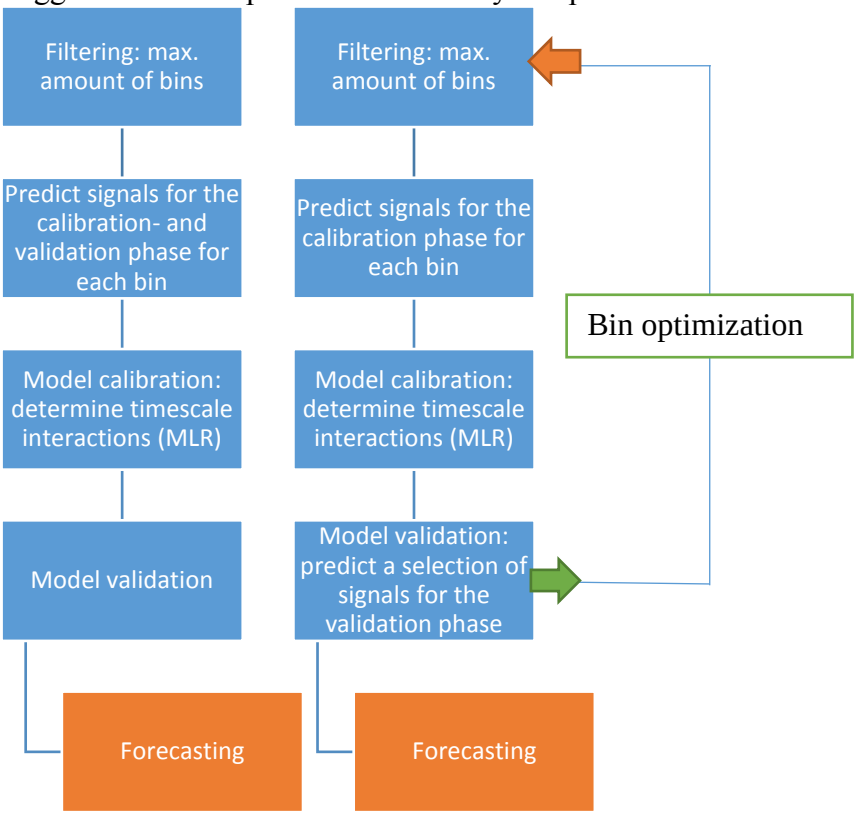

Figure 56: Current modelling structure of the improved model (left) and the suggested modelling structure (right)

Thirdly, the developed filter function is of major importance during all three model improvement steps. It is therefore suggested to use a different filter function to fully explore the consequences of the currently applied one.

The fourth suggestion is to apply the improved model to different datasets for further investigation of general model applicability. An interesting one is the dataset at Gold Coast (Australia), because ShoreFor is designed utilizing this dataset and a lot of morphological data is available here.

The fifth recommendation is about the constraints used for the multiple linear regression analysis. The current constraints filter out most insignificant signals, but it cannot be guaranteed that all used predicted shoreline signals represent the correct physical processes. If an approach can be found such that all predicted signals are justified, the structure of each individual signal within a timescale cluster does not need to be checked anymore. In this way, the grid of timescale interactions indicates in a glance, which timescales are involved in coastline evolution.

The last recommendation is to implement the linear trend term back into the model. A suggestion is to first determine the linear trend with ShoreFor. Subsequently, a linear combination of the total predicted shoreline signal (determined with the improved model) and the linear trend term can give a simple representation.

9 Bibliography

Almar, R., Marchesiello, P., Almeida, L. P., Thuan, D. H., Tanaka, H., & Viet, N. T. (2017). Shoreline response to a sequence of typhoon and monsoon events. *Water (Switzerland)*, *9*(6). https://doi.org/10.3390/w9060364

Battjes, J. A. (n.d.). CHAPTER 26, (1), 466–480.

Coco, G., & Ciavola, P. (2017). *Coastal Storms*.

Coco, G., Senechal, N., Rejas, A., Bryan, K. R., Capo, S., Parisot, J. P., … MacMahan, J. H. M. (2014). Beach response to a sequence of extreme storms. *Geomorphology*, *204*, 493–501. https://doi.org/10.1016/j.geomorph.2013.08.028

Davidson, M. A., Lewis, R. P., & Turner, I. L. (2010). Forecasting seasonal to multi-year shoreline change. *Coastal Engineering*, *57*(6), 620–629. https://doi.org/10.1016/j.coastaleng.2010.02.001

Davidson, M. A., Splinter, K. D., & Turner, I. L. (2013). A simple equilibrium model for predicting shoreline change. *Coastal Engineering*, *73*, 191–202. https://doi.org/10.1016/j.coastaleng.2012.11.002

Davidson, M. A., & Turner, I. L. (2009). A behavioral template beach profile model for predicting seasonal to interannual shoreline evolution. *Journal of Geophysical Research: Earth Surface*, *114*(1), 1–21. https://doi.org/10.1029/2007JF000888

Davidson, M. A., Turner, I. L., Splinter, K. D., & Harley, M. D. (2017). Annual prediction of shoreline erosion and subsequent recovery. *Coastal Engineering*, *130*(January), 14–25. https://doi.org/10.1016/j.coastaleng.2017.09.008

Kriebel, B. D. L., & Dean, R. G. (1993). BEACH-PROFILE RESPONSE, *119*(2), 204–226.

Larson, M., & C. Kraus, N. (1995). Prediction of cross-shore sediment transport at different spatial and temporal scales. *Marine Geology*, *126*(1–4), 111–127. https://doi.org/10.1016/0025-3227(95)00068-A

Lee, G. hong, Nicholls, R. J., & Birkemeier, W. A. (1998). Storm-driven variability of the beach-nearshore profile at Duck, North Carolina, USA, 1981-1991. *Marine Geology*, *148*(3–4), 163–177. https://doi.org/10.1016/S0025-3227(98)00010-3

Miller, J. K., & Dean, R. G. (2004). A simple new shoreline change model. *Coastal Engineering*, *51*(7), 531–556. https://doi.org/10.1016/j.coastaleng.2004.05.006

Milne, I. A., Sharma, R. N., Flay, R. G. J., & Bickerton, S. (2013). Characteristics of the turbulence in the flow at a tidal stream power site Subject Areas :

Ondoa, G. A., Bonou, F., Tomety, F. S., du Penhoat, Y., Perret, C., Degbe, C. G. E., & Almar, R. (2017). Beach response to wave forcing from event to inter-annual time scales at grand popo, benin (Gulf of Guinea). *Water (Switzerland)*, *9*(6). https://doi.org/10.3390/w9060447

Roelvink, D. J. A., & Stive, M. (1989). Bar-generating cross-shore flow mechanisms on a beach, (April). https://doi.org/10.1029/JC094iC04p04785

Southgate, H. N. (1995). The effects of wave chronology on medium and long term coastal morphology. *Coastal Engineering*, *26*(3–4), 251–270. https://doi.org/10.1016/0378-3839(95)00028-3

Splinter, K.D., et al. (2014). A generalized equilibrium model for predicting daily to inter-annual shoreline response, (January 2015), 1–23. https://doi.org/10.1002/2014JF003106

Splinter, K. D., Turner, I. L., Reinhardt, M., & Ruessink, G. (2017). Rapid adjustment of shoreline behavior to changing seasonality of storms: observations and modelling at an open-coast beach. *Earth Surface Processes and Landforms*, *42*(8), 1186–1194. https://doi.org/10.1002/esp.4088

van Rijn, L. C., Wasltra, D. J. R., Grasmeijer, B., Sutherland, J., Pan, S., & Sierra, J. P. (2003). The predictability of cross-shore bed evolution of sandy beaches at the time scale of storms and seasons using process-based profile models. *Coastal Engineering*, *47*(3), 295–327. https://doi.org/10.1016/S0378-3839(02)00120-5

Wright, L. D., Short, A.D., Green, M. O. (1985). Short-term changes in the morphodynamic states of beaches and suf zones: an empirical predictive model. *Marine Geology*, *62*(1182).

Yates, M. L., Guza, R. T., & O'Reilly, W. C. (2009). Equilibrium shoreline response: Observations and modeling. *Journal of Geophysical Research: Oceans*, *114*(9), 1–16. https://doi.org/10.1029/2009JC005359

Appendix A: Relevant coastal processes

In this appendix, a small summary of relevant hydro- and morphodynamic mechanisms is presented, with the emphasis on cross-shore processes.

Hydrodynamics

Waves

When waves in deep water travel towards the beach, they will start to feel the bottom and at a certain moment wave transformation takes place. During this transformation some processes/mechanisms are important, such as shoaling, bottom friction and wave-breaking. As a consequence of these processes, the wave height, wave length and wave energy is transforming/dissipating.

Shoaling

The effect of shoaling over a flat, sloping bottom is initially to decrease but then to increase the amplitude. Under stationary conditions and normal incident waves, a decrease of transport velocity (waves travel slower when the water depth decreases) must be compensated by an increase of the wave amplitude in order to satisfy the energy balance. Furthermore, according to the linear wave theory a decrease of the wave length will be present while the wave period remains constant.

Bottom friction

If waves approach the shore and they start to feel the bottom, a boundary layer is formed (where turbulence is important) between the free stream velocity of the waves and the bottom. The friction in the wave boundary layer results in dissipation of wave energy. Furthermore, the water moving along the bed imposes a shear stress on the bed. The time varying shear stress at the bed is often strong enough to set sediment grains into motion. Moreover, a net transport of sediment due to wave-induced streaming (Longuet-Higgins) can be present.

Wave breaking

A wave crest becomes unstable and starts breaking when the particle velocity exceeds the velocity of the wave crest (the wave celerity). Miche's breaking criterion expresses when a wave starts to break:

$$\left[\frac{H}{L}\right]_{\max} = 0.142 \tanh(kh) \tag{23}$$

Where H is the wave height, L the wave length, k the wave number and h the water depth. In shallow water ($\tanh(kh) \rightarrow kh$) the expression above reduces to:

$$\gamma = \left[\frac{H}{L}\right]_{\max} = \frac{H_b}{h_b} \approx 0.88 \tag{24}$$

With γ the breaker index, H_b the breaking wave height and h_b the water depth at the breaking point. The formula above indicates that the waves start to break when the water depth is the limiting factor (depth induced breaking). The wave breaks because the wave celerity is reduced as the wave approaches the shore and the horizontal particle velocities will increase due to the shoaling. Note that according to the solitary wave theory (a wave theory for shallow water) the breaker index is ≈0.78. The relations presented above are derived based on the fact that the bottom is horizontal.

The breaking process of waves on a sloping bed can be expressed by the Iribarren parameter:

$$\xi = \frac{tan\alpha}{\sqrt{\frac{H_0}{L_0}}} \tag{25}$$

Where *tan(α)* is the steepness of the beach, L_0 the wavelength in deep water and H_0 the wave height in deep water. Depending on the value of the Iribarren parameter, different breaker types can be distinguished (Figure 57) (Battjes, 1974).

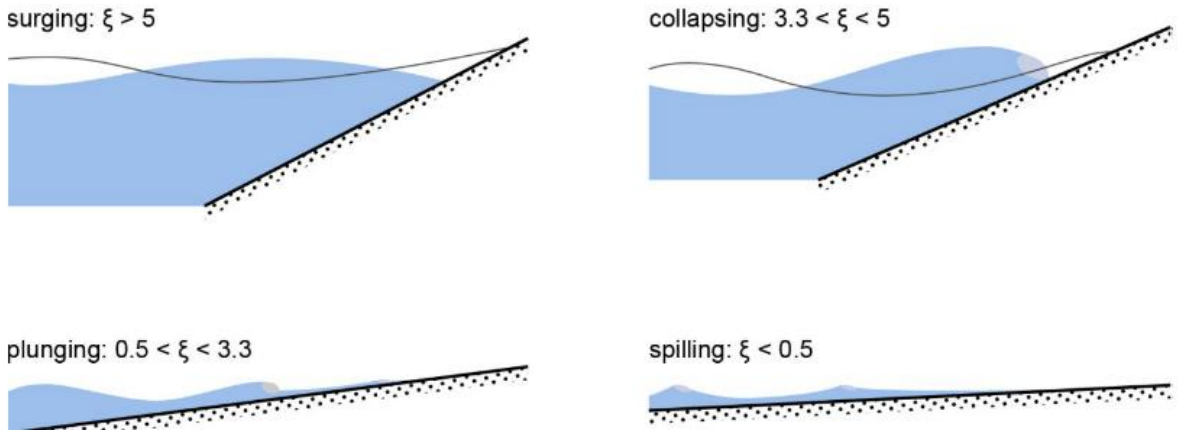

Figure 57: Different breaker types as a function of the Iribarren parameter (based on Battjes, 1974)

Spilling breakers are found along flat beaches and begin breaking at a relatively great distance from the shore. At the beach almost all energy is dissipated in the breaking process. A plunging breaker can be recognized by the curling top. When these waves break, a lot of energy is dissipated into turbulence. Surging breakers occur along steep shores for relatively long swell waves. The waves surge up and down the slope and the breaker zone is very narrow. Moreover, more than half of the energy is reflected back into deeper water. In between these non-breaking surging waves and breaking plunging waves, are the collapsing waves.

Currents

Return current

For breaking waves, the mass transport towards the coast between wave crest and wave trough may be quite large. However, there must be a zero net mass transport through the vertical as otherwise water will increasingly pile up against the coast. Hence, a net velocity below the wave trough level must be present, which is directed away from the coastline to compensate for the flux above the wave trough level. This is called a return current which results in seaward directed velocities under the wave trough level. The return current under breaking waves is usually much larger than steady Longuet-Higgins streaming. For non-breaking waves a relatively small return current is present.

Morphodynamics

Cross shore sediment transport

A variety of mechanisms exist which contribute to cross-shore sediment exchange. For example, during heavy storms the breaking waves cause high sediment concentrations in the lower and middle parts of the water column where the velocity is offshore directed. Due to the return current and this non-uniform sediment concentration over depth a net offshore sediment transport is present.

Roelvink and Stive (1989) showed that the most important contributions to bed load transport are the transport due to the mean current, the transport due to short wave skewness and the transport due to the interaction between the long wave velocity and the short wave velocity variance. The first contribution (mean current) is directed towards the coast outside the surf zone and directed offshore in the surf zone (due to Longuet-Higgins streaming and return current respectively). The second contribution is always onshore directed because due to shoaling short waves become skewed. The last term is offshore directed as long the long wave travels with the wave group (bound long wave). Somewhere in the surf zone this wave becomes released and the contribution to the bedload transport becomes onshore directed. Note that in all three cases the short waves stir up the sediment.

Bar development

A bar can develop in a cross-shore profile if the wave forcing is high enough. The large wave forcing erodes the coastline and the sediment will be deposited somewhere further offshore. A direct consequence of this is that a bar may develop. This bar will break/dissipate the highest waves in the spectrum, causing less energy available for coastline erosion. This means that the bars determine the location and rate of energy dissipation due to wave breaking and they may dictate the morphological response. The surf zone bars respond on forcing event timescales: storm events may move surf zone bars offshore, while more moderate wave action may move them onshore.

Longshore sediment transport

As a result of incoming waves approaching the coastline under an angle, a longshore sediment transport can be expected. When a gradient in longshore sediment transport is absent, cross-shore processes will dominate shoreline change. However, if a gradient in longshore sediment transport is present, two possibilities are may occur: a positive gradient will result in coastline erosion, while a negative gradient in longshore sediment transport will result in accretion.

Appendix B: Developed filter function

In this appendix, the developed filter function will be elaborated. The different filtering steps, the reconstruction of filtered signals to distinguish timescales, the accuracy and limitations are treated.

Before the filter function was developed, the following actions were carried out:

- All the wave- and shoreline signals are interpolated, such that they have a temporal resolution of one day.
- All the wave- and shoreline signals are detrended to exclude the time-series of temporal scales which are larger than the duration of the dataset.

The developed filter function is based on the concept of a running mean. A running mean calculates for each distinct day in the time-series, the mean of the surrounding window (w) days, where the window can be any value starting from one day to the signal duration. When w is one, the running mean and the raw signal are identical. When w becomes larger, the mean of all the surrounding window days is calculated. As an example, w=100 days is taken to construct the running mean in Figure 58 (red line).

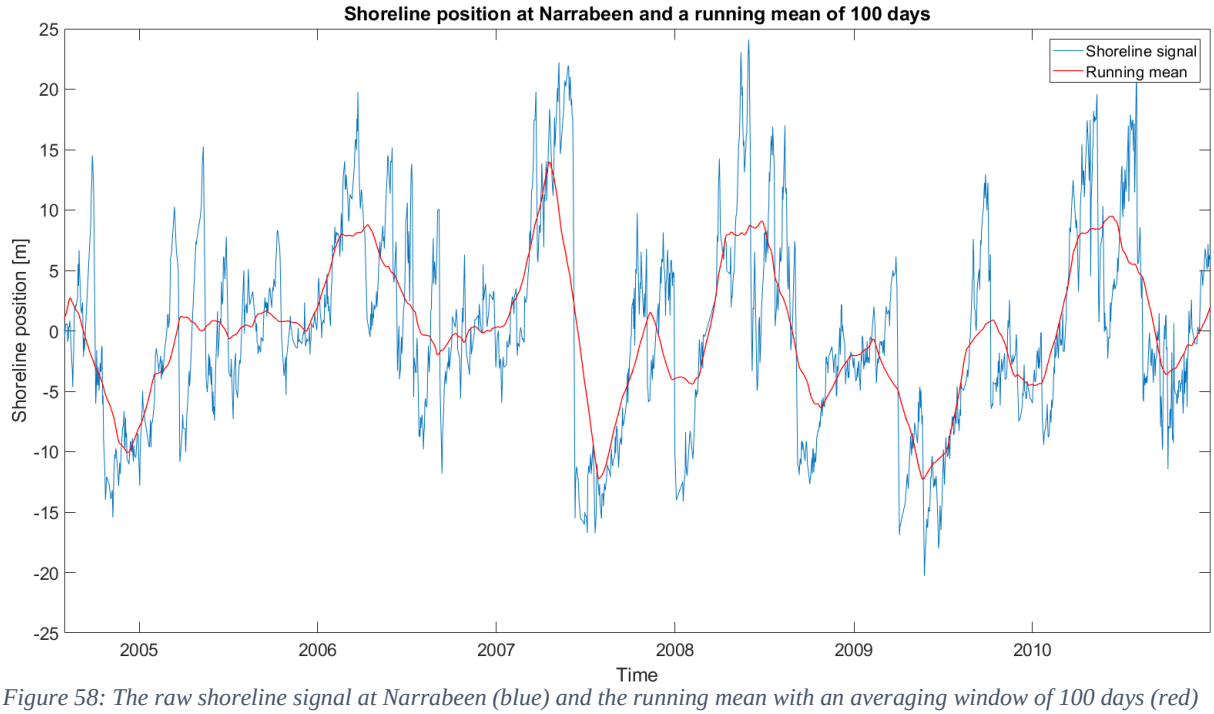

Figure 58: The raw shoreline signal at Narrabeen (blue) and the running mean with an averaging window of 100 days (red)

However, near the time-series ends the running mean cannot be calculated. In that case, the mean of the remaining days is taken. Another problem is to calculate the running mean near data-gaps. By using a tolerance parameter, that problem can be circumvented. The formulas that control the manipulation of data-gaps are as follows:

$$\#NaN > tol * w \rightarrow NaN \quad (26)$$

$$\#NaN \leq tol * w \rightarrow average\ (linear\ interpolation) \quad (27)$$

Where w is the averaging window, NaN is not-a-number and tol the tolerance. The tolerance parameter takes input values ranging from zero to one. If the percentage of NaN values within the total averaging window is smaller than the tolerance, the running mean is calculated where the NaN values are replaced by linear interpolation. If the opposite is true, the running average returns a NaN value. If the tolerance is high, the amount of linear interpolation is also high.

Figure 59 illustrates using a synthetic shoreline signal, the operation of the tolerance parameter. The figure shows the averaging procedure for point five with an averaging window of seven points (from point two until point eight). Note that points three and four are NaN values.

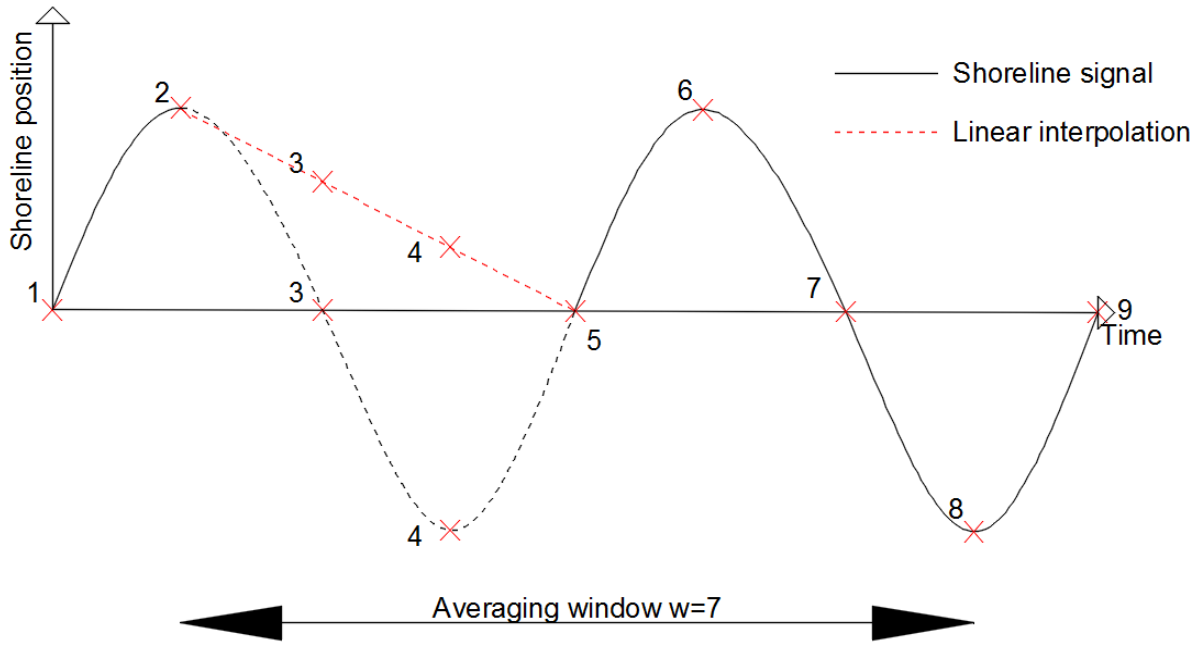

Figure 59: The averaging procedure of point five, if points three and four are NaN values

With formulas 26 and 27, the running average for point five can be calculated:

First, considering a tolerance of 0.2:
$2 > 0.2 * 7 \rightarrow NaN$

Secondly, for a tolerance of 0.3:
$2 \leq 0.3 * 7 \rightarrow linear\ interpolation$

Considering a tolerance of 0.2 or lower, the average of point five will be a NaN value. For a tolerance of 0.3 or higher, the average will be calculated where the NaN values are replaced by linear interpolation. In that case, the average of point five is calculated by including the values on the interpolated (red) line in Figure 59.

Subsequently, the calculated running mean is subtracted from the raw signal, or in Figure 58, the red line is subtracted from the blue line. In this way, the smaller timescales remain in the signal. To illustrate this and the following steps of the filter function in a simple way, a synthetic shoreline signal will be used.

Timescale distributions

The synthetic shoreline signal utilized in this section exists out of three sinusoidal waves with different temporal scales/periods (small, medium and large), but with identical amplitudes. In Figure 60, the synthetic shoreline signal is represented by the black line in the top panel and the running average is represented by the red line. The averaging window is the same as the period of the medium scale signal. When the two signals are subtracted from each other, the red line in the middle panel remains (composed out of the small- and medium scale signals). To separate the small- and medium scale signals, another running average is used. The averaging window of the second running average is exactly half of the one that is used for the first running average. In the next section, it will be explained why this has to be the case. The red line in the bottom panel shows the remaining filtered signal, which is close to the medium scale sinusoidal wave.

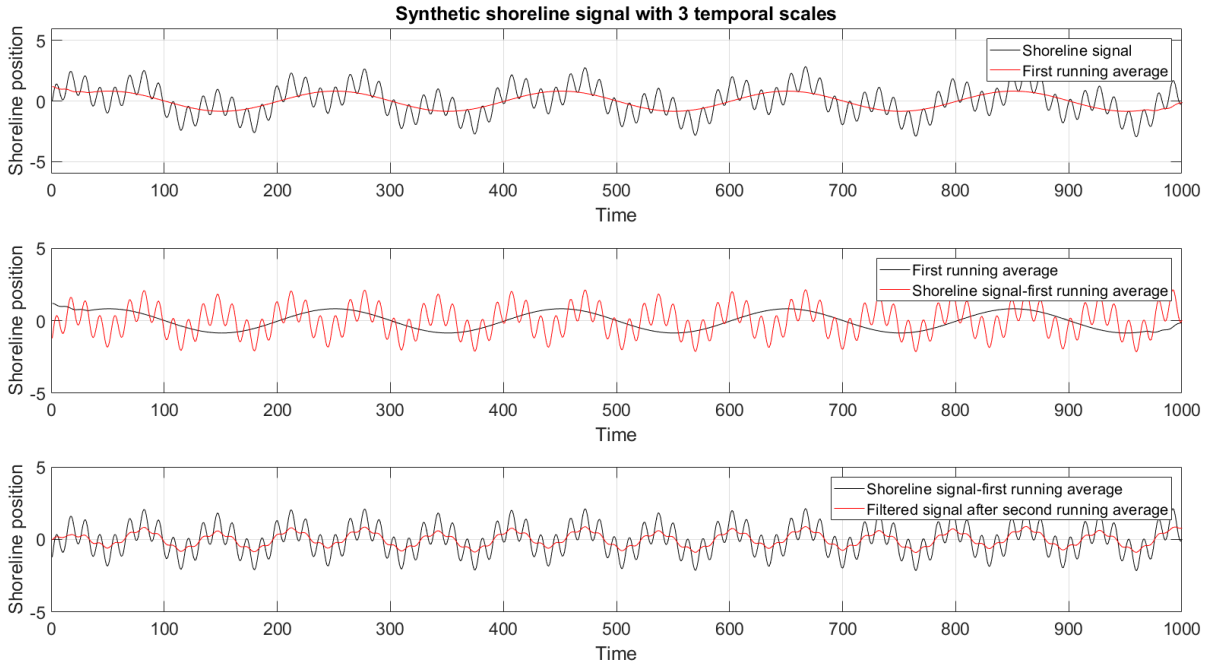

Figure 60: The three steps that make up the filter function. In each panel the black line is the same as the red line in the panel above to highlight the separate steps of the filter function. The black line in the top panel is the synthetic shoreline signal consisting of three sinusoidal waves with different periods. The red line in the bottom panel is the resulting signal, when filtered for the medium period sinusoidal wave.

The temporal spectrum can be found by applying the above described procedure for all different averaging windows. Where the averaging window is ranging from one day to *x* days, in which *x* is the duration of the signal. Subsequently, the standard deviation is calculated for each filtered signal and is plotted as a function of the averaging window. This represents the variability of the different timescales within the total shoreline signal. The temporal spectrum for the synthetic shoreline signal is presented in Figure 61.

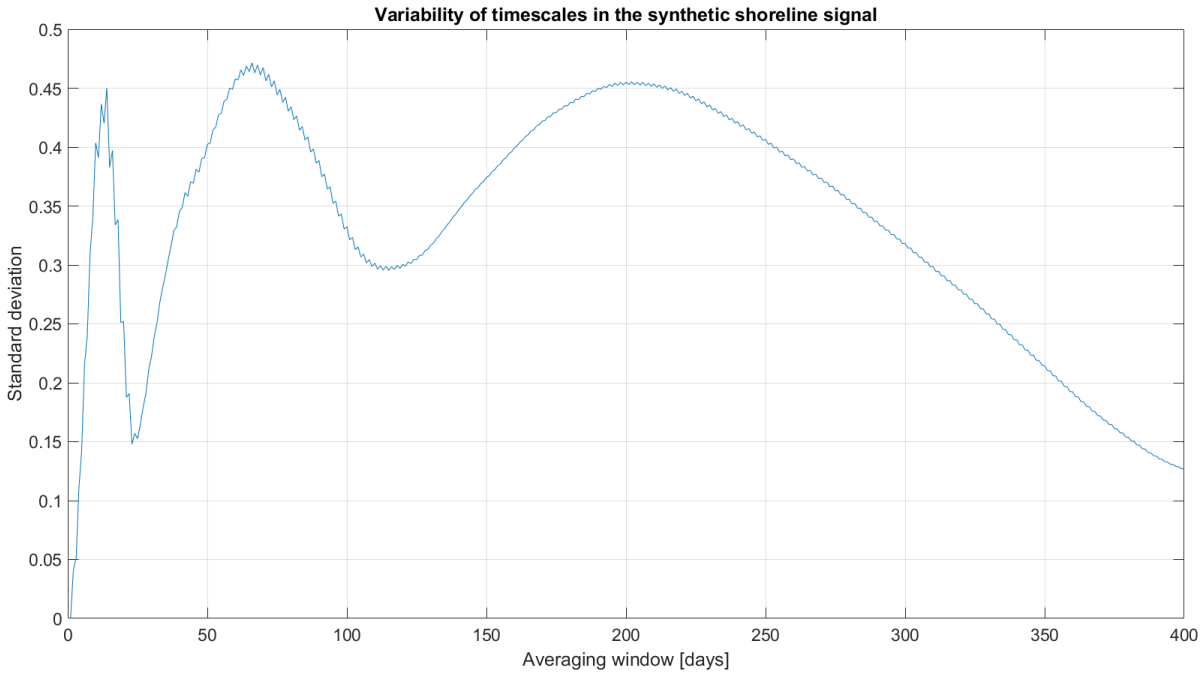

Figure 61: The temporal spectrum of the synthetic shoreline signal. The three peaks represent the three sinusoidal waves in the synthetic time-series.

The three peaks in the temporal spectrum correspond to the three periods of the sinusoidal waves. The peak of the largest averaging window represents the sinusoidal wave with the largest period and the most left peak corresponds to the small period sinusoidal wave. Note that the amplitude of the standard deviation within the spectrum is not the same as the standard deviation of each individual sinusoidal wave. This is a direct consequence of the averaging procedures. More important is that the peaks have the same standard deviation, which should be the case as the three sinusoidal waves have the same amplitude.

The filter function can be written down as follows:

$$fs(rs, w, tol) = ra_2(rs - ra_1(rs, w, tol), n * w, tol) \quad (28)$$

$$= \left(ra_1(rs, w, tol)\right) \quad (28a)$$
$$= \left(rs - ra_1(rs, w, tol)\right) \quad (28b)$$
$$= ra_2(rs - ra_1(rs, w, tol), n * w, tol) \quad (28c)$$

Where *fs* is the filtered signal, *rs* the raw signal, *ra* the running average function, *n* determines the difference in averaging width between the first and second running average and has to be 0.5, *w* the averaging width and *tol* the tolerance of the data-gaps. Note that formulas 28a until 28c represent the distinct steps of the filter function, which correspond to the three red signals in Figure 60.

Figure 62 indicates that only when *n* = 0.5, the positions of the peaks in the temporal spectrum are equal to the periods of the distinct signals that make up the synthetic shoreline signal. If *n* is larger, the peaks in the temporal spectrum are shifted towards a smaller timescale, while the opposite is true if *n* is smaller than 0.5. In those cases, the averaging procedures are causing that the standard deviation is the largest for timescales which are not represented in the synthetic shoreline signal.

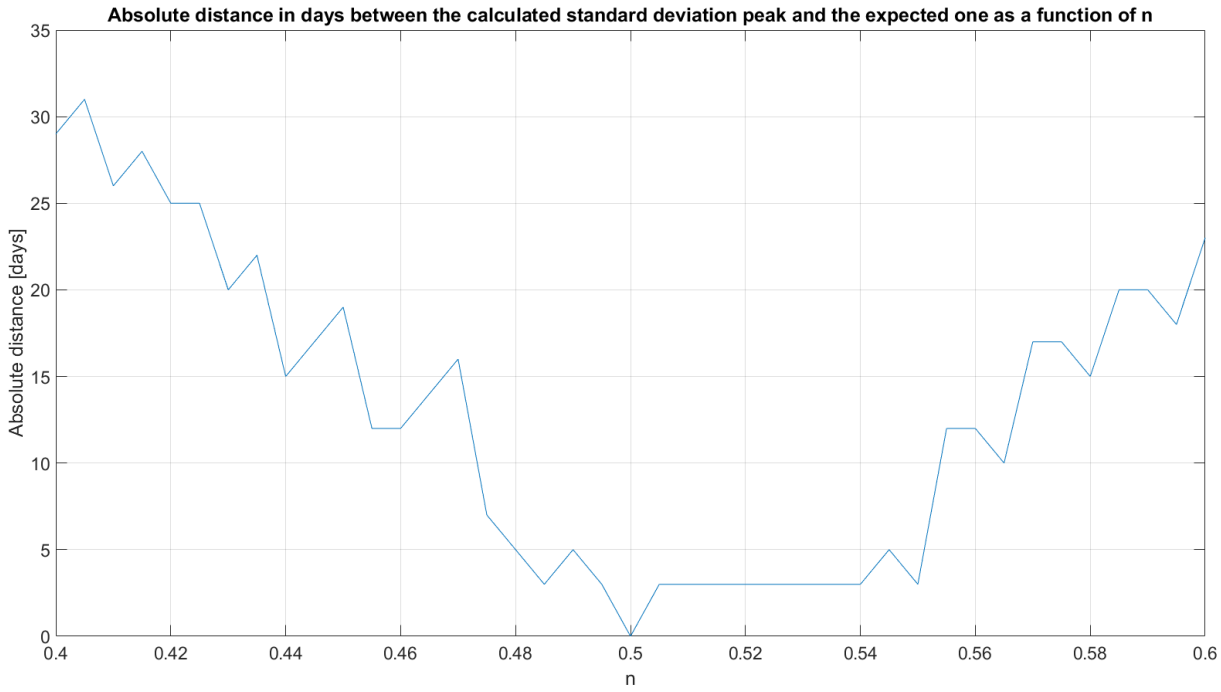

Figure 62: Absolute distance in days between the calculated peak in the temporal spectrum and the expected one for different values of n

An explanation for this shift can be found by realizing that the two running average functions in formula 28 are coupled. To illustrate this, a synthetic shoreline signal is used which only consists of the large period sinusoidal wave. In Figure 63, the period of this wave in the temporal spectrum is indicated by the vertical orange line. The top panel shows the temporal spectrum after the first two steps of the filter function (formula 28b). The peak shift can be explained using Figure 64, in which the first two steps of the filter function are visualized. The applied averaging width is slightly larger than the period of the sinusoidal wave (i.e. in the top panel of Figure 63, slightly to the right of the vertical orange bar). The corresponding average of the signal (red line in the top panel of Figure 64) is out of phase with the raw signal. Subsequently, the signal's standard deviation after subtraction will be larger than when the averaging width matches the period of the sinusoidal wave (then the average is zero). This results in a larger standard deviation for that filtered timescale and a peak shift in the temporal spectrum.

To shift the peak to the orange vertical line in the top panel of Figure 63, the second averaging procedure is used (formula 28c). The peak shift correction for different values of *n*, is presented in the center panel of Figure 63. The combination of the temporal spectrum in the top panel and the correction for different values of *n* is presented in the bottom panel. Only when $n = 0.5$ (red line), the peak in the temporal spectrum matches the vertical orange bar.

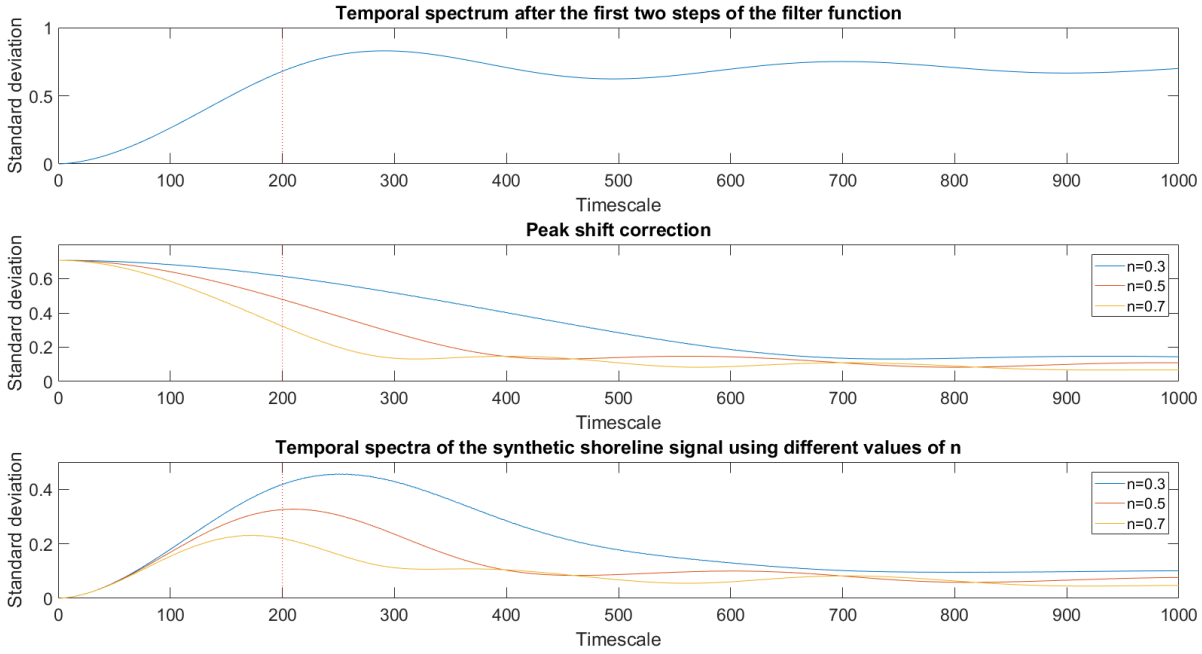

Figure 63: The top panel presents the temporal spectrum of the synthetic shoreline signal calculated with formula 28b. The center panel is the peak shift correction and the bottom panel shows the combination of the first panel and the peak shift correction for different values of n.

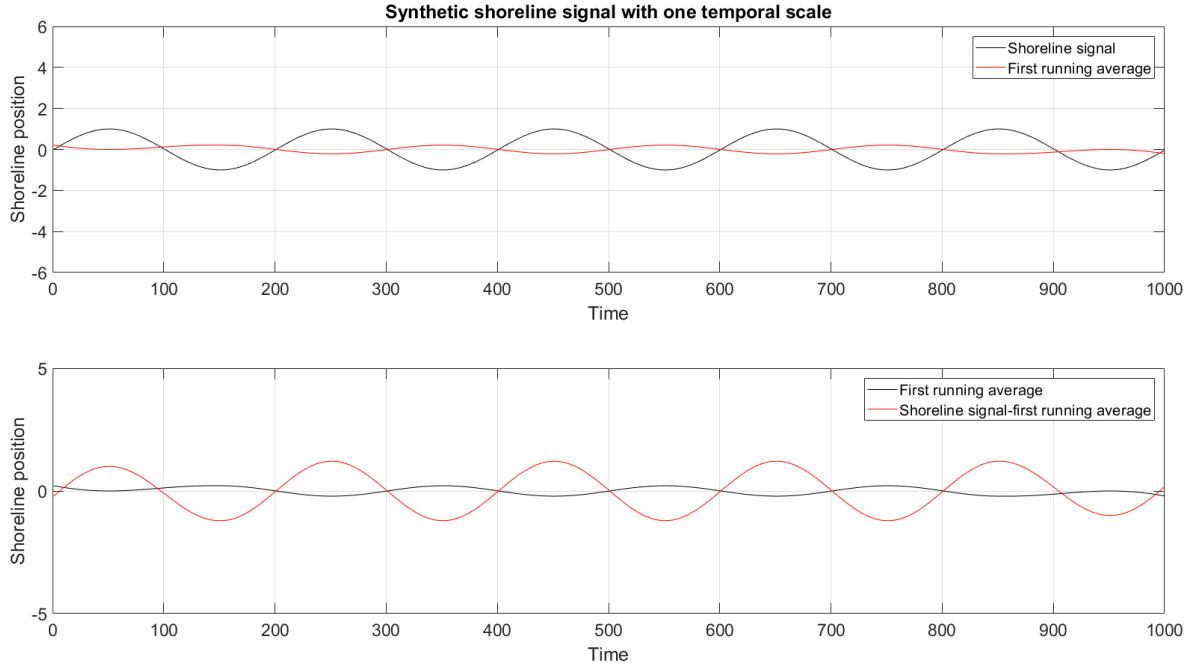

Figure 64: The first two steps of the filter function. When the averaging width is larger than the period of the signal, the resulting signal is out of phase with the shoreline signal (top panel). After subtraction, the standard deviation becomes larger than when the averaging width is equal to the period of the sinusoidal wave which causes a peak shift in the temporal spectrum.

Reconstructing the raw signal

In the previous section, the emphasis lay on finding dominant timescales in a raw signal. The following section will focus on generating time-series with distinct timescales, by using the temporal spectrum. The same synthetic shoreline signal is used, to show the operation of distinguishing timescales. However, before timescales are distinguished, the raw shoreline signal is reconstructed using all filtered signals in the temporal spectrum. This is carried out because an important aspect that has to be fulfilled is energy preservation. Subsequently, parts of the temporal spectrum can be used to generate time-series with distinct timescales. The following procedures are carried out to reconstruct the raw signal:

First, the synthetic shoreline signal is filtered for all timescales using formula 28. Secondly, the amplitude of each filtered signal is divided by the window width. The window width can be calculated by:

$$w - \frac{w}{2} = \frac{w}{2} \tag{29}$$

In which *w* is the averaging width. The window width represents the difference between the two timescales used for the averaging procedures in formula 28. Hence, the window width and the averaging width are not the same. The filtered signals need to be divided by the window width, because Figure 61 indicates that a larger period of the sinusoidal wave yields a wider peak in the temporal spectrum. This phenomenon is caused by the accuracy of the filter function, which will be elaborated later on.

If all filtered signals in the temporal spectrum are added up and the linearly growing window width (*w/2*) is not accounted for, the larger timescales will dominate the reconstructed shoreline signal due to the wider peak in the temporal spectrum. However, this is not the case, because in the synthetic shoreline signal all sinusoidal waves have the same amplitude.

However, the summation of all filtered signals in the temporal spectrum, when accounting for the linearly growing window width, has the same shape as the synthetic shoreline signal but the amplitude is too large. This effect can be eliminated by an optimization process, in which the window width is multiplied by a constant factor, called the extra factor (EF). Figure 65 visualizes the optimization process: the EF yielding the lowest RMSE between the synthetic- and reconstructed signal is chosen.

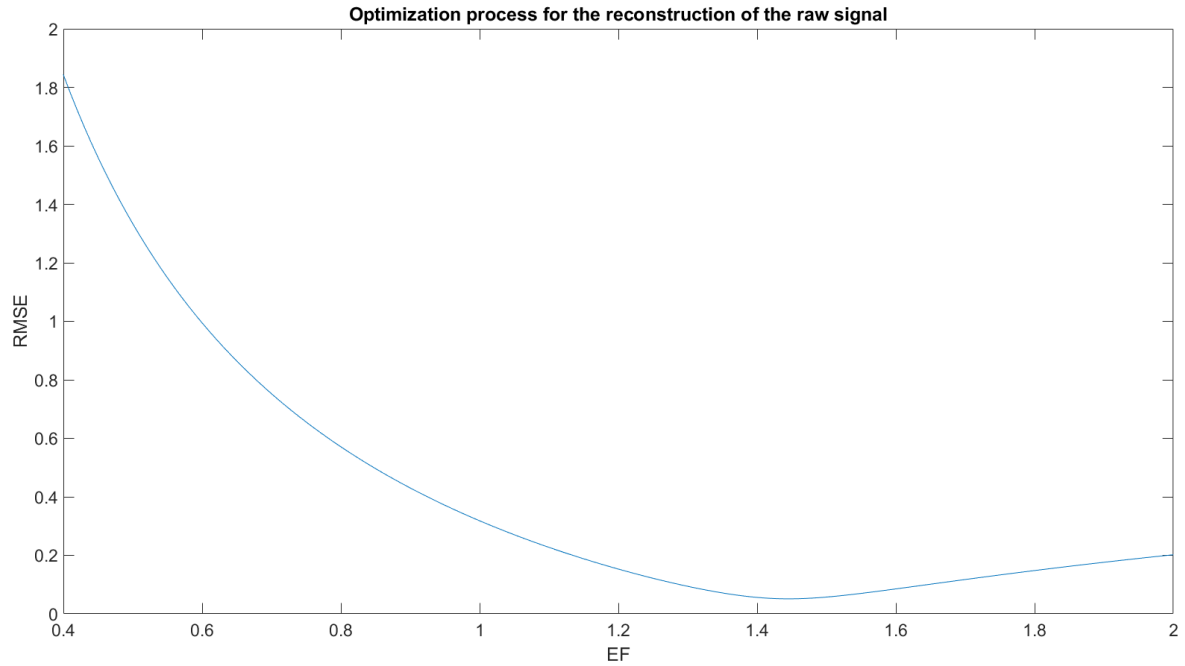

Figure 65: Optimization process for the reconstruction of the synthetic shoreline signal

The procedure described above can be written down as follows:

$$fs(rs, w) = ra_2(rs - ra_1(rs, w), n * w) \quad (30)$$

$$RS(rs, w, EF) = \sum_1^N fs(rs, w)/(WW(w) * EF) \quad (31)$$

Where *N* is the length of the signal, *WW* the window width, *EF* the extra factor, *n* = 0.5, *w* the averaging width, *ra* the running average function, *fs* the filtered signal, *rs* the raw signal and *RS* the reconstructed signal. Figure 66 presents the synthetic- and reconstructed shoreline signals. The overall shape of the raw signal is preserved in the reconstructed signal, but a minor difference in amplitude is present (the RMSE for the optimal EF is not equal to zero (Figure 65)).

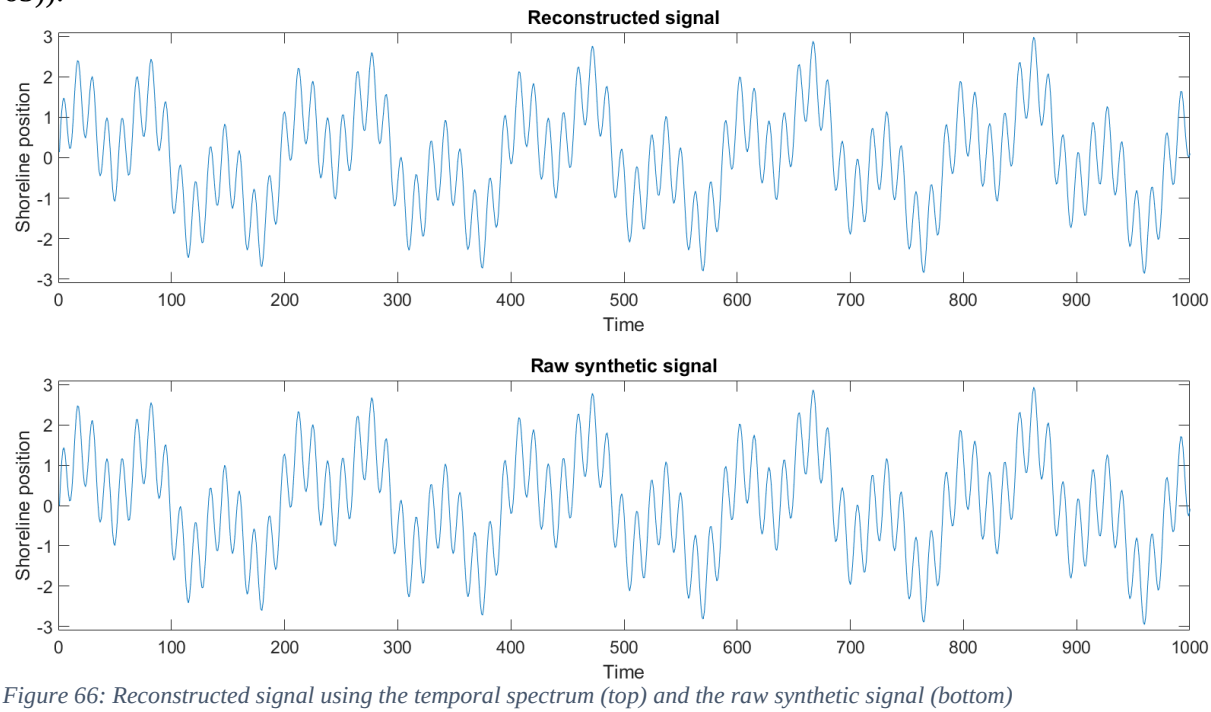

Figure 66: Reconstructed signal using the temporal spectrum (top) and the raw synthetic signal (bottom)

It was already stated above that a larger period sinusoidal wave, yields a wider peak in the temporal spectrum. Figure 67 presents two temporal spectra, one corresponding to a sinusoidal wave with a small period (right) and one with a large period (left). For both cases, the standard deviation goes to zero if the averaging width goes to one. This is due to the fact that for this averaging width, the signal obtained with formula 28a matches the raw signal such that the standard deviation after subtraction (formula 28b) will be zero. In between an averaging window of one and an averaging window equal to the period of the sinusoidal wave, the signal obtained with formula 28a is not equal to the raw signal and a certain variability remains. This explains why the peaks in the temporal spectrum are wider for larger period signals. Moreover it explains why the amplitude of each filtered signal must be divided by the window width to reconstruct the raw signal.

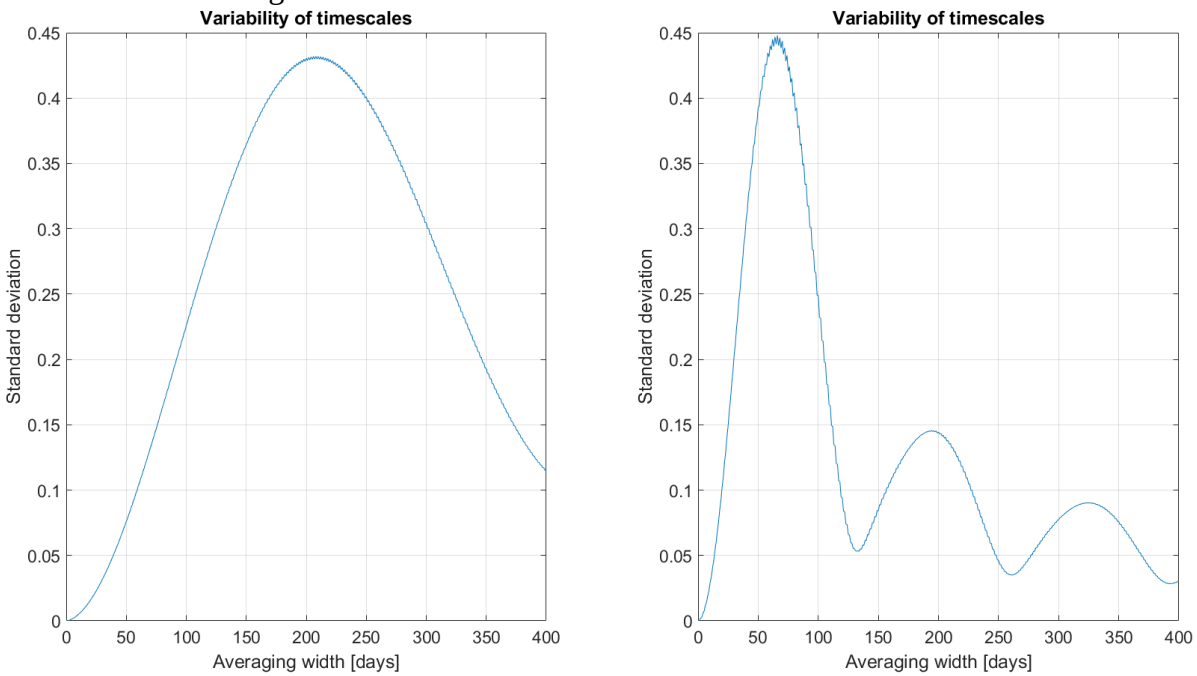

Figure 67: Temporal spectra of the large period- (left) and small period sinusoidal wave (right)

Accuracy of the filter function

The synthetic shoreline signal utilized above had minimal complexity. It was constructed out of three sinusoidal waves, which were easily identified in the temporal spectrum. Using more sinusoidal waves, the accuracy of the filter function could be determined and is presented in Figure 68.

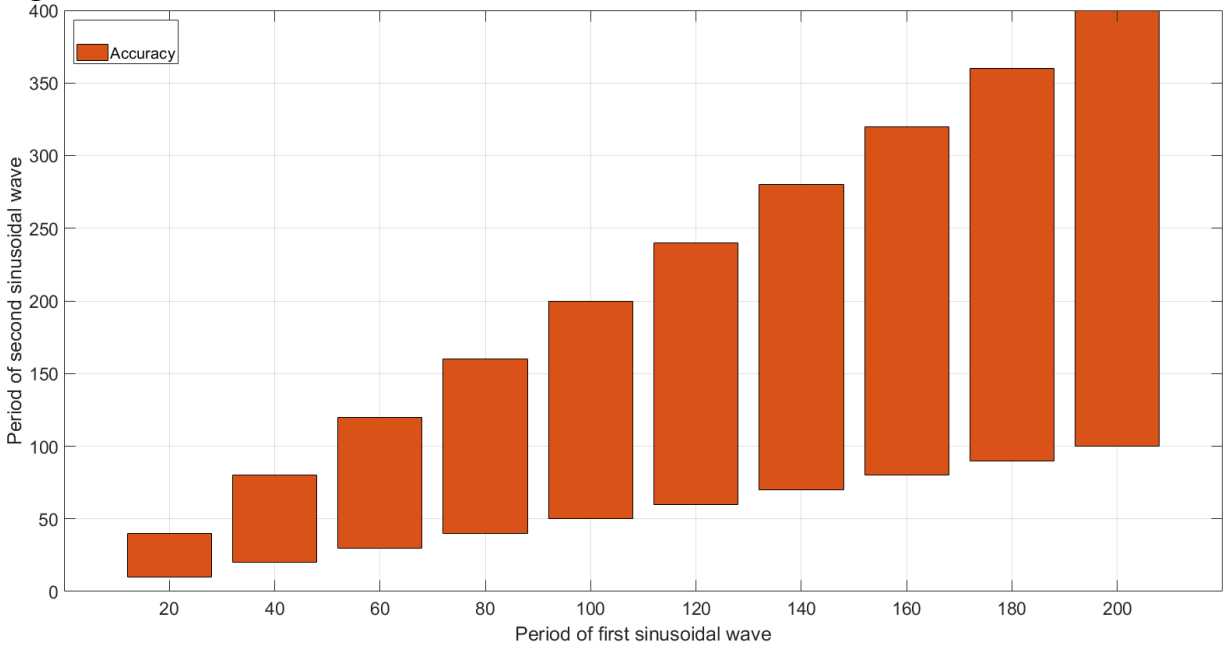

Figure 68: Accuracy of the filter function for two sinusoidal waves

The orange bars in Figure 68 indicate which timescales are not distinguishable from each other in the temporal spectrum. This is the accuracy of the filter function. Note that this accuracy is derived in case of two sinusoidal waves with the same amplitude. For example, if the synthetic shoreline signal is made up out of two sinusoidal waves of which one has a period of 100 days, other sinusoidal waves with the same amplitude and with periods between 50 and 200 days cannot be distinguished in the temporal spectrum. The temporal spectrum should reveal two peaks at the corresponding timescales, but it only shows one peak in between the two separate undistinguishable timescales. Hence, if two sinusoidal waves with the same amplitude fall both within the range of the orange bars in Figure 68, the periods are too close together to be separated by the averaging functions.

Appendix C: Temporal spectra at Narrabeen and Grand Popo

In this appendix, temporal spectra of the shoreline position, wave height, wave period and wave power are presented at Narrabeen and Grand Popo.

Narrabeen

In Figure 69, the temporal spectra at Narrabeen are presented.

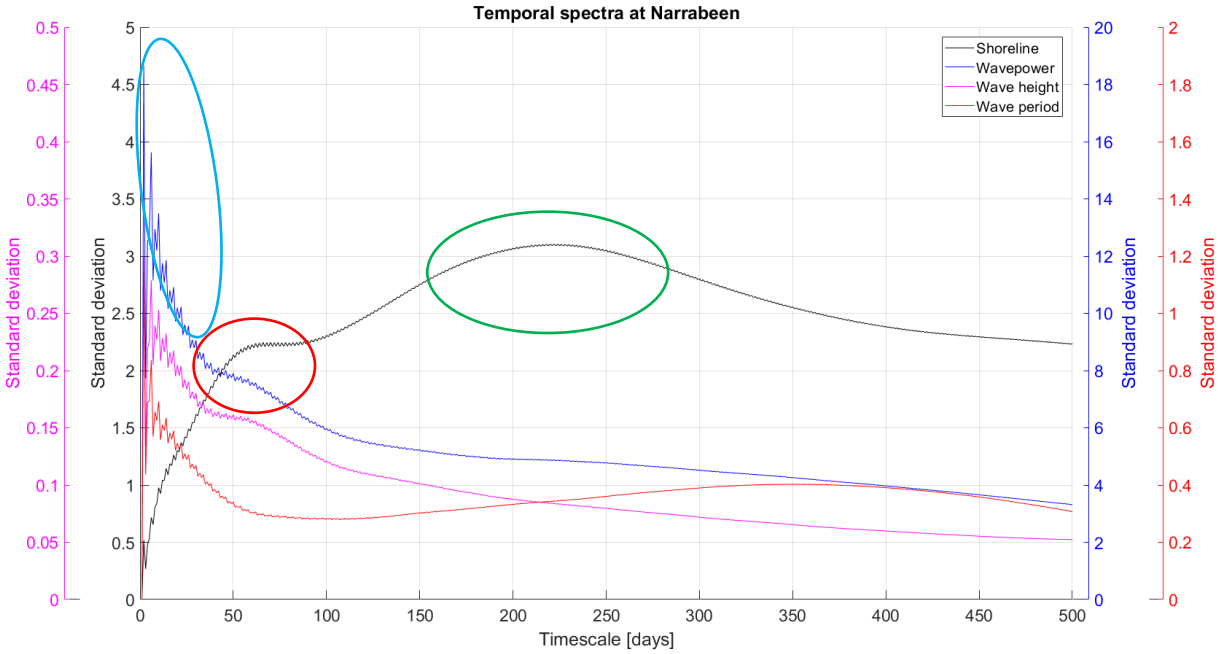

Figure 69: Temporal spectra of the shoreline position, wave height, wave period and wave power at Narrabeen

The shoreline spectrum reveals two dominant timescales, one at ≈60 days (red oval) and one at ≈220 days (green oval). The timescale of 220 days is the most dominant. The wave power spectrum reveals that small (daily) timescales have the most variability (blue oval), opposed to the shoreline spectrum. Both spectra imply that a less dominant timescale (≈60 days) is present as well. This could suggest that shoreline position changes with a temporal scale of ≈60 days are the result of waves with a corresponding timescale. This is not true for the most dominant timescale in the shoreline spectrum with a temporal scale of ≈220 days.

Grand Popo

In Figure 70, the temporal spectra at Grand Popo are presented.

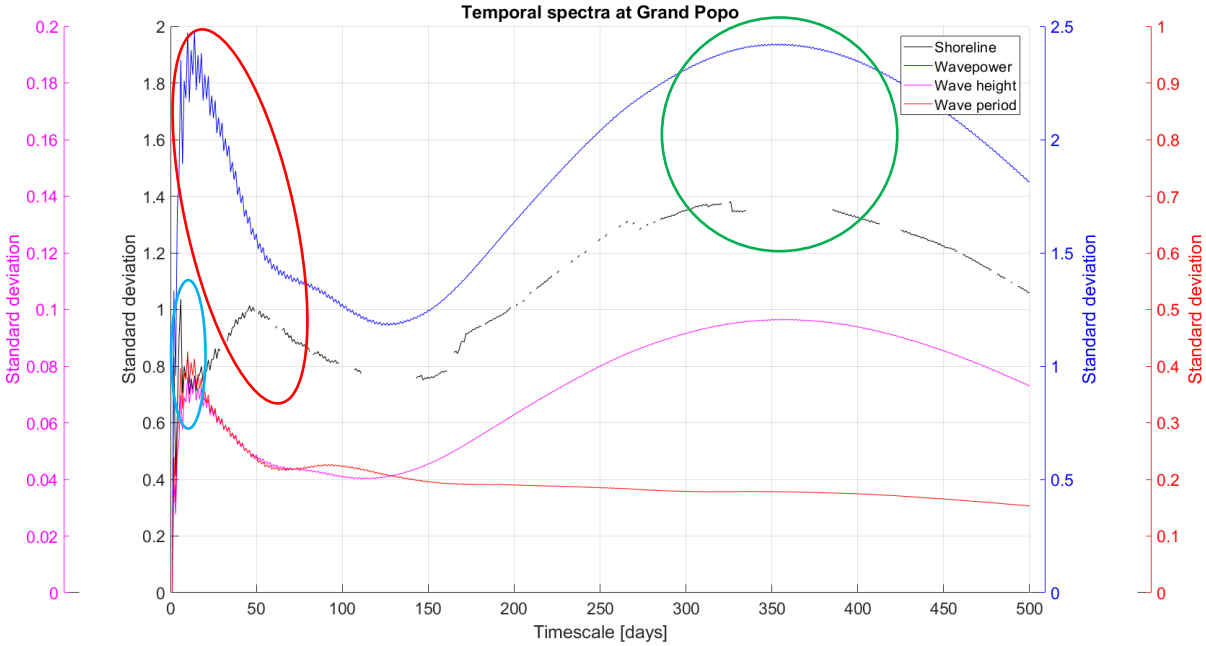

Figure 70: Temporal spectra of the shoreline position, wave height, wave period and wave power at Grand Popo

The seasonal variability (≈365 days) is a dominant mode of shoreline response and wave power (green oval). This can imply that changes in wave forcing with a timescale of ≈365 days are responsible for changes in shoreline position with the identical timescale. Both spectra indicate a large variability in smaller timescales as well (red oval). However, the temporal scales do not correspond to each other: a clear shift is present. A third dominant shoreline response timescale is present, which represents the daily temporal scales (blue oval). Especially at these smaller scales it cannot be stated beforehand which timescales in wave data are responsible for which timescales in shoreline change.

Appendix D: Disability of other approaches to implement multiple timescales

In this appendix, an elaboration is provided about the disability of other approaches to implement multiple beach response timescales in ShoreFor. Before the current approach was found, other methods were tried as well. However, these did not result in the desired outcome as will be shown.

Hardwire timescales

Figure 71 indicates the squared correlation as a function of the memory decay factor when ShoreFor is calibrated on the entire dataset at Nha Trang. The idea was to hardwire ShoreFor with memory decay factors corresponding to peaks in the correlation graph. Those peaks would represent the different dominant beach response timescales. Subsequently, a linear superposition would be carried out to ensure the implementation of multiple timescales.

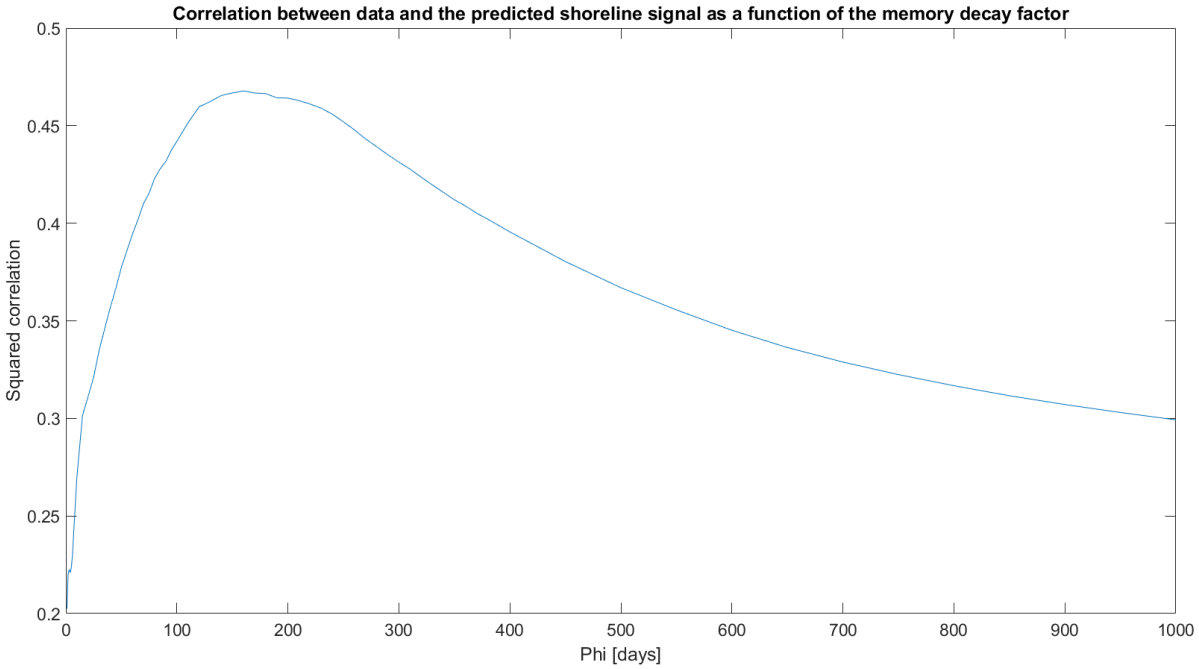

Figure 71: Correlation between data and model prediction as a function of the memory decay factor when ShoreFor is applied to the dataset at Nha Trang

However, the figure indicates that only one correlation peak is present, corresponding to the most dominant timescale (the seasonal timescale). The memory decay factor that represents the monsoon timescale cannot be recognized. Therefore, it is not possible to carry out a linear superposition by hardwiring the most dominant timescales in a signal.

Utilizing filtered shoreline signals and non-filtered forcing signals

Another possible approach to implement multiple timescales is to filter the shoreline signal and force the filtered signals with the raw wave time-series. Subsequently, ShoreFor will find the best fit to each filtered shoreline signal. The corresponding result of the linear superposition is indicated by the black line in Figure 72 (for the Nha Trang dataset). Note that the bin distribution is such that the shoreline response variability within each bin is the same, to exclude consequences which are related to a subjectively chosen distribution. The total amount of bins used in this case is 36.

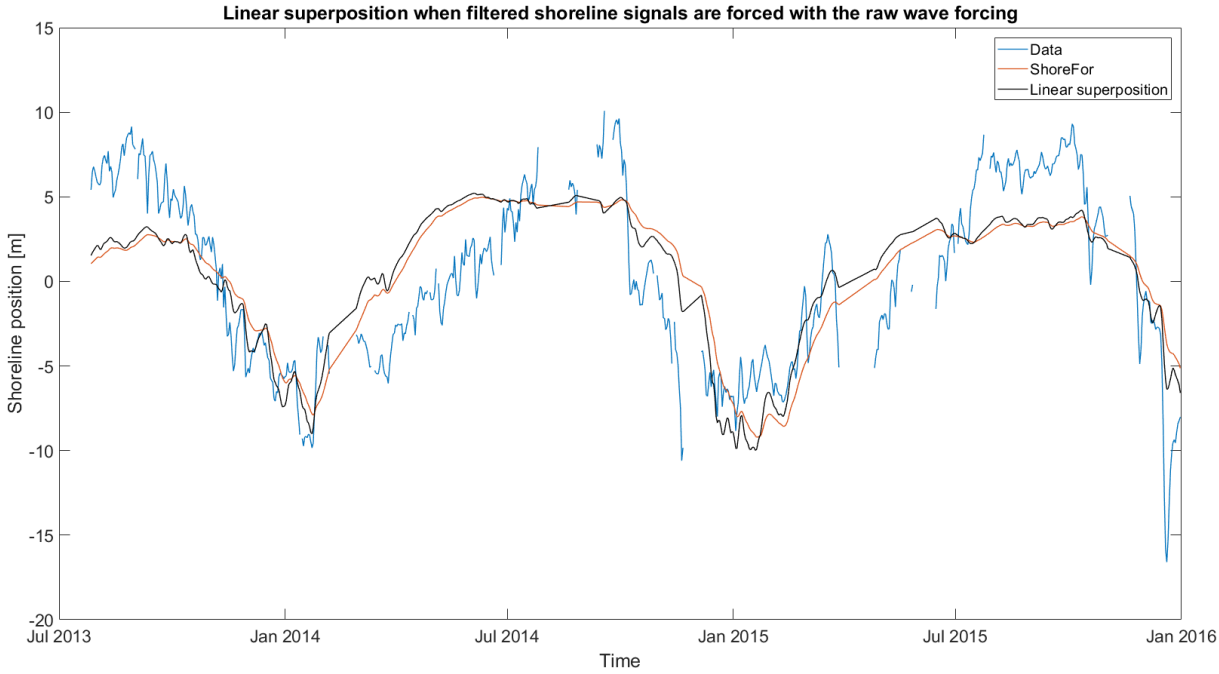

Figure 72: Linear superposition (black) when the shoreline signals are filtered and forced with non-filtered wave signals

However, the approach shows some improvement in predicting smaller timescales, whereas the predicted shoreline signal corresponding to the larger timescales is the same. The reason for this can be observed in Figure 73. If smaller timescales (≈ 1-30 days) in shoreline position (blue line) are forced with the raw wave signal (black line), ShoreFor cannot find a proper relation between the two. This is due to the fact that the dominant seasonal timescale is absent in the filtered shoreline signal, while this scale is still present in the raw wave signal such that it influences the predicted result.

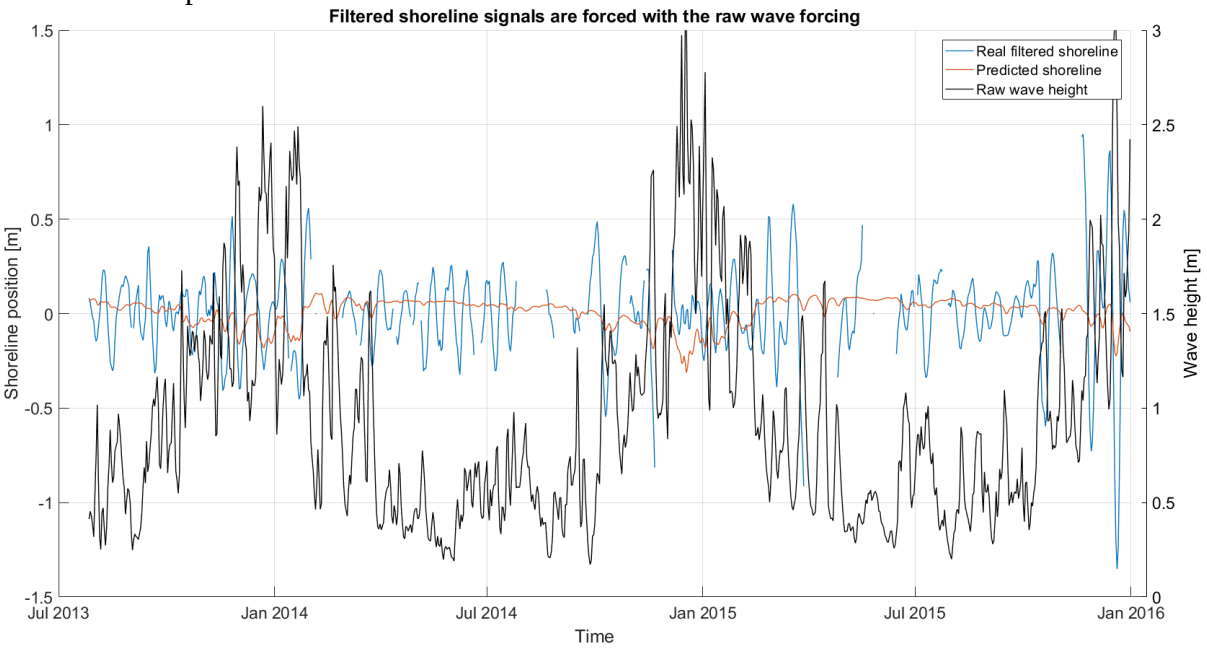

Figure 73: The filtered shoreline signal is forced with the raw forcing signals. ShoreFor cannot find a proper relation between the two as the seasonal timescale is absent in the filtered shoreline signal.